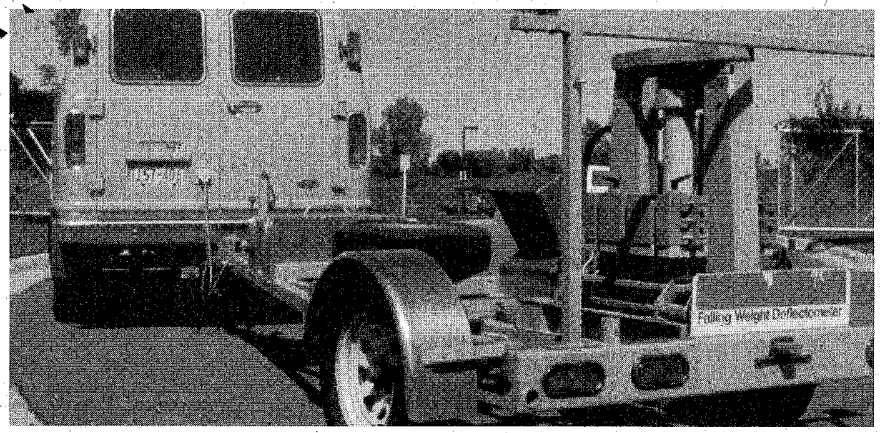
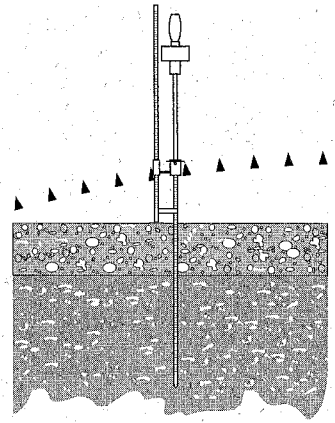




UNIVERSITY OF MINNESOTA
CENTER FOR
TRANSPORTATION
STUDIES

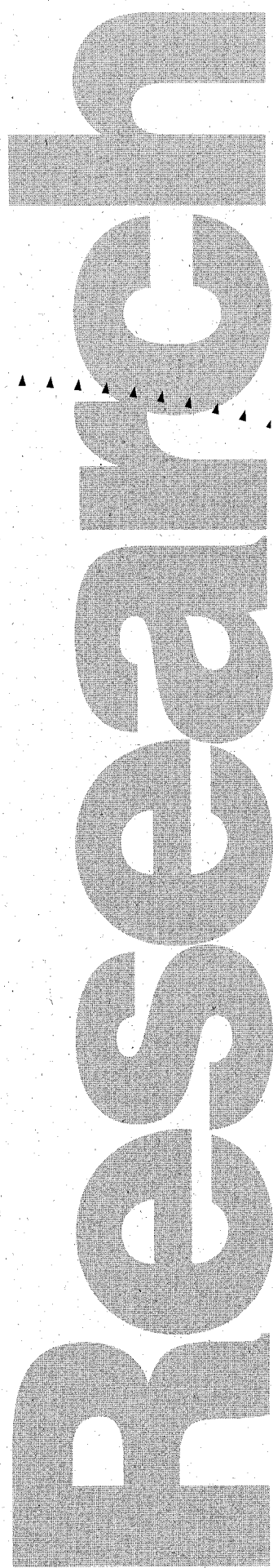


Initial Characterization of Subgrade Soils and Granular Base Materials at the Minnesota Road Research Project

CTS
TE
211
.155
1995



Local Road Research Board



Technical Report Documentation Page

1. Report No. MN/RC - 96/19		2.		3. Recipient's Accession No.	
4. Title and Subtitle INITIAL CHARACTERIZATION OF SUBGRADE SOILS AND GRANULAR BASE MATERIALS AT THE MINNESOTA ROAD RESEARCH PROJECT				5. Report Date December 1995	
				6.	
7. Author(s) David E. Newcomb, Bruce A. Chadbourn, David A. Van Deusen, and Thomas R. Burnham				8. Performing Organization Report No.	
9. Performing Organization Name and Address University of Minnesota Civil Engineering Department 500 Pillsbury Dr. S.E. Minneapolis, Minnesota 55455				10. Project/Task/Work Unit No.	
				11. Contract (C) or Grant (G) No. (C) 68880 TOC #73 (C) 70214 TOC #95	
12. Sponsoring Organization Name and Address Minnesota Department of Transportation 395 John Ireland Boulevard Mail Stop 330 St. Paul, Minnesota 55155				13. Type of Report and Period Covered Final Report 1992-1995	
				14. Sponsoring Agency Code	
15. Supplementary Notes					
16. Abstract (Limit: 200 words) <p>This research was conducted on the behavior of materials at the Minnesota Road Research Project (Mn/ROAD), the construction of which was completed in 1994. Falling-Weight Deflectometer (FWD) tests were conducted on the test sections at all stages of pavement construction (pre-base, post-base, and post pavement). Deflection values were highly variable due to variability in surface condition, soil moisture content, density, and stress-dependent effects.</p> <p>In general, backcalculated subgrade moduli tended to increase with increasing FWD sensor offset (decreasing stress). Post-base and post-pavement testing also indicated an apparent increase in subgrade modulus relative to pre-base values. Moduli values were also determined for granular base results.</p> <p>These results were compared to Dynamic Cone Penetrometer (DCP) penetration index values as well as to resilient moduli values from tests conducted on subgrade and granular base materials in the lab. The backcalculated subgrade soil modulus values compared well with the laboratory resilient modulus values, but no correlation was seen between backcalculated moduli and penetration index values.</p> <p>The results of this testing will provide a baseline for future analysis of the test sections at Mn/ROAD.</p>					
17. Document Analysis/Descriptors Subgrade Soil Falling-Weight Deflectometer (FWD) Dynamic Cone Penetrometer (DCP)				18. Availability Statement No restrictions. Document available from: National Technical Information Services, Springfield, Virginia 22161	
19. Security Class (this report) Unclassified		20. Security Class (this page) Unclassified		21. No. of Pages 149	
				22. Price	

INITIAL CHARACTERIZATION OF SUBGRADE SOILS AND GRANULAR BASE MATERIALS AT THE MINNESOTA ROAD RESEARCH PROJECT

Final Report

Prepared by

David E. Newcomb
Bruce A. Chadbourn

University of Minnesota
Civil Engineering Department
500 Pillsbury Dr. S.E.
Minneapolis, MN 55455-0220

David A. Van Deusen
Thomas R. Burnham

Minnesota Department of Transportation
Office of Minnesota Road Research
1400 Gervais Avenue
Maplewood, MN 55109-2043

December 1995

Published by

Minnesota Department of Transportation
Office of Research Administration
200 Ford Building Mail Stop 330
117 University Avenue
St Paul Minnesota 55155

The contents of this report reflect the views of the authors who are responsible for the facts and accuracy of the data presented herein. The contents do not necessarily reflect the views or policies of the Minnesota Department of Transportation at the time of publication. This report does not constitute a standard, specification, or regulation.

ACKNOWLEDGEMENTS

This work was funded by the Minnesota Department of Transportation and the University of Minnesota Center for Transportation Studies. Their support is gratefully acknowledged. The authors would also like to express their sincere appreciation to the staff of the Non-Destructive Testing, Foundation Soils Laboratory, and Physical Research Sections of the Minnesota Department of Transportation. The work presented in this report represents only a small portion of the total efforts and without the participation of Mn/DOT personnel this work would not have been possible. The authors would also like to thank Dr. Carl A. Lenngren who performed much of the backcalculation analysis, and RST-Sweden who provided the multi-layer backcalculation program used in the study.

TABLE OF CONTENTS

CHAPTER 1 - INTRODUCTION	1
Background	1
Objectives	1
Scope	2
CHAPTER 2 - PREVIOUS WORK	5
CHAPTER 3 - SUBGRADE TESTING PROCEDURES	7
FWD Testing	7
Soil Sampling	8
Dynamic Cone Penetrometer (DCP) Testing	9
CHAPTER 4 - ANALYSIS	11
Deflection Data Validation	11
Homogeneous Backcalculation Analysis	13
Static Multi-Layered Backcalculation Analysis	15
Analysis of Laboratory Data	17
Comparison of Field and Laboratory Data	18
Penetration Index	19
Geostatistical Analysis	20
Effects of Construction on Subgrade Stress and Modulus	21
<i>Stress Calculations</i>	21
<i>Subgrade Tests</i>	22
<i>Granular Base Tests</i>	22
<i>Flexible Pavement Tests</i>	23
<i>PASB Tests</i>	24
<i>Rigid Pavement Tests</i>	25
<i>Aggregate and Chip-Seal Tests</i>	25
Effects of Construction on Granular Base Stress Modulus	26
CHAPTER 5 - CONCLUSIONS AND RECOMMENDATIONS	27
Conclusions	27
Recommendations	28
REFERENCES	29

APPENDICES

(Available at the Mn/Road office at the Minnesota Department of Transportation)

- APPENDIX A Documentation of Subgrade FWD Tests**
- APPENDIX B Documentation of Base FWD Tests**
- APPENDIX C Documentation of Subgrade and Base Soils Sampling and Testing**
- APPENDIX D Backcalculated Subgrade Moduli: Homogeneous Model**
- APPENDIX E Summary of DCP Testing**
- APPENDIX F Construction Effects Summary Data**

LIST OF TABLES

Table 1a.	Variability and correlation of surface deflections from subgrade testing TS 3: entire section.....	31
Table 1b.	Variability and correlation of surface deflections from subgrade testing TS 3: grid test.	32
Table 1c.	Variability and correlation of surface deflections from subgrade testing TS 4: entire section.....	33
Table 1d.	Variability and correlation of surface deflections from subgrade testing TS 4: grid test.	34
Table 2a.	Variability and correlation of surface deflections from base testing TS 3: entire section.	35
Table 2b.	Variability and correlation of surface deflections from base testing TS 3: grid test.	36
Table 2c.	Variability and correlation of surface deflections from base testing TS 4: entire section.	37
Table 2d.	Variability and correlation of surface deflections from base testing TS 4: grid test.	38
Table 3.	Values of half-space deflection factor $f(r)$ for several values of Poisson's ratio.	39
Table 4.	Summary statistics for thin-walled sample data.	41
Table 5.	Summary statistics for bag sample data.	43
Table 6a.	Comparison of backcalculated and laboratory resilient moduli by test section.....	47
Table 6b.	Comparison of backcalculated and laboratory resilient moduli by facility sub-section.	48
Table 7a.	Summary of selected backcalculated moduli and penetration index values: subgrade testing.	49
Table 7b.	Summary of selected backcalculated moduli and penetration index values: base testing.....	51
Table 8.	Summary of backcalculation results from testing on sections with thin granular layers.	53
Table 9.	Summary of backcalculation data from all conventional flexible test sections.	54
Table 10.	Summary of average backcalculation data from all full-depth sections.	55
Table 11.	Summary of subgrade modulus and deviator stress changes for all conventional, flexible test sections, at different stages.....	56
Table 12.	Summary of backcalculation results from testing on sections after construction of permeable asphalt-stabilized base (PASB).	57
Table 13.	Effective pavement modulus data for rigid sections.	58
Table 14.	Summary of backcalculation results from testing on aggregate and chip-seal test sections	59

Table 15. Summary of subgrade modulus and stress increases for the aggregate and chip-seal test sections.	59
Table 16. Summary of average test section results for backcalculation analyses of granular base materials.	60

LIST OF FIGURES

Fig. 1.	Location and site layout for the Mn/ROAD project.....	61
Fig. 2.	Mn/ROAD test section diagrams.	62
Fig. 3.	Comparison of FWD deflections for TS 6, D_0 sensor, taken two days apart.	67
Fig. 4.	Comparison of FWD deflections for TS 6, D_{600} sensor, taken two days apart.....	68
Fig. 5.	Comparison of FWD deflections for TS 6, D_{1800} sensor, taken two days apart.	69
Fig. 6.	Relationship between D_{1800} and D_{600} sensor deflections, TS 6 variability study.....	70
Fig. 7.	Comparison of FWD deflections for TS 7, D_0 sensor, taken two days apart.	71
Fig. 8.	Comparison of FWD deflections for TS 7, D_{600} sensor, taken two days apart.....	72
Fig. 9.	Comparison of FWD deflections for TS 7, D_{1800} sensor, taken two days apart.	73
Fig. 10.	Relationship between D_{1800} and D_{600} sensor deflections, TS 7 variability study.....	74
Fig. 11.	Backcalculated moduli for all sensor offsets from TS 10 and 24.....	75
Fig. 12.	Variation of backcalculated subgrade moduli for mainline test sections, lane 1.....	76
Fig. 13.	Variation of backcalculated subgrade moduli for mainline test sections, lane 4.....	77
Fig. 14.	Variation of backcalculated subgrade moduli for mainline test sections, lane 7.....	78
Fig. 15.	Variation of backcalculated subgrade moduli for low-volume test sections, lane 1.	79
Fig. 16.	Variation of backcalculated subgrade moduli for low-volume test sections, lane 4.	80
Fig. 17.	Variation of backcalculated subgrade moduli for low-volume test sections, lane 7.	81
Fig. 18.	Average backcalculated subgrade moduli for mainline test sections, lane 1.....	82
Fig. 19.	Average backcalculated subgrade moduli for mainline test sections, lane 4.....	83
Fig. 20.	Average backcalculated subgrade moduli for mainline test sections, lane 7.....	84
Fig. 21.	Average backcalculated subgrade moduli for low-volume test sections, lane 1.....	85
Fig. 22.	Average backcalculated subgrade moduli for low-volume test sections, lane 4.....	86
Fig. 23.	Average backcalculated subgrade moduli for low-volume test sections, lane 7.....	87
Fig. 24.	Variation of backcalculated post-base subgrade moduli for mainline test sections, lane 1.....	88
Fig. 25.	Variation of backcalculated post-base subgrade moduli for mainline test sections, lane 4.....	89
Fig. 26.	Variation of backcalculated post-base subgrade moduli for mainline test sections, lane 7.....	90
Fig. 27.	Variation of backcalculated post-base subgrade moduli for low-volume test sections, lane 1.....	91
Fig. 28.	Variation of backcalculated post-base subgrade moduli for low-volume test sections, lane 4.....	92
Fig. 29.	Variation of backcalculated post-base subgrade moduli for low-volume test sections, lane 7.....	93
Fig. 30.	Average backcalculated post-base subgrade moduli for mainline test sections, lane 1.....	94
Fig. 31.	Average backcalculated post-base subgrade moduli for mainline test sections, lane 4.....	95

LIST OF FIGURES, CONT.

Fig. 32. Average backcalculated post-base subgrade moduli for mainline test sections, lane 7.	96
Fig. 33. Average backcalculated post-base subgrade moduli for low-volume test sections, lane 1.	97
Fig. 34. Average backcalculated post-base subgrade moduli for low-volume test sections, lane 4.	98
Fig. 35. Average backcalculated post-base subgrade moduli for low-volume test sections, lane 7.	99
Fig. 36. Comparison of backcalculated moduli obtained from pre- and post-base tests on the mainline sections.	100
Fig. 37. Comparison of backcalculated moduli obtained from pre- and post-base tests on the low-volume sections.	101
Fig. 38. Comparison of moduli obtained from homogeneous and multi-layered approaches: 5-year designs.	102
Fig. 39. Comparison of moduli obtained from homogeneous and multi-layered approaches: 10-year designs.	103
Fig. 40. Variation of laboratory soil moisture content obtained during subgrade FWD testing, mainline test sections.	104
Fig. 41. Variation of laboratory soil moisture content obtained during subgrade FWD testing, low-volume test sections.	105
Fig. 42. Variation of laboratory granular base moisture content obtained during base FWD testing, mainline test sections.	106
Fig. 43. Variation of laboratory granular base moisture content obtained during base FWD testing, low-volume test sections.	107
Fig. 44. Effect of saturation level on resilient modulus of thin-walled (undisturbed) samples.	108
Fig. 45. Comparison of resilient moduli and compressive strength of thin-walled (undisturbed) samples.	109
Fig. 46. Distribution of deviator stresses in half-space: normal and principal stress differences.	110
Fig. 47. Variation of backcalculated and laboratory subgrade moduli.	111
Fig. 48. Comparison of backcalculated and thin-walled (undisturbed) laboratory subgrade resilient moduli: average test section data.	112
Fig. 49. Variation of sub-layer penetration index values for the mainline test sections, subgrade testing (right lane).	113
Fig. 50. Variation of sub-layer penetration index values for the mainline test sections, subgrade testing (left lane).	114
Fig. 51. Variation of sub-layer penetration index values for the low-volume test sections, subgrade testing (right lane).	115
Fig. 52. Variation of sub-layer penetration index values for the low-volume test sections, subgrade testing (left lane).	116
Fig. 53. Variation of sub-layer penetration index values for the mainline test sections, base testing (right lane).	117

LIST OF FIGURES, CONT.

Fig. 54. Variation of sub-layer penetration index values for the mainline test sections, base testing (left lane).....	118
Fig. 55. Variation of sub-layer penetration index values for the low-volume test sections, base testing (right lane).....	119
Fig. 56. Variation of sub-layer penetration index values for the low-volume test sections, base testing (left lane).....	120
Fig. 57. Variation of penetration index values and moduli for the mainline test sections, subgrade testing (right lane).....	121
Fig. 58. Variation of penetration index values and moduli for the mainline test sections, subgrade testing (left lane).....	122
Fig. 59. Variation of penetration index values and moduli for the low-volume test sections, subgrade testing (right lane).....	123
Fig. 60. Variation of penetration index values and moduli for the low-volume test sections, subgrade testing (left lane).....	124
Fig. 61. Variation of penetration index values and moduli for the mainline test sections, base testing (right lane).....	125
Fig. 62. Variation of penetration index values and moduli for the mainline test sections, base testing (left lane).....	126
Fig. 63. Variation of penetration index values and moduli for the low-volume test sections, base testing (right lane).....	127
Fig. 64. Variation of penetration index values and moduli for the low-volume test sections, base testing (left lane).....	128
Fig. 65. Comparison of DCP penetration index and backcalculated modulus from subgrade testing.....	129
Fig. 66. Comparison of DCP penetration index and backcalculated modulus from base testing.....	130
Fig. 67. Variograms for subgrade moduli base on log-transformed data.....	131
Fig. 68. Variation of backcalculated and estimated (kriged) moduli with station.....	132
Fig. 69. Comparison of moduli from laboratory data and values estimated at thin-walled locations using kriging.....	133
Fig.70. Contributions of geostatic and load-induced stresses to principal stresses in half-space.....	134
Fig. 71. Backcalculation model configurations.....	135
Fig. 72. Locations of points for subgrade stress calculations.....	138
Fig. 73. Increase in subgrade modulus after construction vs. initial subgrade modulus and pavement thickness.....	141

EXECUTIVE SUMMARY

The Minnesota Department of Transportation recently (1994) completed construction of the Minnesota Road Research Project (Mn/ROAD), a cold regions pavement research facility, on Interstate 94 in central Minnesota. The purpose of the facility is to verify and improve existing pavement design models, to learn more about the factors that affect pavement response and performance, and to develop new pavement models that will make it possible to build and maintain safer, smoother, longer lasting, and more economical roadways.

Many factors affect the structural design of a pavement, including the physical and mechanical characteristics of the subgrade soils and granular base materials. Knowledge of pavement materials characteristics is essential to the design engineer and researcher for rehabilitation and performance prediction.

The study presented in this paper was undertaken to assess the properties of the subgrade soils at the site. Several different methods of sampling were used including retrieval of bulk and undisturbed soil samples, nondestructive deflection testing, and penetration testing.

The purpose of the final report is to present the basic information that has been gathered and analyses that have been completed.

Highly variable deflections from the subgrade and base testing were observed owing to variability in surface condition, soil moisture content, density, and stress-dependent effects. For a given test, a significant increase in backcalculated moduli with increasing sensor offset was noted. This was attributed to nonlinear stress-dependent soil modulus effects. Moduli backcalculated from the deflection testing on the subgrade compared well with laboratory values. A preliminary comparison of penetration index and backcalculated soil modulus was made but the results did not show a correlation.

The effects of construction on the observed subgrade and base moduli were analyzed. In most cases, increases in the moduli after each step of construction were observed. On the basis of the analyses conducted, it is reasonable to conclude the following:

- The variability studies suggest that, at least for the embankment at Mn/ROAD, a relatively large amount of deflection variability can be expected even at short testing intervals.
- Within the variability encountered, the backcalculated and laboratory moduli compared well, but moisture and density differences must be reconciled.
- The surface condition of the soil had a noticeable impact upon the variability of the measured deflections, especially at the inner sensor locations.

- Over the range of moisture contents observed in the undisturbed specimens, the degree of saturation had little impact on the laboratory resilient modulus.
- The multi-layered backcalculation approach did not provide any advantage in interpreting falling-weight deflectometer (FWD) deflections from pre-base subgrade testing relative to the homogeneous approach.
- For the majority of the sections, the post-base subgrade modulus increased relative to before base construction. This was not always accompanied by a decrease in the deviator stresses, as would be expected.
- For all conventional flexible sections, the subgrade modulus did increase when going from base to pavement construction. This was accompanied by a uniform *increase* in the deviator stress, not a *decrease* as would be expected.
- Overall, the apparent subgrade modulus did increase after pavement construction, relative to pre-base construction. Sections with initially lower average subgrade moduli showed the greatest increase after construction. Also, sections with the largest total pavement thickness showed the greatest relative modulus increase, while sections with the lowest total pavement thickness showed the least relative modulus increase.
- Overall increases in the subgrade moduli from pre- and post-construction tests on the permeable asphalt-stabilized base (PASB) sections were observed. These increases in moduli were accompanied by decreases in the calculated deviator stresses.
- For the aggregate and chip-seal sections, the increase in modulus in each section, on average, was accompanied by a decrease in the deviator stress.
- The effects of changes in bulk modulus stress state in the granular materials on observed moduli were investigated. No trend could be established.

The results of the laboratory and field testing can be used as a baseline for future analysis of test section pavement response modeling and prediction. Further research should address the following points:

- Effects of moisture and density on observed subgrade FWD deflections and moduli
 - A large number of moisture contents were taken from various depths at selected FWD testing stations. Moisture information is abundant and density data are sparse. A method is needed to determine the degree of saturation in a situation like this.
- Effects of moisture and density on DCP penetration index
- Further exploration of possible relationships between penetration index and deflection data
- Statistical analysis of variance on moduli from the following subsets of data:
 1. Five-year versus 10-year versus low-volume road (LVR) designs
 2. Pre-base versus post-base versus post-pavement testing
 3. Sections with base versus sections without base

- **Effects of moisture on post-base backcalculated moduli**

A detailed multi-layered backcalculation of post-base testing has been completed. The results of the granular base resilient modulus tests should be compared to the in situ modulus values. Incorporate in situ moisture content data from samples taken during post-base testing to assess the effects of moisture. Determine the relationship between gravimetric, post-base moisture content and the moisture state after paving (volumetric, post-construction time domain reflectometer (TDR)).

- **Stress-dependency effects**

A backcalculation analysis of selected post-paving deflection data has been done and a preliminary, quantitative description of stress-dependency effects has been presented. The conclusions from these results need to be formalized.

- **Effects of soil embankment cut depth on observed subgrade deflections.**

CHAPTER 1

INTRODUCTION

Background

In 1994, the Minnesota Department of Transportation completed construction of the Minnesota Road Research Project (Mn/ROAD), a cold regions pavement research facility, on Interstate 94 in central Minnesota. The facility consists of forty 150 m pavement test sections. Twenty-three of these test sections are being loaded with existing freeway traffic and the remainder are being loaded with calibrated trucks. Over 4000 sensors embedded in the roadway collect pavement response data throughout the year. The purpose of the facility is to learn more about the factors that affect pavement response and performance, to verify and improve existing pavement design models, and to develop new pavement models that will allow us to build and maintain safer, smoother, longer lasting, and more economical roadways.

Many factors affect the structural design of a pavement, including the physical and mechanical characteristics of the subgrade soils. The study presented in this paper was undertaken to assess the properties of the subgrade soils at the site.

Objectives

The objectives of this study were to arrive at an a) initial assessment of the magnitude and variability of the subgrade properties at the facility, b) to compare two different methods of resilient modulus determination, and c) to discern the changes in the resilient modulus as the layers of the pavement structure were constructed.

The property that is of primary interest is the resilient modulus of the subgrade soil, a parameter that is used in pavement design. Since the performance of the individual test sections may be influenced by the resilient modulus of the subgrade soils, it is important to have a sound understanding of how this parameter varies along the pavement embankment. The properties were determined by nondestructive test methods as well as analysis of disturbed and undisturbed soil samples.

The main focus in the final report is to present all available data. Analyses related to subgrade falling-weight deflectometer (FWD) data backcalculation, laboratory soils data analyses, granular base and pavement FWD testing backcalculation of base and subgrade moduli, and construction effects are presented here. At the time of publication several major tasks were

incomplete: (1) laboratory testing of all granular base and subbase materials and (2) entry of data into the Mn/ROAD database. It was decided that most of the analysis would be much easier to perform once all laboratory testing was complete and data were verified and entered into the database. A detailed list of recommendations for further analysis will be presented in the conclusions and recommendations section of this report.

Scope

Mn/ROAD is located in east-central Minnesota on I-94 (see Fig. 1) The facility is divided into high and low traffic volume experiments. The high volume mainline experiment consists of 23 different test sections and is open to public and commercial traffic. The low volume experiment is a closed test track constructed of 17 different sections with two turnaround loops. Diagrams of the pavement layers in each cell are shown in Fig. 2.

Native soils at the site are primarily silty clay. The existing topography was up to 5 m above the elevation of the planned subgrade excavation. The depth of subgrade excavation below the top of the constructed (pavement) surface was 1.5 m for the sections which were built on native soils. Four sections were constructed on sand fill with a 2 m deep subgrade excavation. A detailed discussion of the experimental design of the facility is given by Newcomb *et al.* (1).

The subgrade testing procedures discussed in this paper marked the beginning of the material sampling and testing program at the facility. Falling-weight deflectometer (FWD) tests were conducted at regularly spaced intervals along the embankment. About half of the 40 test sections were tested during fall of 1991 while the remaining sections were finished in early summer of 1992. Disturbed and undisturbed soil samples were retrieved from selected locations within each section on the same day as the FWD testing. In addition to the subgrade survey, FWD testing was conducted on the granular base, granular subbase, and permeable asphalt-stabilized base (PASB) as they were constructed for each section. These tests began in 1992 and were completed in 1993. The data were analyzed and compared to the subgrade data to assess the effects of construction. Since the time paving was completed, the sections have been tested numerous times with the FWD. Representative pavement deflection data from these tests were selected for comparison to the subgrade data to provide a further indication of the effects of construction.

These current data are important to future data analysis at Mn/ROAD in that the baseline values (*e.g.*, resilient modulus, moisture content, and dynamic cone penetrometer (DCP) penetration index) obtained in this study will be used with future pavement response and performance data.

There are several appendices to this report that can be obtained from the Mn/ROAD office at the Minnesota Department of Transportation. These appendices contain information on subgrade and base FWD testing documentation, subgrade and base soils sampling and testing, tabulated backcalculation results, and a summary of DCP testing.

CHAPTER 2

PREVIOUS WORK

Although the focus in this report is on the analysis of FWD data, a brief review of other site surveys is included here. Previous studies of laboratory and in situ property correlation have focused on comparisons of moduli determined by field (backcalculated) and laboratory (resilient modulus) methods. The problem with this sort of approach lies in the fact that soil samples with vastly different volumes are being compared. For example, in the thin-wall sampling method, the volume of soil sampled is very small relative to the volume sampled by the FWD (2).

Newcomb (3) and Lee *et al.* (4) performed FWD tests on existing pavements in Washington. Each 300 m long test section was tested using the FWD at 15 m intervals. Disturbed soil samples were retrieved from the shoulders of these pavements and re-compacted in the laboratory. The data from this study indicated that the means of the field and laboratory values compared well. Janoo and Berg (5) conducted tests directly on a clay layer prepared in a concrete test pit. This study indicated that the center FWD sensor (D_0) sensor reading exhibited a higher degree of variability relative to the other sensors and oftentimes gave values which exceeded the 2 mm range of the sensors. Houston and Perera (6) conducted a series of tests at 20 different pavement sites. At each site, FWD tests were sampled at 3 m intervals over a 28 m section of the pavement. They concluded that most of the variability in the deflections within a section were due to variability in the subgrade materials and that these variations occurred over distances less than 28 m for the structures tested. They also stated that the variability was mostly contained within the native (basement) foundation soils and not in the engineered (compacted) soils. Houston *et al.* (2) discussed the problem of volume size contrast and suggested that it is only exacerbated by the usual sample retrieval procedures of taking material from the upper 300 to 600 mm of the subgrade. They also suggested a remedy to the sampling volume problem that involves retrieving between 6 and 10 samples from the soil in the vicinity of an FWD station. While this approach may address the volume-variability relationship it seems impractical to employ in a large-scale field test.

CHAPTER 3

SUBGRADE TESTING PROCEDURES

FWD Testing

Dynatest Model 8000 machines were used for the FWD testing discussed in this report. During the fall 1991 test series only one machine was used while in 1992 and 1993 two machines were used due to time constraints. The testing pattern for each section was originally designed for a series of 9 test stations located longitudinally at 15 m intervals along three different transverse offsets. These offset lines were situated along the roadway centerline and at 3 m to either side, *i.e.*, the anticipated outer wheel paths of the two lanes. At the beginning of the 1992 tests, the sampling plan was changed to add one more test point per test section.

A large diameter (450 mm) plate was used for all of the tests and velocity sensors were located at the center of the plate (0 mm) and at offsets of 300, 450, 600, 900, 1350, and 1800 mm from the center. The loading patterns for the 1992 tests differed slightly from those used in 1991. In 1991 three seating loads plus three load drops each at three different drop heights were used. The maximum loads ranged from 12-25 kN. The drop height was increased for each successive set. The loading pattern was changed slightly for 1992 and 1993 to include four seating drops plus three load drops from three heights in progressive order. In addition to the original nine drops, data from the seating drops were stored in the data file. This was done in order to address the effects the seating load drops and load repetitions had on sensor deflections. Similar load levels were used for each series of tests.

A complete tabulation of all testing that was conducted on the subgrade is given at the end of Appendix A. Details on test section, lane, date, machine, and stations tested are included. The first table lists information from the original data files. The second gives basically the same information with corrections. These corrections address the following:

- On the very first day of testing (23-Sep-91) the operator entered stations numbered 1 through 9. The data files were changed to reflect the actual project stationing.
- During most of 1991, the stations were entered with a "+" separating the station and offset. This character presented a problem for some of the backcalculation software which did not read non-numeric characters. All "+" separators were deleted from those data files.

- It was not always possible to test every planned station in a test section. The second table reflects this in that stations that were skipped are blank.

Note that these changes were made only to data files possessed by the authors of this report. These changes may not necessarily have been made in the data that was entered into the Mn/ROAD database.

Procedures for base course testing were essentially identical to those used for subgrade testing. This testing was started during late summer 1992 just prior to construction of the 5-year pavement test sections. A complete tabulation of all testing that was conducted on the base is given at the end of Appendix B. Details on test section, lane, date, machine, and stations tested are included. Again, the first table lists information from the original data files and the second gives the same information with corrections.

When feasible, each test site was inspected prior to loading and the visual appearance of the surface was noted. In cases where the station was unsuitable for testing due to loose surface material, wheel ruts, or other surface irregularities, attempts were made to remedy the situation. In most cases, the preparation work amounted to clearing loose material with a shovel or filling in divots. In some cases the surface appeared to be uniform but out-of-range deflections resulted after a few load drops. This was most likely due to a thin layer of highly compressible soil or material that was perhaps saturated at some depth. In these cases, the test station was shifted forward or backward 1 to 2 m and the test was repeated. If the test was not successful at this point, the test site was abandoned.

Soil Sampling

The primary objective of the accompanying soil sampling program was to obtain the physical parameters that are useful in interpreting the mechanical properties of the soil. Since the silty-clay subgrade is quite moisture-sensitive it is important to have an estimate of the soil moisture and in-place density at selected stations along the embankment.

During the FWD testing small jar samples were retrieved from three different locations within each section. Two of the samples were taken at two different locations from the upper 0.3 m of the subgrade while at the third location three samples were taken from depths down to 1 m. These samples were used to determine the *in situ* moisture content of the soil.

Disturbed bag samples obtained from auger borings were also retrieved from selected locations within each section. Several different tests were conducted on these samples including Atterberg limits (AASHTO T 90), sieve and hydrometer analyses (AASHTO T 88), Proctor density tests (AASHTO T 99 and T 180), and stabilometer (R-value) tests. Undisturbed samples were retrieved using thin-walled tubes from depths ranging from 300 mm to over 2 m.

Gravimetric analyses and unconfined compression tests (AASHTO T 208) were performed on these samples. Resilient modulus tests (SHRP Protocol P 46) were also conducted, but with the following two differences relative to the SHRP Protocol: (1) specimens were compacted using a Proctor hammer and (2) the load cell used in the apparatus was located inside the triaxial vessel. Data from the soil sampling and testing program are tabulated in Appendix C.

Dynamic Cone Penetrometer (DCP) Testing

The dynamic cone penetrometer (DCP) is a device that is commonly used during geotechnical site investigations. The device consists essentially of a narrow rod with a conic tip at one end. A mass is dropped from a specified height onto the top of the rod and the penetration of the tip into the soil embankment is recorded as the number of blows progresses. Portable DCP devices generally have total depths of penetration of about 1 m. The penetration index (mm/Blow) is calculated as the average amount of penetration per hammer blow and is a rough measure of the soil shear strength. Various correlation models exist for estimating soil shear strength or modulus from the penetration index profile. A thorough review of the use of the DCP in pavement engineering field research and as used by Mn/DOT is given in (7).

Penetration tests of both the subgrade and base were conducted using a DCP. The scheme for DCP testing consisted of testing at 30 m intervals at two different transverse offsets along the embankment. DCP testing on a given section was generally performed within 1 to 2 days of the FWD testing.

CHAPTER 4

ANALYSIS

Deflection Data Validation

During the course of this study, several techniques were used to analyze and interpret the data. The first part of the analysis approach involved the validation of deflection data. In essence, this procedure involved investigating the basins and verifying that they were sensible. A statistical analysis of the deflection data from each section was also useful in establishing spatial correlation and trend of the data as well as detecting outlying values that may be suspect due to considerations discussed shortly.

The first focus was on detecting erroneous data. By inspecting the deflection basins and identifying sets with (1) extremely large deflection values, (2) negative slopes, or (3) null deflections, it was possible to sort out basins unsuitable for analysis. With respect to item (1), excessively large deflections were observed under the plate (D_0) sensor. This was presumably due to the variable nature of the soil surface with conditions of either a soft layer or brittle crust present at the surface that would lead to inelastic deformation (*e.g.*, compaction or punching). Item (2) refers to basins in which an outer sensor yielded a deflection value higher than its interior neighbor. Occurrences of item (3) may have occurred when the sensor was either resting on a piece of debris or otherwise not properly seated with the soil surface.

Several special tests were conducted to investigate the repeatability of the FWD deflection sensor responses. In the first set of tests, the outer wheel path of sections TS 6 and TS 7 were retested at the original locations about 48 hours after the original tests. These sections were selected due to the fact that the surface appearance was very smooth and uniform relative to the other sections. The deflection readings from each of the two series of tests were normalized to a uniform load intensity of 100 kPa and plotted against one another on a scatter chart. Results from TS 6 showing the comparison between the two sets of D_0 , D_{600} , and D_{1800} sensor readings are given in Fig. 3-5, respectively. Scatter due to variability in FWD load-plate placement, soil moisture, and load level is evident. The coefficient of determination (R^2) values for the sensor reading correlations were 0.87, 0.81, and 0.68 for the D_0 , D_{600} , and D_{1800} pairings, respectively. Correlation coefficients for these pairings were 0.93, 0.90, and 0.82, respectively, indicating a fairly strong positive correlation. Note that, while the higher R^2 value for the D_0 sensor indicates a higher correlation, there is a significant offset in the No. 2 series of data relative to No. 1. For the D_{600} sensor (see Fig. 4), the correlation is better except for one cluster of data points which

represent a single station. The results for the D_{1800} sensor (see Fig. 5) appear much more evenly distributed. Normally, one would expect a positive relationship between adjacent deflections as a function of load (with all other variables held constant); the apparent negative relationship shown between the D_{1800} and D_{600} sensors in Fig. 6 is peculiar and is most likely due to the effects of the two outlying data points. The main cluster of data in Fig. 6 displays a positive relationship as expected. A similar analysis was conducted for TS 7. Results from TS 7 showing the comparison between the two sets of D_0 , D_{600} , and D_{1800} sensor readings are given in Fig. 7-10, respectively.

The scatter in the D_0 sensor comparison is thought to be due to placement of the FWD which would obviously affect the plate contact and sensor location. Also, during the period between the two tests, the weather conditions were sunny and windy, which would allow for drying, especially near the surface, thus changing the soil properties. However, the effects of soil drying should be less for the D_{1800} sensor than for the D_0 sensor since greater offsets from the loading plate correspond to responses from deeper in the structure. Thus, scatter observed in the D_{1800} readings for these tests was probably due to poor sensor-soil contact. These data verify that there is a high degree of deflection variability to be expected in tests conducted directly on soil surfaces. This is due to the variable nature of the surface, *i.e.*, nonuniform features such as ruts and loose compressible surface material, moisture content and density variations, and stress-dependent effects.

Another series of tests was conducted in which TS 3 and 4 were retested using the normal 15 m spacing but with additional tests conducted within the sections on a close-set grid. In these additional tests, the FWD plate was positioned at nine different stations within a 3.7 m square, forming a grid size of 1.85 m. Summary statistics from these data sets are shown in Table 1. For the most part, the variability in the sensor deflections is consistently smaller for the cluster test, as would be expected. This is due to the fact that at small separation distances, the subgrade properties do not vary as much relative to larger distances. However, even at the short separation distance, the coefficient of variation (CV) of the deflections ranges from 18 to 35 percent. Again, these variations are attributable to both spatial changes in the soil parameters as well as test variability due to surface effects.

The variability study was repeated in TS 3 and 4 after the construction of the base layer. Since TS 4 is a full-depth section, it was essentially unchanged since the previous test save for variances in grade elevation and surface grading. The summary statistics from these tests are presented in Table 2. Note the significant decrease in the central deflections for TS 3 due to the increased strength afforded by the granular base.

The effects of the seating drops and load repetition were addressed by investigating the change in deflections with successive load applications at a given test station for all of the subgrade FWD test data. Each sensor deflection was normalized to a standard load. Significant

variations in readings from the two innermost sensors occurred. In some cases an increase in normalized deflection for these sensors was observed while in others a decrease was noted. No trend could be established.

Homogeneous Backcalculation Analysis

The first step in the backcalculation analysis was to assume a homogeneous soil mass. The moduli of the soil can be estimated from the load and deflection data using the Boussinesq solution for a uniformly distributed load on the surface of an isotropic, elastic half-space (8). The surface deflection of the half-space due to a uniformly distributed circular load is given by the following equation:

$$w = \begin{cases} \frac{2(1-\nu^2)qa}{E} & (r=0) \\ \frac{4(1-\nu^2)qr}{\pi E} \left[\int_0^{\frac{\pi}{2}} \sqrt{1-\frac{a^2}{r^2} \sin^2 \theta} d\theta - \left(1-\frac{a^2}{r^2}\right) \int_0^{\frac{\pi}{2}} \frac{d\theta}{\sqrt{1-a^2/r^2 \sin^2 \theta}} \right] & (r>a) \end{cases} \quad (\text{Eq. 1})$$

where

- w = vertical deflection
- θ = integration variable
- r = radial offset from center of loaded area
- ν = Poisson's ratio
- a = radius of loaded area
- q = applied pressure
- E = Young's modulus of material

The integrals in the second part of Eq. 1 were evaluated analytically using special functions presented in Abramowitz and Stegun (9). In essence, the vertical deflection at the surface of the half-space can be represented by Eq. 2:

$$w = \frac{q}{E} r f(r) \quad (\text{Eq. 2})$$

where

$$f(0) = 2(1-\nu^2)a$$

$$f(r) = \frac{4(1-\nu^2)}{\pi} \left[\int_0^{\frac{\pi}{2}} \sqrt{1-\frac{a^2}{r^2} \sin^2 \theta} d\theta - \left(1-\frac{a^2}{r^2}\right) \int_0^{\frac{\pi}{2}} \frac{d\theta}{\sqrt{1-a^2/r^2 \sin^2 \theta}} \right] \quad (r>a)$$

Values for the function $f(r)$ are tabulated in Table 3 for a range of offsets (r/a) and several values of Poisson's ratio.

It is important to address the differences between the test conditions and the assumed model. Key deviations from the assumptions implicit to the theory of elasticity are as follows:

1. Imperfect sensor contact may cause erroneous deflection measurements.
2. Imperfect plate contact may produce a nonuniform surface pressure distribution.
3. The effects of repeated FWD load drops on the subgrade soil may change the properties of the soil near the plate.
4. FWD tests are quasi-dynamic by nature while the backcalculation analysis is based upon static elasticity.
5. Deformations may not be reversible.
6. The soil response may be stress-dependent.

Item (1) above is a consequence of the surface condition, *e.g.*, the presence of ruts, desiccation cracks, and loose material. These conditions can presumably result in zero deflections or negative slopes as discussed above, and such data were excluded from the analysis. Items (2) and (3) are also due to surface conditions but it was assumed that the effects of nonuniform plate contact were local, *i.e.*, they were negligible at some distance away from the plate. Also, the observed changes in normalized deflections of the outer sensors with load repetition were small compared to those of the innermost sensors. Item (4) cannot be accounted for in the analysis and induces a systematic error in the backcalculated moduli which cannot be determined. Item (5) also cannot be accounted for with the linear elastic analysis that is presented in this paper. As a consequence of the above considerations, it is believed that the deflections measured by the innermost sensors (especially D_0 and D_{300}) were influenced by surface irregularities to a greater degree than the outer sensors. Item (6) is commonly observed in laboratory tests. This type of response cannot be modeled directly using linear elastic theory but is usually evident through an observed change in backcalculated modulus with load level and depth.

All deflection data were first analyzed using the homogenous half-space model; the equations given above were implemented in a computer program that reads the raw FWD data files directly. The backcalculated modulus for each testing station was summarized for a surface pressure intensity of 100 kPa. This was done by conducting a regression analysis of backcalculated modulus versus load for each testing station. The resulting relationship was used to determine the modulus for a surface pressure of 100 kPa. These results are tabulated in Appendix D.

If the embankment were perfectly homogenous and not stress-dependent, the moduli values backcalculated from sensor deflections at different offsets would be identical. In reality, a variation in the backcalculated modulus with offset was observed. This implies that the modulus changes with depth due to the combined effects of non-homogeneity (moisture content and density variations) and stress-dependency. Typical examples are shown in Fig. 11 with modulus profiles from two sections (TS 10 and 24). The sand-fill section (TS 24) shows a series of fairly

uniform backcalculated modulus values for all sensor offsets while for the silty-clay section (TS 10) this is not true. This difference is primarily due to the effects of stress-dependency on the silty-clay material.

The variations in backcalculated moduli with station for all test sections are shown in Fig. 12-17. Average moduli for each test section are shown in Fig. 18-23. A similar set of plots for the variations in moduli with station and average test section moduli from the post-base testing are shown in Fig. 24-29 and Fig. 30-35, respectively.

Note that test sections 24 and 25 (station 160+00 to 180+00) in the South loop and 36 and 37 (station 80+00 to 90+00) in the North loop were constructed over approximately 2 m of granular fill. In addition, sections 24, 36, and 37 all have a granular base layer which was constructed and bladed shortly before testing. Apparently the moduli for these sections are less variable as indicated by the more consistent deflections. This is attributable to the smoother surface condition in these sections relative to the regular sections. It may also suggest that the sand fill is more homogeneous than the native soil.

A comparison of backcalculated moduli from tests conducted before and after base construction are shown in Fig. 36 and 37. The values in these graphs represent moduli backcalculated from the D_{1800} sensor. This figure shows that for most of the test sections there was an apparent increase in the backcalculated moduli. One would expect this due to stress-dependent effects. The added stiffness of the granular material serves to decrease the stresses in the soil beneath it. A more detailed analysis of this problem will be covered in a later section of this chapter.

Static Multi-Layered Backcalculation Analysis

The load and deflection data were also used as input in a multi-layered backcalculation program to arrive at estimates of the soil properties for an assumed structure. The program CLEVERCALC 3.5 was used for the backcalculation. CLEVERCALC is a derivative version of EVERCALC developed in the state of Washington (10). It utilizes metric units and includes other research-oriented features. The program is based on the CHEVRON linear elastic layer analysis program and the iteration process stops if one of the following occurs:

1. The mean root-mean-square of the relative difference between measured and backcalculated reading is less than a given value.
2. The combined change of modulus for all layers from one iteration to the next is less than a given value.
3. The maximum number of given iterations has been reached.

The purpose of the first criterion is obvious: If the match is near perfect, the search is stopped. The difference between the two basins is referred to as the *deflection error*. It is expressed as the root-mean-square (RMS) deviation.

The second criterion requires some explanation. The program bases the adjusted moduli on the effect a change in the logarithm of the modulus has on the deflection error. This is expressed as a slope, and a slope is determined for each unknown layer. A steep slope will lead to a quick solution, but a shallow slope may take longer or even lead to non-convergence. Further, the resolution of the sensors may not be adequate to reach the stipulated RMS-criterion. In addition, the shortcomings of the linear elastic model, faulty assumption of layer thicknesses, or both, may deter a perfect match of the basins. Thus, when the change of modulus is small for each layer, the program is unable to arrive at a better match anyway and the iteration procedure stops. Such basins should always be checked critically, but may be accepted if the deviation from the measured basin is not too large.

The purpose of the last criterion is as obvious as the first, and it is needed for practical reasons. The criteria used in the present study was an RMS tolerance of one percent, a change of modulus of one percent, and a maximum of 10 iterations.

As the stiffness of the subgrade may vary with depth, a three-layer system was assumed for the subgrade structure. Initial attempts with a two-layer system yielded high RMS values. This was due to difficulties in fitting measured basins with only two layer parameters. In backcalculation analysis, an important assumption is the selection of layer thicknesses. The approach taken in this analysis was to choose a reasonable set of thicknesses and perform backcalculations from deflection basins at representative test stations. Preliminary calculations were performed by assuming a thickness of either 150 or 250 mm for layer one (the top layer), and varying the thickness of layer two from 50 to 600 mm. These thicknesses are believed to be reasonable, as they are on the order of the thicknesses of the lifts used in constructing the embankment. It was found that the backcalculated moduli of the second layer were highly sensitive to thickness ratios (H_1/H_2) greater than about 0.3, regardless of the thickness of layer one. Ultimately, the backcalculations were performed for data from all tests using thicknesses of 150 mm and 450 mm for layers one and two, respectively. Poisson's ratio was assumed to be 0.4 for all three layers.

Since in a multi-layered system the modulus backcalculated for layer one is dependent on the inner sensor deflections, it could be expected that the modulus value for this layer may be erroneous due to the departures from the theory as noted in the section above. The technique adopted in this analysis was to exclude the two innermost sensors (D_0 and D_{300}) from the backcalculation. Thus, the moduli backcalculated for layer one, while essential to the calculation, are not used in the analysis of the resulting moduli. Only the final drop from each drop height was

used for backcalculation; the others were used to monitor seating effects. It was noted that a large percentage of the basins failing the validation criterion discussed above yielded RMS values greater than 15 percent and the values of these moduli were exceedingly large. As such, these stations were excluded from any subsequent analysis.

Comparisons of moduli obtained from the two different approaches are shown in Fig. 38 and Fig. 39 for the mainline 5-year and 10-year designs, respectively. For the multi-layered approach, only backcalculated moduli for layer three were considered for this comparison due to the surface effects on measured deflections; for the homogeneous approach, the moduli obtained from the D_{1800} sensor were used. The comparisons for both sets of data are good, especially the 5-year sections. The reason for the larger amount of scatter in the 10-year sections is not known.

At this point it seems reasonable to conclude that the multi-layered backcalculation approach does not provide any advantage in interpreting FWD deflections from subgrade testing relative to the homogeneous approach.

Analysis of Laboratory Data

A complete tabulation of soils data from bag, jar, and thin-walled specimens can be found in Appendix C. The data from the thin-walled specimens are summarized in Table 4. Data from the bag samples are summarized in Table 5. The test procedures used for determination of the soil resilient modulus were in accordance with SHRP Protocol P 46. A regression analysis of the data from each test was performed to determine the constants to be used in Eq. 3:

$$M_R = K_1 \sigma_d^{K_2} \quad (\text{Eq. 3})$$

where

M_R = resilient modulus

K_1, K_2 = material constants

σ_d = deviator stress

For all tests, the constant K_2 was found to be negative. This is to be expected since fine-grained soils normally exhibit a decrease in modulus for increasing σ_d . In both tables, the values shown for the resilient modulus were obtained from the laboratory $M_R - \sigma_d$ regression relationship. A value of 0.8 kPa was assumed for σ_d . The significance of this value will be discussed in detail in the following section.

The spatial variation of moisture contents obtained from the FWD jar samples for the mainline and low-volume test sections are shown in Fig. 40 and 41, respectively. The variation of moisture contents for FWD tests taken during the base testing are shown in Fig. 42 and 43.

Other researchers have investigated the correlation between resilient moduli and various soil parameters such as degree of saturation (11). The effect of the degree of saturation on the laboratory resilient modulus was investigated. This is shown in Fig. 44. Over the range of degree of saturation observed (85-105 percent) no significant effects can be seen. A graph of resilient modulus versus the unconfined compressive strength is shown in Fig. 45. This plot shows a fair correlation between the two parameters. One might expect to see a correlation between a measure of soil strength and the resilient modulus, mainly because these parameters both depend on other factors that influence the stability of the soil, such as density and moisture content.

Comparison of Field and Laboratory Data

When comparing field and laboratory resilient modulus data, it is necessary to reconcile the differences in the testing conditions between the two cases. For a given soil type, the primary factors affecting the resilient modulus are moisture content and density.

The laboratory resilient modulus test is a test that attempts to simulate the response of an element of soil material with principal stresses acting on it. To estimate the field resilient modulus of fine-grained soils using the laboratory regression relationship, a deviator stress must be selected. One may compute a stress difference at a certain location within the structure, but care must be taken to use a value that reflects the inherent assumption of principal stresses. The usual practice of using normal stresses may lead to problems since away from the vertical axis of the load, shear stresses will usually be present. In addition to this, the normal stress differences may become negative within a zone beneath the load. This is depicted in Fig. 46 in which vertical deviatoric stress profiles are shown for a range of radial offsets. At the center of the plate ($r/a = 0$), the normal stress difference $\sigma_d = \sigma_z - \sigma_r$ is positive, but for other values of r/a , the normal stress difference is negative at some point. In this case, the laboratory relationship becomes useless and defies interpretation, because σ_d in an equation of the form $M_R = K_1 \sigma_d^{K_2}$ cannot be negative. The rational alternative would be to use the principal stress difference $\sigma_d = \sigma_1 - \sigma_3$, since this is in agreement with the assumptions made in the resilient modulus test and because it is always positive. The deviator stress used to compute resilient moduli from the laboratory relationships in this report was taken to be the principal stress difference at a point 900 mm beneath the D₁₈₀₀ sensor. Using the WES5 program (12), the calculated deviator stress $\sigma_d = \sigma_1 - \sigma_3$ at this point due to a 100 kPa surface pressure was 0.8 kPa .

A comparison of the homogeneous backcalculated moduli and laboratory moduli is shown in Fig. 47. Backcalculated subgrade moduli from the subgrade and base testing are denoted as pre-base and post-base, respectively. A direct comparison of the laboratory and field data is not possible without utilizing some sort of interpolation technique such as kriging (13), because FWD

tests and thin-walled samples were not conducted at exactly the same points. This issue will be addressed in a later section of this chapter. A dramatic increase in the backcalculated moduli after construction of the base layer is apparent. However, the data in Fig. 47 suggest a fair, but far from strong correlation. This is apparent in Fig. 48 in which the average lab and field moduli are compared. The backcalculated values represent moduli computed from the D_{1800} sensor deflection referenced to a surface pressure of 100 kPa. The laboratory moduli reflect the assumption that $\sigma_d = 0.8$ kPa. It appears that the lab values are consistently smaller than the backcalculated values. This discrepancy may be due to either (1) the natural variation of moisture and density in the test section that has not been reconciled or (2) the deviator stress selected for laboratory moduli. To address item (1), a relationship between the backcalculated moduli and *in situ* degree of saturation (S) could be used to adjust the data to an arbitrary reference saturation. In order to compute S it would be necessary to have detailed information of the *in situ* density and moisture content profile at as many FWD test stations as possible. However, only the moisture content profile was determined at selected FWD test stations. Summary statistics broken down by test section and facility subsection for pre-base subgrade and laboratory moduli are shown in Table 6.

Penetration Index

The presentation of the DCP data in this report will be limited to graphs showing the spatial variation and a preliminary correlation analysis between backcalculated moduli and penetration index. In order to summarize the data, the average penetration index at four different depth increments was computed for each test station. The total possible penetration of the device is about 1 m, so layers of 0.25 m were selected. A summary of the tests conducted and sub-layer averages are tabulated in Appendix E. The variation of penetration index with station for the subgrade and base testing are shown in Fig. 49-52 and Fig. 53-56, respectively. A comparison of backcalculated moduli and DCP penetration index for the subgrade and base testing are shown in Fig. 57-60 and Fig. 61-64, respectively. The moduli represent values computed from the D_{1800} sensor; the penetration index values shown in these graphs are the average penetrations from depths beneath 0.75 m.

As alluded to earlier, one might expect to see a relationship between soil stiffness and strength (see Fig. 45) although the two are not directly related. For the sake of comparison, average moduli from several offsets and penetration index values for each test section are shown in Table 7. A correlation analysis was performed on these data. The pairings showing the highest degree of correlation for the whole set were D_{300} versus 250-500 mm and D_{600} versus 750-1000 mm; the data are plotted in Fig. 65. For the base testing, the best pairings were D_{300} versus

500-750 mm and D_{600} versus 750-1000 mm; these data are plotted in Fig. 66. The R^2 value was less than 0.6 for both comparisons, indicating a poor relationship. A log-log regression calculation was performed but this did not improve the fit. The poor fit is most likely due to the fact that the DCP test is destructive in nature and the penetration index is a measure of the shear strength of the soil. By contrast, the FWD test and subsequent backcalculated resilient moduli are nondestructive in nature. While both backcalculated modulus and penetration index are likely affected by the same soil parameters, *e.g.*, density and moisture content, the assumption that there is a relationship between the two is questionable.

Geostatistical Analysis

The spatial correlation of the data were investigated using geostatistics and are expressed in the form of a variogram. A variogram expresses the variance of the sample data as a function of separation distance. A discussion of geostatistics and its potential application to pavement design are given in (13).

The experimental variograms for the log-transformed moduli of the D_{600} and D_{1800} moduli from lane one of the mainline test sections are shown in Fig. 67. The variogram is the variance of the transformed backcalculated resilient moduli values. By itself this relationship is of little use, but it is essential for an interpolation analysis such as kriging.

Another comparison between the backcalculated and laboratory moduli was attempted using kriging. The variogram for the D_{1800} moduli in Fig. 67 was used to model the raw data set in order to obtain estimates of the backcalculated modulus at the points where thin-walled specimens were taken. The program used for this analysis was GEOEAS, which is available as public domain (14). A comparison of the kriged and backcalculated values is shown in Fig. 68. It can be seen that in effect, kriging smoothes the data. The kriged moduli obtained from this analysis are plotted against the laboratory modulus values in Fig. 69. This comparison appears slightly better than the one obtained from the average test section data (see Fig. 48). Again, the relationship would undoubtedly improve if the effects of moisture and density variation could be reconciled.

Effects of Construction on Subgrade Stress and Modulus

In a previous section, subgrade modulus calculations were made using the homogeneous model from deflection data obtained before and after base construction. Those results showed that base construction resulted in an increase in the subgrade modulus, at least for the outer (D_{1350}

and D_{1800}) sensors. A subsequent analysis was undertaken to arrive at a more quantitative assessment of the subgrade stress and modulus changes due to granular base construction.

In this section, data from before and after base construction, and after pavement construction will be compared to assess the effects of layer construction on the calculated subgrade modulus. In addition, the effects of changes in the estimated bulk stress in granular base layers from before and after pavement construction will be investigated.

Stress Calculations

All stresses were computed using a Cartesian coordinate system (see Fig. 70). In general, away from the axis of symmetry of a loaded half-space, the axis of major principal stress will not be aligned with the vertical coordinate axis. For this analysis, the effects of overburden on principal stress differences will be considered, as shown in Fig. 70. Principal stresses from geostatic and load-induced stress states cannot be added directly; it is necessary to sum the Cartesian stresses first, and then compute principal stresses.

For all the stress calculations, the geostatic stresses were estimated by assuming uniform bulk densities for the various materials. For unbound materials, (subgrade and granular base) a bulk density of 2100 kg/m^3 was assumed. This was determined to be the average bulk density of all thin-walled subgrade samples and was also fairly close to the available data for the granular base and subbase materials. For all asphalt concrete material, the bulk density was assumed to be 2300 kg/m^3 . A value of 0.5 was assumed for the ratio of horizontal to vertical pressure.

A multi-layer backcalculation analysis was performed to estimate layer moduli from most of the granular base FWD data, as well as all PASB, flexible pavement, aggregate, and chip-seal FWD data (see Fig. 71). Specifics of these analyses are given in the following sections. The backcalculated moduli were used as input to the computer program WES5 in order to calculate the load-induced stresses (12). Then, the total deviator stresses for selected FWD data on granular base, PASB, aggregate, and flexible pavement surfaces were computed at two different points for comparison with moduli from two different offsets (see Fig. 72). The specific locations selected for stress calculations were based on (1) type of surface being tested and (2) FWD sensor configuration. The total deviator stress was calculated by (1) adding corresponding geostatic and normal load-induced stress components, (2) computing the principal stresses, and (3) taking the difference between the major and minor principal stresses.

Bulk stresses in the granular base layers were also forward-calculated using WES5. This was done only for those FWD tests (before and after construction) conducted on sections that would later have a flexible pavement constructed on them. Bulk stresses were calculated at points within the base layer, along the axis of symmetry of the load plate.

Subgrade Tests

The subgrade moduli calculated from tests done on the subgrade surface will be used as a baseline for the comparisons. The method used to calculate these subgrade moduli (using the homogeneous model) was presented in a previous section (see Fig. 71a). Data from lane 1 were selected for this analysis. For each testing station, subgrade moduli from the 300 and 1800 mm sensors and intermediate drop height (roughly 100 kPa surface pressure) were selected. These values are denoted as E_{300} and E_{1800} , respectively.

Points 150 and 900 mm below the 300 and 1800 mm FWD sensors, respectively, were selected for stress computation and comparison with the E_{300} and E_{1800} modulus values (see Fig. 72a). At these two points, the ratios of principal stress difference to applied surface pressure are 0.33 and 0.15, respectively. These values, appropriately scaled to the applied load, can be applied to all subgrade tests because stresses within a half-space are not dependent on modulus.

Granular Base Tests

The base FWD testing data were approached a bit differently. A multi-layer backcalculation analysis using EVERCALC 3.3 was performed. Only data from lane 1 were selected. Reasonable results were obtained from all sections tested except for those with thin granular base layers less than about 125 mm (sections 6, 11, 12, 13, 24, 36, 38, 39, and 40). For these sections, the homogeneous model was used in a fashion similar to the subgrade data analysis (see Fig 72b). For all other sections with granular base layers, the backcalculations were done using EVERCALC 3.3. In all cases, a three-layer system was modeled. In cases where the total granular material thickness was less than 300 mm, the granular layer was modeled as one layer with a 300 mm thick intermediate subgrade layer beneath it (see Fig. 71c). In cases where the granular base layer had a total thickness of greater than 300 mm, the granular layer was split into two equal layers (see Fig. 71d). Stress values were computed at the same points relative to the top of the subgrade layer as in the subgrade tests, *i.e.*, at points 300 and 1800 mm away from the load, and 150 and 900 mm beneath the base/subgrade interface, respectively (see Fig. 72b).

A summary of backcalculation results from testing on sections with thin base layers is shown in Table 8. Note that in most sections, a relative increase in the apparent subgrade modulus was noted after base construction for moduli from both sensor offsets. A full tabulation of all data from the tests done on sections with thin base layers is given in Appendix F, Table F1.

A comparison of the subgrade moduli and stresses obtained from post-base tests will be presented in the next paragraphs. Comparisons of post-base and post-construction granular base moduli and stress will be presented in a later section.

Flexible Pavement Tests

Multi-layer backcalculations were performed for the post-construction (pavement) FWD testing data with the exception of the concrete data. All selected data were from October 1993, ensuring that comparable support conditions were obtained. Only data from lane 1 were chosen for the analysis. Recall that, with the exception of the 5-year sections, which were paved in fall 1992, all of the test sections were paved in late summer-early fall 1993. No post-construction FWD testing had been conducted on the 5-year sections during fall 1992.

The various layer configurations used in the backcalculation analysis are shown in Fig. 71g and Fig. 71h for the full-depth and conventional section data, respectively. A three-layer system was used in all cases. For the full-depth sections, an intermediate subgrade layer was used (see Fig. 71g).

The greatest difficulty in the backcalculation was encountered with the sections having total asphalt concrete layer thicknesses less than about 100 mm. These particular sections were TS 24, 28, and 31 on the low-volume road. The problem was due primarily to the size of the plate relative to the asphalt thickness; the thin profile of the asphalt layer contributed little strength to the structure. The FWD sensor spacing was another factor, because the first sensor offset from the plate (a distance of 200 mm) gave little information on the deformation of the asphalt layer. The end result was a backcalculation analysis with poor RMS values and inconsistent asphalt layer moduli. An attempt was made to fix the modulus of the asphalt layer based on pavement temperature but this was not successful.

The first step in the stress analysis was to compute the effective stress bulb radius (a_e) using the procedure in the 1993 *AASHTO Guide for Design of Pavement Structures* (15). This information was used to determine the minimum radial offset at which to compute the stresses in the subgrade. As suggested in the AASHTO Guide, the radial offset should be greater than 0.7 times the effective radius, *i.e.*, $r \geq 0.7a_e$. It was found that this condition was satisfied by the 1500 mm FWD sensor and, with the exception of only the thickest sections, the condition was also met for the 600 mm sensor. Thus, the two points selected for calculation of stresses were offset by 600 and 1500 mm radially from the load (see Fig. 72c and 72d).

The results for the conventional and full-depth flexible sections are given in Tables 9 and 10. These data represent average test section values. A complete tabulation of all data can be found in Appendix F, Table F2 (conventional) and Table F3 (full-depth). A summary of subgrade

modulus and deviator stress changes is presented in Table 11. Relative changes in the backcalculated subgrade moduli after each stage of construction are shown. The following observations were noted:

- For the majority of the sections, the subgrade modulus after base construction increased relative to before base construction. This was not accompanied by a uniform decrease in the deviator stresses.
- For all sections, the modulus did increase when going from base to pavement construction. This was accompanied by a uniform *increase* in the deviator stress, not a decrease as would be expected.
- Overall, the apparent subgrade modulus did increase after pavement construction, relative to pre-base construction. Sections with lower average subgrade moduli initially showed the greatest increase after construction. Also, sections with the largest total pavement thickness showed the greatest relative modulus increase, while sections with the lowest total pavement thickness showed the least relative modulus increase. This is shown in Fig. 73.

It should be noted that, due to the time between the various construction stages, moisture conditions within the subgrade of each section undoubtedly changed. This analysis does not account for moisture changes.

PASB Tests

Multi-layer backcalculation analyses were done on the four sections with PASB layers, shortly after construction of the PASB layers. The PASB sections in TS 7, 8, and 9 were paved and tested during late summer 1992, and the PASB in TS 10 was paved and tested in summer 1993.

The layer configuration used in the backcalculation analysis is shown in Fig. 71i. A three-layer system was used in all cases. Each of the four test sections has 100 mm of PASB constructed over a 75 mm granular subbase. This subbase was not isolated during the backcalculations, as shown in Fig. 71i.

Average test section data are summarized in Table 12. A complete tabulation can be found in Appendix F, Table F4. Note that TS 7 through 9 were tested on the same day, starting with TS 9 and finishing with TS 7. Temperature conditions during the time TS 9 was being tested were unseasonable cool, but warmed as the day went on. The conditions for TS 7 testing were fairly warm. It appears that the moduli for the PASB layer are fairly temperature-dependent, as would be expected. In general, slight increases in the subgrade moduli were noted (compare E_2

with E_{300} and E_3 with E_{1800}). These changes were accompanied by decreases in the calculated deviator stresses, as expected.

Rigid Pavement Tests

Because of the difficulties associated with performing multi-layered backcalculation analyses on rigid pavement sections, a different method was used to calculate the post-construction subgrade modulus from the rigid pavement tests. To compute the subgrade modulus from PCC pavement sections, the AASHTO subgrade modulus calculation procedure was used (15). The layer configuration used in this analysis is shown in Fig. 71f. Deflection data from FWD tests conducted at the geometric center of the panels within each test section were selected. These data were taken from a routine FWD test run done during fall 1993. Five panels per lane within each section were tested.

Although the analysis showed that, for the majority of the basin, the effective subgrade stress radius was larger than the distance to the D_{1500} sensor, the D_{900} sensor was selected for the subgrade modulus calculation. This was done to obtain a measurement that was representative of the subgrade response, yet not affected by the nearby transverse joint. Also, the locations of the FWD test points on the PCC slabs do not coincide with the original subgrade and base test locations, so the data will be compared on an average test section basis. The results are summarized in Table 13.

In general, increases in the average subgrade moduli were observed after construction. It is interesting to note that the effective pavement moduli (E_p) for each of the three groups (5-year, 10-year, and low-volume) of pavements are comparable. The 5-year section with the lowest E_p is TS 5, which has a relatively thick granular subbase layer.

Aggregate and Chip-Seal Tests

Multi-layer backcalculation analyses were done on the four sections with aggregate and chip-seal pavement layers. Deflection data from lane 1 were selected. These data were from tests completed during fall 1994, several months after test traffic began operating on the sections and over two years after the subgrade tests were conducted. The granular pavement layer was divided into two equal layers for the backcalculation (see Fig. 71e) and the contribution of the chip-seal (TS 32 and 35) was neglected. Stresses were calculated at points similar to those used in the granular base tests (see Fig. 72e).

Average test section results are summarized in Table 14. A complete tabulation by station number is given in Appendix F, Table F5. a summary of subgrade stress and modulus increases is

given in Table 15. As shown in Table 14, increases were observed for post-construction testing relative to both pre-construction sensor offsets. On average, for the 1800 mm sensor offset, the increase in modulus in each section was accompanied by a decrease in the deviator stress.

Effects of Construction on Granular Base Stress Modulus

The backcalculated moduli results obtained for the granular base layers from the analyses discussed in the previous section will be analyzed here. For post-base tests in each conventional flexible pavement test section, the bulk stress was computed at the mid-point of the layer(s) used in the model. In cases where two layers were used to model the total granular layer, bulk stresses were calculated at the mid-point of that layer. For post-construction tests, the bulk stresses were calculated at two points within the base layer: At depths of 0.4 and 0.6 times the total thickness of the granular base/subbase material.

A complete summary by station is given in Appendix F, Table F6, and a summary by test section average is shown in Table 16. Bulk stresses and moduli for the results in these tables are from the intermediate drop height corresponding to a nominal load level of about 20 kN for the post-base tests and 40 kN for the post-construction tests. Note that no base testing data were available for TS23; this section has a composite PASB/granular subbase structure. Also, there are no post-base backcalculations for TS 24 because this has a thin base. No overall trend could be established between the changes in bulk stress and moduli.

CHAPTER 5

CONCLUSIONS AND RECOMMENDATIONS

Conclusions

The study presented in this paper was undertaken to assess the properties of the subgrade and granular base soil materials at Mn/ROAD. Several different methods of sampling were used including retrieval of bulk and undisturbed soil samples, nondestructive deflection testing, and penetration testing. The basic information and raw data that have been gathered to date were presented. In addition, results from both laboratory testing of the field materials and theoretical analyses of the deflection data were presented.

Highly variable deflections from the subgrade and base testing were observed. This is likely due to variability in surface condition as well as variations in soil moisture content, density, and stress-dependent effects. For a given test, a significant increase in backcalculated moduli with increasing sensor offset was noted and was attributed to nonlinear stress-dependent soil modulus effects. Moduli backcalculated from the deflection testing on the subgrade compared well with laboratory values, while post-paving backcalculated moduli were higher than the laboratory values due to stress-dependency effects. A preliminary comparison of penetration index and backcalculated soil modulus was made but the results did not show a correlation.

On the basis of the analysis conducted thus far it is reasonable to conclude the following:

- The variability studies suggest that, at least for the embankment at Mn/ROAD, a relatively large amount of deflection variability can be expected even at short testing intervals.
- Within the variability encountered, the backcalculated and laboratory moduli appear to compare well, but moisture and density differences must be reconciled.
- The surface condition of the soil has a noticeable impact upon the variability of the measured deflections, especially the inner sensor locations.
- Over the range of moisture contents observed in the undisturbed specimens, the degree of saturation had little impact on the laboratory resilient modulus.
- The multi-layered backcalculation approach did not provide any advantage in interpreting FWD deflections from subgrade testing relative to the homogeneous approach.

The following observations regarding pavement construction effects were noted:

- For the majority of the sections, the post-base subgrade modulus increased relative to before base construction. This was not accompanied by a uniform decrease in the deviator stresses.

- For all conventional flexible sections the subgrade modulus from post-construction FWD tests did increase relative to moduli from tests done on the granular base. This was despite a uniform increase in the deviator stress (not a decrease as would be expected). The reason for this is that, while the load-induced stresses did decrease, they were overshadowed by the net increase in overburden stresses after construction.
- Overall, the apparent subgrade modulus did increase after pavement construction, relative to pre-base construction. Sections with initially lower average subgrade moduli showed the greatest increase after construction. Also, sections with the largest total pavement thickness showed the greatest relative modulus increase, while sections with the lowest total pavement thickness showed the least relative modulus increase.
- Overall increases in the subgrade moduli from pre- and post-construction tests on the PASB sections were observed. These increases in moduli were accompanied by decreases in the calculated deviator stresses.
- For the aggregate and chip-seal sections, the increase in modulus in each section, on average, was accompanied by a decrease in the deviator stress (for the 1800 mm sensor offset).

Recommendations

Further analysis should address the following issues:

- Effects of moisture and density on observed subgrade FWD deflections and moduli
- Effects of moisture and density on DCP penetration index
- Further exploration of possible relationships between penetration index and deflection data
- Statistical analysis of variance on moduli from the following subsets of data:
 1. Five-year versus 10-year versus low-volume road (LVR) designs
 2. Pre-base versus post-base versus post-pavement testing
 3. Sections with base versus sections without base
- Comparison of laboratory resilient modulus data on granular materials to backcalculation results from tests on base and pavement surfaces.
- Effects of soil embankment cut depth on observed subgrade deflections.

REFERENCES

1. D. E. Newcomb, R. Benke, and G. R. Cochran. Minnesota Road Research Project - An Overview. Cold Regions Engineering, In *Proceedings of the Sixth International Specialty Conference*, 1991, pp. 463-471.
2. W. N. Houston, M. S. Mamlouk, and R. W. S. Perera. Laboratory versus Nondestructive Testing for Pavement Design. *ASCE Journal of Transportation Engineering*, Vol. 118, No. 2, March/April 1992, pp. 207-222.
3. D. E. Newcomb. Comparisons of Field and Laboratory Estimated Resilient Moduli of Pavement Materials. *Asphalt Paving Technology*, Association of Asphalt Paving Technologists, Vol. 56, February 1987, pp. 91-106.
4. S. W. Lee, J. P. Mahoney, and N. C. Jackson. In *Transportation Research Record 1196*, TRB, National Research Council, Washington, D.C., 1988, pp. 85-95.
5. V. C. Janoo and R. L. Berg. *Predicting the Behavior of Asphalt Concrete Pavements in Seasonal Frost Areas Using Nondestructive Techniques*. Report 90-10, U.S. Army Corps of Engineers Cold Regions Research and Engineering Laboratory, 1990.
6. S. L. Houston and R. Perera. Impact of Natural Site Variability on Nondestructive Test Deflection Basins. *ASCE Journal of Transportation Engineering*, Vol. 117, No. 5, September/October 1991, pp. 550-565.
7. T. Burnham and D. Johnson. In Situ Characterization Using the Dynamic Cone Penetrometer. Minnesota Department of Transportation, Physical Research Section. Report No. 93-05, May 1993.
8. S. P. Timoshenko and J. N. Goodier. *Theory of Elasticity*. McGraw-Hill, New York, 1970.
9. M. Abramowitz and I. A. Stegun. *Handbook of Mathematical Functions*. Dover, New York, 1972.
10. Washington State Transportation Center, University of Washington, Washington State Department of Transportation. Evercalc User's Guide 1.1, April 1987.
11. M. R. Thompson and Q. L. Robnett. *ASCE Transportation Engineering Journal*, Vol. 105, No. TE1, January 1979, pp. 71-89.
12. U.S. Army Corps of Engineers, Waterways Experiment Station. Investigation of Pressures and Deflections for Flexible Pavements, Report No. 4, Homogeneous Sand Test Section. Technical Memorandum No. 3-323, December 1954.
13. L. P. Aboulkheir. Geostatistics for Pavement Design on Variable Soils. Masters Thesis, University of Minnesota, Dept. of Civil & Mineral Engineering, June 1991.
14. U.S. EPA Environmental Monitoring Systems Laboratory. Geo-EAS Reference Manual, May 1990.
15. American Association of State Highway and Transportation Officials, *AASHTO Guide for Design of Pavement Structures*, 1993.

Table 1a. Variability and correlation of surface deflections from subgrade testing: entire section.

SUBGRADE TS 3 - ENTIRE SECTION
SUMMARY STATISTICS FOR DEFLECTIONS (μm)

	D_0	D_{300}	D_{450}	D_{600}	D_{900}	D_{1350}	D_{1800}
Mean	1218	503	229	120	61	38	34
Median	1130	440	177	88	51	35	26
S.D.	427	219	129	76	31	10	48
Range	2108	1135	641	343	231	75	480
Min.	451	185	73	40	28	9	14
Max.	2558	1320	713	383	258	83	495
Count.	710	710	710	710	710	710	710

CORRELATION MATRIX

	D_0	D_{300}	D_{450}	D_{600}	D_{900}	D_{1350}	D_{1800}
D_0	1						
D_{300}	0.8391	1					
D_{450}	0.7401	0.9130	1				
D_{600}	0.6465	0.8162	0.9573	1			
D_{900}	0.3990	0.4666	0.6421	0.7220	1		
D_{1350}	0.3307	0.3064	0.3461	0.3361	0.3573	1	
D_{1800}	0.2047	0.2567	0.3452	0.4094	0.4631	0.3509	1

NOTE:

Subscripts represent sensor offsets (mm).

Table 1b. Variability of surface deflections from subgrade testing: grid test.

SUBGRADE TS 3 - GRID TEST

SUMMARY STATISTICS FOR DEFLECTIONS (μm)

	D_0	D_{300}	D_{450}	D_{600}	D_{900}	D_{1350}	D_{1800}
Mean	956	421	177	86	46	34	25
Median	952	414	175	83	45	33	25
S.D.	173	95	41	16	5	4	3
Range	697	407	177	63	18	18	12
Min.	613	266	117	68	40	26	20
Max.	1310	673	294	130	59	44	32
Count.	90	90	90	90	90	90	90

CORRELATION MATRIX

	D_0	D_{300}	D_{450}	D_{600}	D_{900}	D_{1350}	D_{1800}
D_0	1						
D_{300}	0.8646	1					
D_{450}	0.7370	0.9298	1				
D_{600}	0.6476	0.8484	0.9430	1			
D_{900}	0.7432	0.7199	0.6629	0.7659	1		
D_{1350}	0.6832	0.8089	0.7922	0.7503	0.6735	1	
D_{1800}	0.6346	0.7399	0.6956	0.5968	0.4329	0.7202	1

Table 1c. Variability of surface deflections from subgrade testing: entire section.

SUBGRADE TS 4 - ENTIRE SECTION
SUMMARY STATISTICS FOR DEFLECTIONS (μm)

	D_0	D_{300}	D_{450}	D_{600}	D_{900}	D_{1350}	D_{1800}
Mean	695	397	207	121	47	26	22
Median	632	357	197	111	43	25	21
S.D.	341	172	86	59	16	8	7
Range	3202	994	573	747	114	72	64
Min.	246	118	74	50	23	0	2
Max.	3448	1111	648	797	137	72	66
Count.	710	710	710	710	710	710	710

CORRELATION MATRIX

	D_0	D_{300}	D_{450}	D_{600}	D_{900}	D_{1350}	D_{1800}
D_0	1						
D_{300}	0.6703	1					
D_{450}	0.6753	0.9367	1				
D_{600}	0.4413	0.5277	0.6029	1			
D_{900}	0.5698	0.5977	0.6782	0.7530	1		
D_{1350}	0.5562	0.5356	0.5902	0.5389	0.7733	1	
D_{1800}	0.5081	0.5792	0.6466	0.5848	0.6884	0.7703	1

Table 1d. Variability of surface deflections from subgrade testing: grid test.

SUBGRADE TS 4 - GRID TEST
SUMMARY STATISTICS FOR DEFLECTIONS (μm)

	D_0	D_{300}	D_{450}	D_{600}	D_{900}	D_{1350}	D_{1800}
Mean	686	395	211	122	52	26	21
Median	669	349	202	123	53	27	21
S.D.	155	105	39	15	5	4	4
Range	660	398	158	52	18	20	24
Min.	403	268	155	96	45	13	6
Max.	1063	666	313	148	63	32	30
Count	90	90	90	90	90	90	90

CORRELATION MATRIX

	D_0	D_{300}	D_{450}	D_{600}	D_{900}	D_{1350}	D_{1800}
D_0	1						
D_{300}	0.7842	1					
D_{450}	0.6841	0.9622	1				
D_{600}	0.3892	0.6020	0.7598	1			
D_{900}	-0.0758	0.0096	0.1675	0.6884	1		
D_{1350}	0.4978	0.4402	0.3381	-0.123	-0.4374	1	
D_{1800}	0.4172	0.4610	0.4172	0.1988	-0.2178	0.5546	1

Table 2a. Variability and correlation of surface deflections from base testing: entire section.

BASE TS 3 - ENTIRE SECTION

SUMMARY STATISTICS FOR DEFLECTIONS (μm)

	D_0	D_{300}	D_{450}	D_{600}	D_{900}	D_{1350}	D_{1800}
Mean	319	132	67	44	28	19	14
Median	308	131	67	43	28	18	13
S.D.	74	20	7	4	3	6	2
Range	410	108	33	76	21	143	17
Min.	205	87	51	34	19	12	7
Max.	615	195	84	111	40	155	24
Count.	710	710	710	710	710	710	710

CORRELATION MATRIX

	D_0	D_{300}	D_{450}	D_{600}	D_{900}	D_{1350}	D_{1800}
D_0	1						
D_{300}	0.5839	1					
D_{450}	0.5444	0.918	1				
D_{600}	0.4438	0.4817	0.6168	1			
D_{900}	0.2736	0.2286	0.4028	0.5599	1		
D_{1350}	0.2609	0.0514	0.1048	0.7217	0.3075	1	
D_{1800}	0.1258	0.1691	0.2594	0.4614	0.5761	0.3613	1

NOTE:

Subscripts represent sensor offsets (mm).

Table 2b. Variability and correlation of surface deflections from base testing: grid test.

BASE TS 3 - GRID TEST

SUMMARY STATISTICS FOR DEFLECTIONS (μm)

	D_0	D_{300}	D_{450}	D_{600}	D_{900}	D_{1350}	D_{1800}
Mean	347	131	66	43	28	18	13
Median	370	131	66	43	28	18	13
S.D.	87	15	5	2	1	3	2
Range	341	55	18	10	7	16	13
Min.	205	100	55	39	25	12	9
Max.	545	155	73	49	33	28	21
Count.	90	90	90	90	90	90	90

CORRELATION MATRIX

	D_0	D_{300}	D_{450}	D_{600}	D_{900}	D_{1350}	D_{1800}
D_0	1						
D_{300}	0.5623	1					
D_{450}	0.4036	0.9271	1				
D_{600}	0.2526	0.8094	0.8424	1			
D_{900}	0.1512	0.0752	0.0126	0.2093	1		
D_{1350}	0.2827	0.0668	-0.0895	0.1718	0.3182	1	
D_{1800}	0.3209	0.2339	0.2834	0.1008	0.3030	-0.0068	1

Table 2c. Variability and correlation of surface deflections from base testing: entire section.

**BASE TS 4 - ENTIRE SECTION
SUMMARY STATISTICS FOR DEFLECTIONS (μm)**

	D_0	D_{300}	D_{450}	D_{600}	D_{900}	D_{1350}	D_{1800}
Mean	982	466	252	142	52	28	24
Median	944	443	236	131	50	26	23
S.D.	549	237	110	54	19	8	8
Range	2700	1166	615	361	145	50	57
Min.	174	101	68	46	8	14	12
Max.	2874	1267	682	407	153	64	69
Count	710	710	710	710	710	710	710

CORRELATION MATRIX

	D_0	D_{300}	D_{450}	D_{600}	D_{900}	D_{1350}	D_{1800}
D_0	1						
D_{300}	0.9512	1					
D_{450}	0.8626	0.9638	1				
D_{600}	0.7034	0.8366	0.9393	1			
D_{900}	0.2228	0.2988	0.4222	0.6628	1		
D_{1350}	0.6967	0.6633	0.6260	0.6248	0.6349	1	
D_{1800}	0.8303	0.8323	0.7971	0.7387	0.4652	0.8367	1

Table 2d. Variability and correlation of surface deflections from base testing: grid test.

BASE TS 4 - GRID TEST
SUMMARY STATISTICS FOR DEFLECTIONS (μm)

	D_0	D_{300}	D_{450}	D_{600}	D_{900}	D_{1350}	D_{1800}
Mean	738	381	228	151	71	30	22
Median	623	352	214	142	70	28	22
S.D.	381	170	73	40	15	7	6
Range	1382	619	264	151	58	27	25
Min.	309	180	132	97	50	20	13
Max.	1691	799	395	248	108	48	38
Count	90	90	90	90	90	90	90

CORRELATION MATRIX

	D_0	D_{300}	D_{450}	D_{600}	D_{900}	D_{1350}	D_{1800}
D_0	1						
D_{300}	0.9850	1					
D_{450}	0.9219	0.9698	1				
D_{600}	0.8253	0.9009	0.9765	1			
D_{900}	0.5939	0.7030	0.8510	0.9310	1		
D_{1350}	0.7868	0.8505	0.9156	0.9326	0.8778	1	
D_{1800}	0.8138	0.8695	0.9345	0.9429	0.8720	0.9312	1

Table 3. Values of $f(r)$ for several values of Poisson's ratio.

r/a	Poisson's ratio			
	0.3	0.35	0.4	0.45
0	1.82000	1.75500	1.68000	1.59500
1	1.15864	1.11726	1.06951	1.01540
2	0.23538	0.22697	0.21727	0.20628
3	0.10258	0.09891	0.09469	0.08990
4	0.05733	0.05528	0.05292	0.05024
5	0.03658	0.03528	0.03377	0.03206
6	0.02537	0.02446	0.02342	0.02223
7	0.01862	0.01795	0.01719	0.01632
8	0.01425	0.01374	0.01315	0.01249
9	0.01125	0.01085	0.01039	0.00986
10	0.00911	0.00879	0.00841	0.00799

THIS PAGE INTENTIONALLY BLANK

Table 4. Summary statistics for thin-walled (undisturbed) subgrade soil sample data.

5-year	M_R (MPa)	LL (per.)	PI (per.)	q_u (kPa)	ρ_w (kg/m ³)	ρ_d (kg/m ³)	m.c. (per.)
Mean	69	34	14	141	2142	1835	17
Median	66	33	14	141	2139	1832	17
S.D.	27	2.5	2.5	33	40	68	2.7
Var.	727	6.1	6.1	1078	1630	4677	7.5
Min.	34	29	10	92	2024	1597	15
Max.	123	38	18	214	2203	1914	27
Count	18	19	19	17	19	19	18
10-year							
Mean	104	33	13	118	2150	1851	16
Median	76	34	13	105	2143	1834	16
S.D.	61	3.4	3.0	55	47	69	2.1
Var.	3674	12	9.2	2995	2198	4694	4.4
Min.	36	24	5.8	47	2063	1749	12
Max.	232	41	20	232	2258	2010	20
Count	24	25	25	23	24	24	25
LVR South							
Mean	90	35	16	173	2132	1836	16
Median	73	34	15	151	2131	1834	16
S.D.	39	3.1	3.2	68	38	56	1.6
Var.	1541	9.5	10	4603	1447	3090	2.5
Min.	50	30	9.7	89	2064	1760	13
Max.	189	39	19	325	2200	1946	18
Count	12	12	12	12	12	12	12

Table 4, cont. Summary statistics for thin-walled (undisturbed) subgrade soil sample data.

<i>LVR</i>	M_R	LL	PI	q_u	ρ_w	ρ_d	m.c.
<i>North</i>	(MPa)	(per.)	(per.)	(kPa)	(kg/m ³)	(kg/m ³)	(per.)
Mean	77	39	20	125	2108	1793	18
Median	79	38	19	127	2119	1796	17
S.D.	32	5.8	5.8	19	27	37	1.5
Var.	1004	34	33	374	708	1364	2.3
Min.	36	30	12	87	2064	1720	15
Max.	145	48	29	150	2138	1840	20
Count	11	11	11	10	10	10	10
<i>Overall</i>							
Mean	87	35	15	136	2137	1834	17
Median	71	34	14	130	2133	1830	17
S.D.	46	4.1	4.2	52	42	64	2.2
Var.	2158	17	17	2657	1803	4099	4.7
Min.	34	24	5.8	47	2024	1597	12
Max.	232	48	29	325	2258	2010	27
Count	65	67	67	62	65	65	65

NOTES:

M_R = Resilient modulus.

LL = Liquid limit (Atterberg).

PI = Plasticity index.

q_u = Bearing capacity.

ρ_w = Wet density.

ρ_d = Dry density.

m.c. = moisture content.

Table 5. Summary statistics for bag subgrade soil sample data.

	LL (per.)	PI (per.)	Proctor		R-Value	Data at optimum moisture content						
			o.m.c. (per.)	ρ_{max} (kg/m ³)		M_R (MPa)	q_u (kPa)	ρ_w (kg/m ³)	ρ_d (kg/m ³)	m.c. (per.)		
5-year												
Mean	35	17	17	1743	14	199	111	2025	1744	16		
Median	34	16	17	1749	14	194	124	2029	1763	16		
S.D.	2.1	1.9	0.71	24	0.94	36	20	59	49	0.62		
Var.	4.2	3.6	0.50	573	0.88	1320	406	3466	2374	0.38		
Min.	33	14	16	1701	13	129	79	1936	1672	15		
Max.	38	19	18	1771	16	241	128	2101	1798	17		
Count	10	10	10	10	9	7	7	7	7	7		
10-year												
Mean	37	17	17	1730	14	205	119	2025	1744	16		
Median	37	17	17	1737	14	207	121	2045	1762	16		
S.D.	5.3	2.8	1.4	40	1.1	42	9.1	65	51	0.99		
Var.	28	7.9	1.8	1595	1.1	1733	83	4248	2601	0.98		
Min.	30	10	14	1646	12	148	105	1920	1661	15		
Max.	59	21	21	1808	16	261	131	2107	1792	18		
Count	23	23	23	23	22	7	6	6	6	6		

Table 5, cont. Summary statistics for bag subgrade soil sample data.

	LL (per.)	PI (per.)	Proctor		R-Value	Data at optimum moisture content						
			o.m.c. (per.)	ρ_{\max} (kg/m ³)		M_R (MPa)	q_u (kPa)	ρ_w (kg/m ³)	ρ_d (kg/m ³)	m.c. (per.)		
LVR South												
Mean	39	21	15	1772	13	183	96	2025	1726	17		
Median	38	20	17	1734	13	187	102	2029	1744	16		
S.D.	4.9	5.1	4.4	110	0.62	37	13	36	58	2.0		
Var.	24	26	19	12033	0.38	1362	165	1309	3388	4.0		
Min.	30	12	7.3	1673	12	145	81	1987	1661	16		
Max.	45	28	20	2019	14	218	105	2059	1773	20		
Count	7	7	10	10	7	3	3	3	3	3		
LVR North												
Mean	32	14	16	1788	15	166	86	2028	1743	16		
Median	32	13	17	1760	15	159	85	2041	1745	16		
S.D.	2.6	3.1	2.3	65	1.1	29	21	66	41	1.3		
Var.	6.6	9.6	5.3	4207	1.2	826	447	4295	1700	1.7		
Min.	29	11	12	1739	13	138	63	1938	1691	15		
Max.	36	19	18	1901	16	206	111	2091	1792	18		
Count	7	7	9	9	6	4	4	4	4	4		

Table 5, cont. Summary statistics for bag subgrade soil sample data.

	LL (per.)	PI (per.)	Proctor		R-Value	Data at optimum moisture content					
			o.m.c. (per.)	ρ_{max} (kg/m ³)		M_R (MPa)	q_u (kPa)	ρ_w (kg/m ³)	ρ_d (kg/m ³)	m.c. (per.)	
Overall											
Mean	36	17	17	1750	14	192	106	2025	1741	16	
Median	36	17	17	1745	14	191	108	2037	1749	16	
S.D.	4.8	3.6	2.4	64	1.1	37	20	55	46	1.2	
Var.	23	13	5.6	4112	1.3	1404	400	3030	2103	1.3	
Min.	29	10	7.3	1646	12	129	63	1920	1661	15	
Max.	59	28	21	2019	16	261	131	2107	1798	20	
Count	47	47	52	52	44	21	20	20	20	20	

NOTES:

LL = Liquid limit (Atterberg).

PI = Plasticity index.

o.m.c. = Optimum moisture content.

ρ_{max} = Maximum density.

M_R = Resilient modulus.

q_u = Bearing capacity.

ρ_w = Wet density.

ρ_d = Dry density.

m.c. = moisture content.

THIS PAGE INTENTIONALLY BLANK

Table 6a. Comparison of backcalculated (pre-base) and laboratory (thin-walled, undisturbed) subgrade resilient moduli by test section.

TS	BACKCALCULATED (MPa)				LABORATORY (MPa)		
	M_R	S.D.	MAX.	MIN.	M_R	MAX.	MIN.
1	105	15	135	81	47	48	47
2	85	31	142	33	46	56	36
3	78	29	133	14	37	40	34
4	104	26	166	59	43	64	
5	89	22	130	44	68	68	68
6	108	50	322	59	95	123	67
7	88	12	119	68	67	77	55
8	91	11	117	66	89	114	73
9	112	28	184	70	97	120	73
10	177	56	307	76	232	232	232
11	162	73	418	76	129	189	60
12	144	55	311	70	120	194	
13	75	13	96	47	40	40	40
14	110	41	268	59	77	87	67
15	92	28	160	56	98	165	58
16	66	14	99	47	46	46	46
17	81	20	112	40	121	121	121
18	92	32	166	48	185	185	185
19	75	17	117	46	56	56	56
20	69	11	102	50	55	65	46
21	104	28	185	67	36	36	36
22	130	50	280	54	55	55	55
23	147	69	326	41	47	47	47
24	85	9.8	100	54			
25	91	7.6	105	73			
26	98	21	155	59	82	97	68
27	130	45	253	56	63	79	47
28	158	39	227	77	58	58	58
29	124	47	240	361	108	108	108

Table 6a, cont. Comparison of backcalculated (pre-base) and laboratory (thin-walled, undisturbed) subgrade resilient moduli by test section.

TS	BACKCALCULATED (MPa)				LABORATORY (MPa)		
	M_R	S.D.	MAX.	MIN.	M_R	MAX.	MIN.
30	110	40	214	34	45	45	45
31	103	22	177	81	114	145	84
32	96	26	158	64	57	79	36
33	87	21	122	53	103	134	72
34	89	24	135	57	61	71	50
35	116	30	169	61	153	189	117
36	93	8.7	109	76			
37	83	5.9	96	65			
38	63	16	108	39	69	77	61
39	85	25	167	53	82	95	69
40	76	34	165	36	72	74	67

Table 6b. Comparison of subgrade moduli broken down by facility sub-sections.

Sub-section	BACKCALCULATED (MPa)				LABORATORY (MPa)			
	M_R	S.D.	MAX.	MIN.	M_R	S.D.	MAX.	MIN.
<i>5-year</i>	96	27	322	14	69	27	123	34
<i>10-year</i>	109	42	418	40	104	61	232	36
<i>LVR North</i>	110	32	253	34	90	39	189	50
<i>LVR South</i>	87	23	169	36	77	32	145	36

Table 7a. Summary of selected backcalculated moduli and penetration index values:
subgrade testing.

TS	MODULI (MPa) FROM 300, 600, AND 1800 mm OFFSETS			PEN. INDEX (mm/BLOW) FOR SEVERAL SUB-LAYERS (mm)			
	E_{300}	E_{600}	E_{1800}	000-250	250-500	500-750	750-1000
1	47	123	105	16	27	11	4.8
2	26	64	85	20	32	27	17
3	32	87	78	20	27	24	16
4	41	68	104	11	21	21	18
5	51	55	89	15	18	27	19
6	42	64	108	9.9	19	23	17
7	39	64	88	11	22	22	21
8	37	60	91	12	21	22	17
9	41	73	112	11	27	21	19
10	87	132	177	10	13	13	12
11	86	150	162	12	14	13	14
12	29	101	144	13	28	14	12
13	47	50	75	18	28	26	29
14	66	93	110	14	22	19	17
15	56	67	92	18	21	21	20
16	40	54	66	20	25	26	22
17	54	74	81	15	24	24	30
18	89	93	92	22	18	19	26
19	44	57	75	26	27	20	19
20	47	59	69	21	26	27	25
21	70	73	104	23	24	26	23
22	49	97	130	22	23	20	17
23	39	71	147	22	37	68	38
24	71	89	85	19	8.3	7.1	6.0
25	83	95	91	11	6.7	7.4	7.2
26	35	66	98	10	18	16	14
27	51	107	130	13	22	24	16

Table 7a, cont. Summary of selected backcalculated moduli and penetration index values: subgrade testing.

TS	MODULI (MPa) FROM 300, 600, AND 1800 mm OFFSETS			PEN. INDEX (mm/BLOW) FOR SEVERAL SUB-LAYERS (mm)			
	E_{300}	E_{600}	E_{1800}	000-250	250-500	500-750	750-1000
28	61	130	158	10	25	24	13
29	56	81	124	8.9	24	20	15
30	54	78	110	12	26	18	17
31	57	61	103	9.8	28	16	14
32	46	68	96	14	30	24	15
33	53	62	87	15	27	31	26
34	46	61	89	16	27	26	17
35	58	80	116	16	19	25	20
36	80	96	93	16	9.8	7.7	5.1
37	75	85	83	17	8.9	7.7	5.9
38	37	54	63	13	20	21	27
39	36	65	85	13	28	25	23
40	35	55	76	11	21	26	31

Table 7b. Summary of selected backcalculated moduli and penetration index values: base testing.

TS	MODULI (MPa) FROM 300, 600, AND 1800 mm OFFSETS			PEN. INDEX (mm/BLOW) FOR SEVERAL SUB-LAYERS (mm)			
	E_{300}	E_{600}	E_{1800}	000-250	250-500	500-750	750-1000
1	102	148	154	8.8	5.5	3.8	11
2	102	116	124	11	5.0	3.6	11
3	118	161	160	8.2	4.1	3.5	5.5
4	38	57	107				
5	139	162	156	4.7	3.3	3.6	12
6	69	65	95	8.7	10	20	19
7	70	83	100	9.2	17	23	18
8	63	79	115	11	17	24	22
9	69	81	129	9.8	23	22	18
10	64	143	216	7.4	15	14	13
11	45	128	188	13	20	12	13
12	38	116	168	19	27	20	14
13	43	93	150	21	22	21	16
14							
15							
16	111	144	152	5.5	3.4	4.1	13
17	121	143	154	4.6	3.3	3.9	14
18	81	91	108	3.2	2.7	11	18
19	128	141	154	2.5	2.4	3.7	15
20	133	143	147	3.6	3.2	3.4	14
21	109	118	139	3.7	3.1	13	17
22	90	100	147	3.5	3.8	14	18
23							
24	127	120	120	5.2	3.8	3.5	4.5
25							
26	53	68	107				
27	59	87	132	6.4	8.2	15	18

Table 7b, cont. Summary of selected backcalculated moduli and penetration index values: base testing.

TS	MODULI (MPa) FROM 300, 600, AND 1800 mm OFFSETS			PEN. INDEX (mm/BLOW) FOR SEVERAL SUB-LAYERS (mm)			
	E_{300}	E_{600}	E_{1800}	000-250	250-500	500-750	750-1000
28	66	90	139	5.3	7.9	16	20
29	82	96	163	4.1	15	21	21
30	63	76	137	4.6	12	24	21
31	68	81	139	3.3	5.7	18	21
32				6.3	9.5	22	23
33				6.6	12	19	21
34				2.3	7.3	19	19
35				6.0	9.4	15	18
36	112	119	115	9.0	8.0	8.9	6.1
37	118	126	124	7.3	4.5	4.6	5.2
38	34	54	80	17.9	18	17	24
39	34	60	88	13.8	18	20	26
40	42	53	90	16.7	16	19	32

Table 8. Summary of backcalculation results from testing on sections with thin granular layers.

TS	300 mm sensor moduli			1800 mm sensor moduli (MPa)		
	Subgrade ¹ E_{300} (MPa)	Post-base ² E_{300b} (MPa)	Relative Change ³ (percent)	Subgrade ¹ E_{1800} (MPa)	Post-base ² E_{1800b} (MPa)	Relative Change ³ (percent)
6	27	47	76	116	91	-21
11	104	45	-57	196	164	-16
12	22	42	91	145	154	7
13	51	43	-16	99	131	33
24	61	121	99	82	116	41
36	92	103	12	110	109	-1
38	25	34	37	56	73	30
39	22	34	54	77	78	1
40	20	46	127	76	83	10

NOTES:

[1] E_{300} , E_{1800} = Pre-base subgrade moduli from 300 and 1800 mm sensors, respectively.

[2] E_{300b} , E_{1800b} = Post-base subgrade moduli from 300 and 1800 mm sensors, respectively.

[3] Relative Change values were calculated as follows: $100 \frac{E_{after} - E_{before}}{E_{before}}$

Table 9. Summary of backcalculation data from all conventional flexible test sections.

TS	Pre-base Moduli and Stresses ¹				Post-base Moduli and Stresses ²				Post-pavement Moduli and Stresses ³		
	E_{300} (MPa)	σ_d^A (kPa)	E_{1800} (MPa)	σ_d^B (kPa)	E_2 (MPa)	E_3 (MPa)	σ_d^A (kPa)	σ_d^B (kPa)	E_3 (MPa)	σ_d^A (kPa)	σ_d^B (kPa)
1	33	39	97	18		162	19	18	183	21	20
2	20	40	77	19		147	20	18	177	21	20
3	28	39	74	18		189	19	20	196	21	22
16	37	34	67	16		142	18	17	184	19	20
17	52	36	83	17		145	18	17	192	19	20
18	96	37	107	17		108	21	15	165	17	18
19	35	33	77	16		155	18	17	209	19	20
20	38	34	69	16		149	18	17	186	21	20
21	87	36	122	16		141	21	16	198	20	18
22	57	36	151	16		139	23	14	221	19	16
23	35	43	131	20					231	13	14
24	66	37	85	17					147	16	11
27	25	39	142	18	28	111	26	12	141	20	13
28	48	43	151	20		122	25	13	159	21	13
29	62	35	115	16	34	143	22	12	187	17	13
30	62	34	121	16		104	19	13	152	19	14
31	59	35	114	16		121	24	14	169	23	14

NOTES:

- [1] E_{300}, E_{1800} = Subgrade moduli from 300 and 1800 mm sensors, respectively.
 σ_d^A, σ_d^B = Deviator stress at Points A and B, respectively (see Fig. 72a).
- [2] E_2 = Modulus of the intermediate subgrade, where applicable (see Fig. 71c).
 E_3 = Subgrade modulus.
 σ_d^A, σ_d^B = Deviator stress at Points A and B, respectively (see Fig. 72b).
- [3] E_3 = Subgrade modulus.
 σ_d^A, σ_d^B = Deviator stress at Points A and B, respectively (see Fig. 72c).

Table 10. Summary of average backcalculation data from all full-depth sections.

TS	Pre-base Moduli and Stresses ¹				Post-pavement Moduli and Stresses ²			
	E_{300} (MPa)	σ_d^A (kPa)	E_{1800} (MPa)	σ_d^B (kPa)	E_2 (MPa)	σ_d^A (kPa)	E_3 (MPa)	σ_d^B (kPa)
4	25	40	94	19	107	13	215	12
14	61	36	115	16	114	12	287	13
15	72	35	112	16	110	11	279	13
25	83	38	87	18	104	13	115	11
26	19	38	75	17	88	12	147	11

NOTES:

- [1] E_{300}, E_{1800} = Subgrade moduli from 300 and 1800 mm sensors, respectively.
 σ_d^A, σ_d^B = Deviator stress at Points A and B, respectively (see Fig. 72a).
- [2] E_2 = Modulus of the intermediate subgrade, where applicable (see Fig. 71g).
 E_3 = Subgrade modulus.
 σ_d^A, σ_d^B = Deviator stress at Points A and B, respectively (see Fig. 72d).

Table 11. Summary of subgrade modulus and deviator stress changes for all conventional, flexible test sections, at different construction stages.

TS	Percent change in backcalculated subgrade modulus and deviator stress					
	Pre-base (<i>SG</i>) to Post-base (<i>BS</i>)		Post-base (<i>BS</i>) to Post-pavement (<i>AC</i>)		Pre-base (<i>SG</i>) to Post-pavement (<i>AC</i>)	
	$E_{SG} \rightarrow E_{BS}$	$\sigma_d^{SG} \rightarrow \sigma_d^{BS}$	$E_{BS} \rightarrow E_{AC}$	$\sigma_d^{BS} \rightarrow \sigma_d^{SG}$	$E_{SG} \rightarrow E_{AC}$	$\sigma_d^{SG} \rightarrow \sigma_d^{AC}$
1	91	3	14	11	116	14
2	100	-2	23	11	144	8
3	154	9	5	10	182	21
16	116	9	30	16	178	27
17	103	3	34	16	160	20
18	21	-9	53	16	76	6
19	111	11	35	16	186	28
20	118	9	25	14	170	24
21	20	-4	38	14	73	10
22	1	-11	60	13	60	0
23					83	-32
27	3	-30	27	3	30	-28
28	-14	-34	31	2	13	-33
29	31	-24	30	6	67	-19
30	-17	-18	51	6	28	-13
31	14	-14	38	3	53	-11

Table 12. Summary of backcalculation results from testing on sections after construction of permeable asphalt-stabilized base (PASB).

TS	Pre-base Moduli and Stresses ¹				Post-base (PASB) Moduli and Stresses ²				
	E_{300} (MPa)	σ_d^A (kPa)	E_{1800} (MPa)	σ_d^B (kPa)	E_1 (MPa)	E_2 (MPa)	σ_d^A (kPa)	E_3 (MPa)	σ_d^B (kPa)
7	25	39	70	18	660	35	29	74	11
8	24	37	84	17	1363	32	25	90	11
9	29	37	113	17	3819	46	21	116	11
10	98	37	183	17	521	49	29	196	11

NOTES:

- [1] E_{300}, E_{1800} = Subgrade moduli from 300 and 1800 mm sensors, respectively.
 σ_d^A, σ_d^B = Deviator stress at Points A and B, respectively (see Fig. 72a).
- [2] E_1 = PASB modulus.
 E_2 = Modulus of the intermediate layer (see Fig. 71i).
 E_3 = Subgrade modulus.
 σ_d^A, σ_d^B = Deviator stress at Points A and B, respectively (see Fig. 72b).

Table 13. Effective pavement modulus data for rigid sections.

TS	Subgrade	Base	Rigid	
	E_{SG} (MPa)	E_{SG} (MPa)	E_p (MPa)	E_{SG} (MPa)
5	68	148	2481	195
6	121	91	8866	153
7	71	73	7301	177
8	83	90	7118	174
9	110	115	7506	193
10	205	196	8667	226
11	222	164	9708	190
12	141	154	9874	210
13	89	131	9806	193
36	105	108	7694	126
37	86	125	3019	127
38	58	72	6298	95
39	79	77	6670	111
40	69	83	8909	125

NOTES:

Rigid

E_{SG} , E_p =effective subgrade and pavement modulus as calculated using the AASHTO procedure (15)

Base

E_{SG} =subgrade modulus calculated using either the homogenous model (D_{1800}) or EVERCALC (E_3) as follows:

- | | |
|---|---------------------------|
| TS 5 and 37 (thick granular base): | EVERCALC 3 layer analysis |
| TS 7 through 10 (PASB): | EVERCALC 3 layer analysis |
| TS 6, 11 through 36, 38 through 40 (thin base): | homogenous model |

Subgrade

E_{SG} =subgrade modulus computed from the homogenous model (D_{1800} sensor)

Table 14. Summary of backcalculation results from testing on aggregate and chip-seal test sections.

TS	Pre-base subgrade moduli (MPa) and stresses (kPa) ¹				Post-construction subgrade moduli (MPa) and stresses (kPa) ²		
	E_{300}	σ_d^A	E_{1800}	σ_d^B	E_3	σ_d^A	σ_d^B
32	33	39	92	18	135	39	13
33	55	46	84	21	100	48	13
34	32	44	69	20	128	49	13
35	56	45	111	21	155	48	13

NOTES:

- [1] E_{300} , E_{1800} = Subgrade moduli from 300 and 1800 mm sensors, respectively.
 σ_d^A , σ_d^B = Deviator stress at Points A and B, respectively (see Fig. 72a).
- [2] E_2 = Modulus of the intermediate subgrade, where applicable (see Fig. 71g).
 E_3 = Subgrade modulus.
 σ_d^A , σ_d^B = Deviator stress at Points A and B, respectively (see Fig. 72e).

Table 15. Summary of subgrade modulus and stress changes for the aggregate and chip-seal test sections.

TS	Percent change in backcalculated subgrade modulus and deviator stress			
	Percent change, Point A ¹ (300 mm offset)		Percent change, Point B ¹ (1800 mm offset)	
	$E_{300} \rightarrow E_3$	$\sigma_d^{SG} \rightarrow \sigma_d^{Agg}$	$E_{1800} \rightarrow E_3$	$\sigma_d^{SG} \rightarrow \sigma_d^{Agg}$
32	344	-1	52	-29
33	131	5	19	-38
34	340	12	88	-35
35	191	9	42	-37

NOTES:

- [1] Stress evaluation locations (see Fig. 72a and b).
 E_{300} , E_{1800} = Subgrade moduli from 300 and 1800 mm sensors, respectively.
 E_3 = Subgrade modulus from post-base (PASB) testing.
 σ_d^{SG} = Deviator stress from pre-base testing.
 σ_d^{Agg} = Deviator stress from post-base (PASB) testing.

Table 16. Summary of average test section results for backcalculation analyses of granular base materials.

TS	Base ¹				Pavement ²		
	E_1 (MPa)	θ^A (kPa)	E_2 (MPa)	θ^B (kPa)	E_2 (MPa)	θ^A (kPa)	θ^B (kPa)
1	97	126	140	52	105	65	60
2	134	138	134	52	106	63	58
3	139	120	152	51	134	62	57
5	137	145	239	49			
16	96	126	129	51	153	56	52
17	97	129	144	52	128	55	53
18	176	163	59	68	82	54	54
19	120	121	133	50	131	56	54
20	146	123	151	48	134	65	59
21	149	161	89	65	116	69	64
22	348	157	37	81	61	72	71
23					44	75	75
24					166	316	267
27	83	195		115	33	163	153
28	370	152	17	110	41	151	138
29	257	205		82	31	123	121
30	602	116	10	84	43	112	107
31	300	161	26	93	74	140	119

NOTES:

- [1] E_1 = Granular base modulus.
 E_2 = Subgrade modulus.
 θ^A, θ^B = Bulk stress at Points A and B, respectively (see Fig. 72b).
- [2] E_2 = Granular base modulus.
 θ^A, θ^B = Bulk stress at Points A and B, respectively (see Fig. 72c).

MnROAD

Minnesota Road Research Project

Cell Locations



- 1-4 - Bituminous
- 5-9 - Concrete
- 10-13 - Concrete
- 14-23 - Bituminous
- 24-31 - Bituminous
- 32-35 - Aggregate
- 36-40 - Concrete
- 41-46 - Concrete Loops

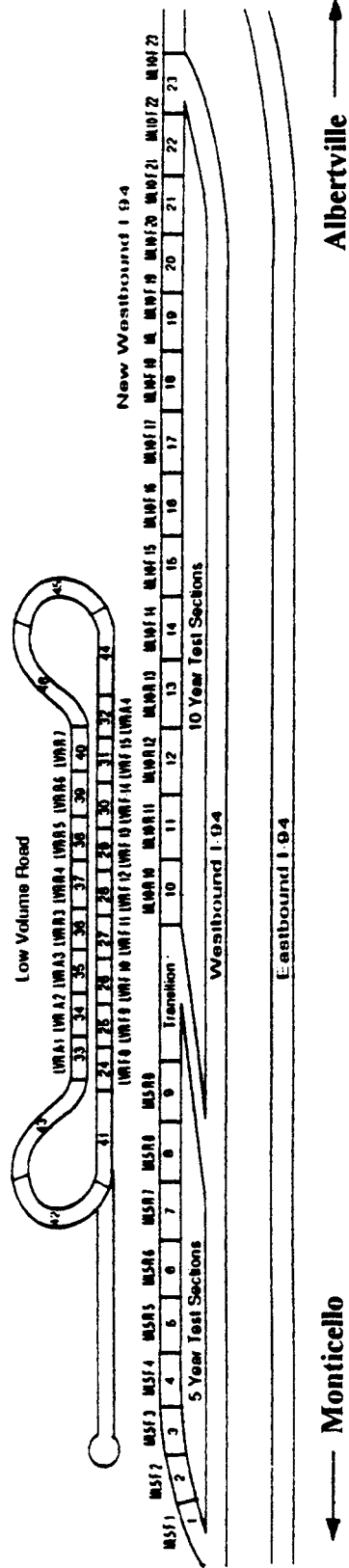
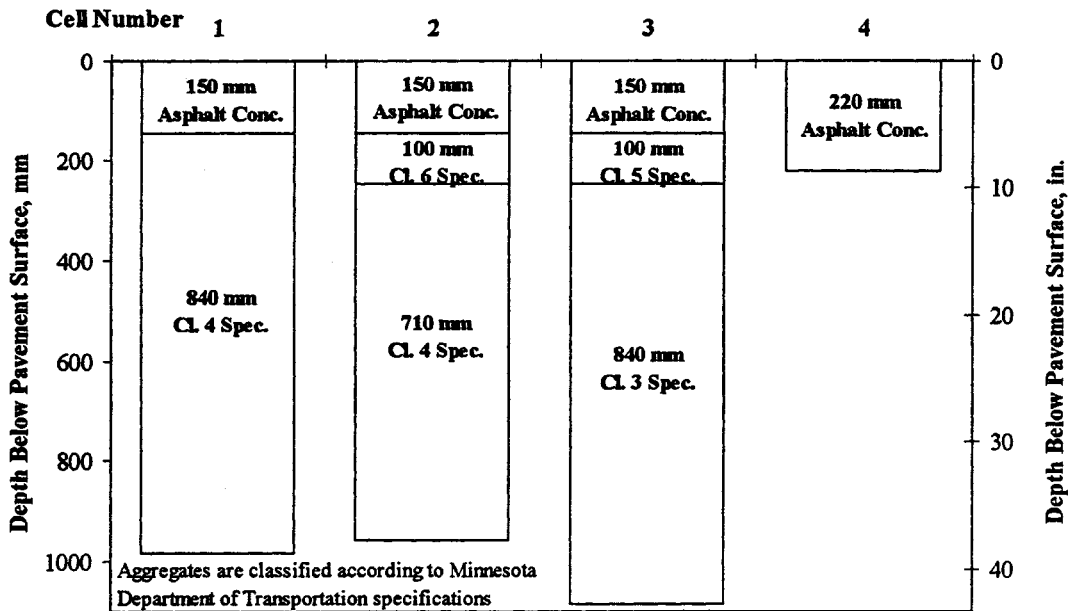


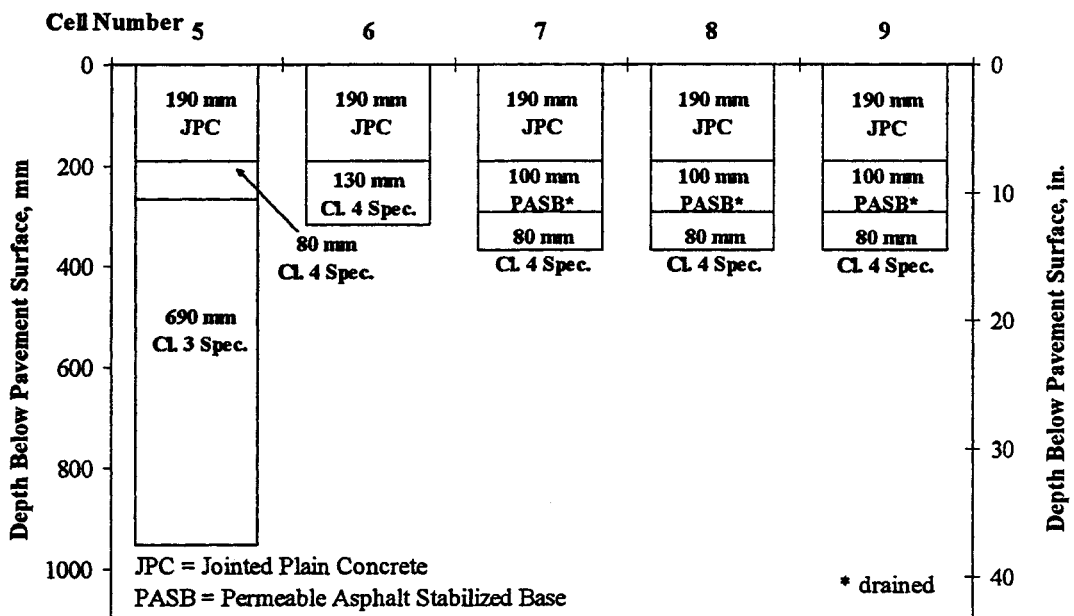
Fig. 1. Location and site layout for the Mn/ROAD project.

**5-Year Mainline Bituminous Test Sections
Cells 1 - 4**



(a)

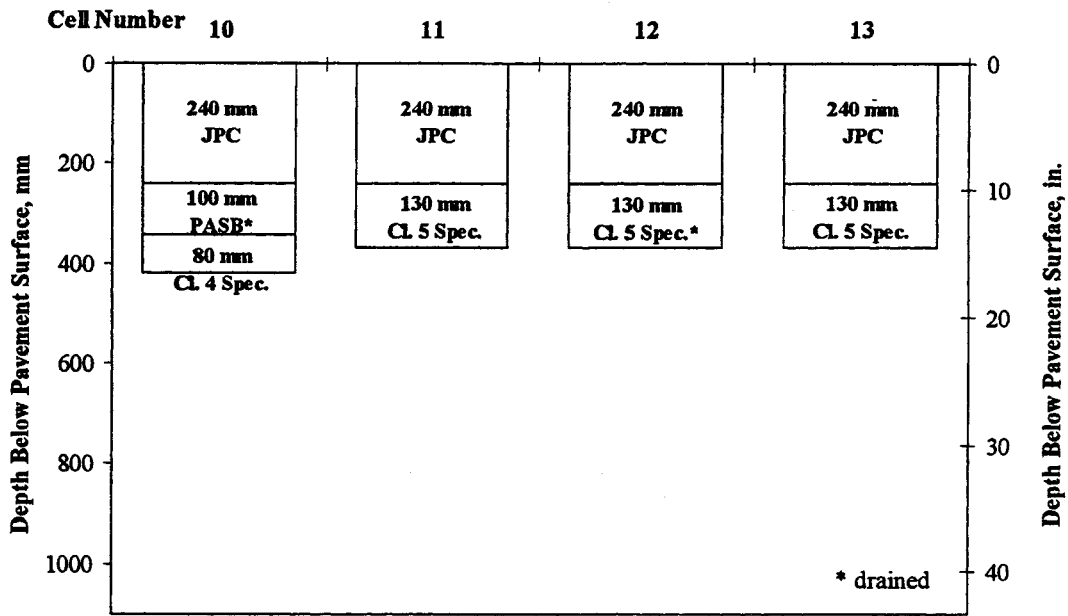
**5-Year Mainline Concrete Test Sections
Cells 5 - 9**



(b)

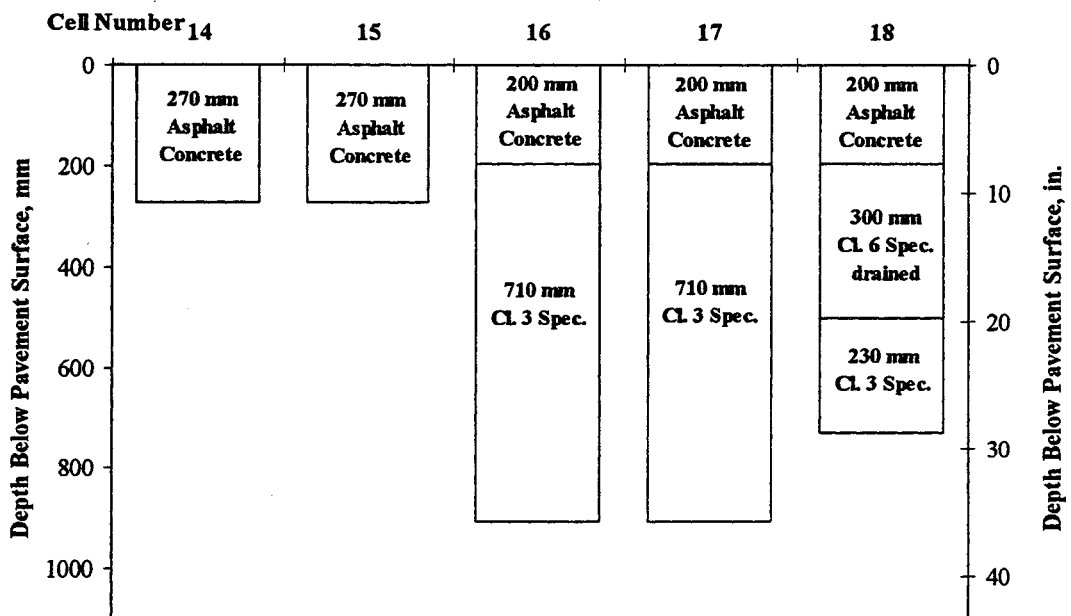
Fig. 2. Mn/ROAD test section diagrams.

**10-Year Mainline Concrete Test Sections
Cells 10 - 13**



(c)

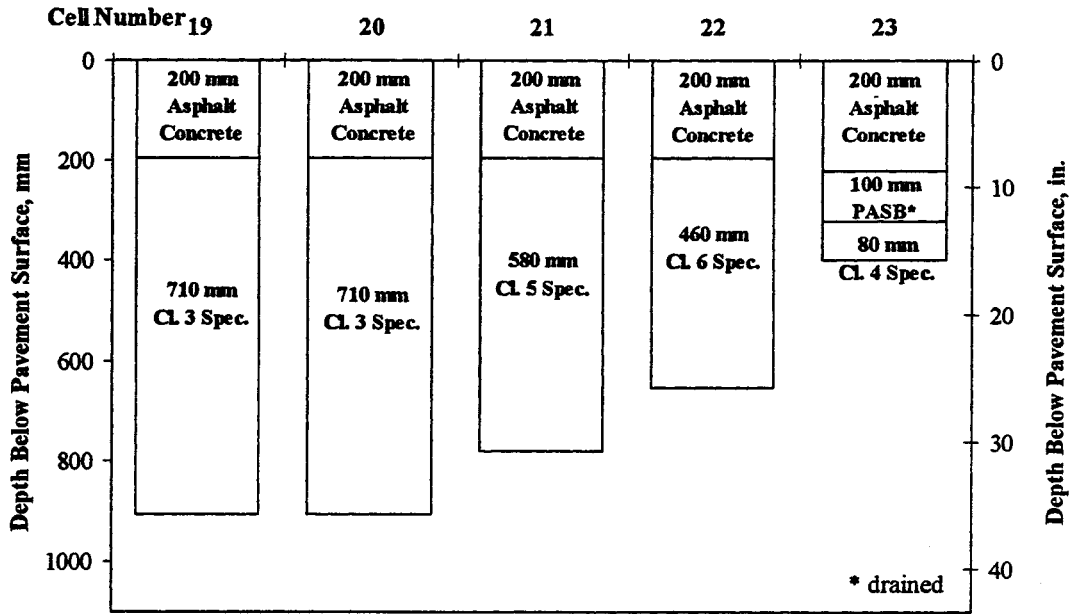
**10-Year Mainline Bituminous Test Sections
Cells 14 - 18**



(d)

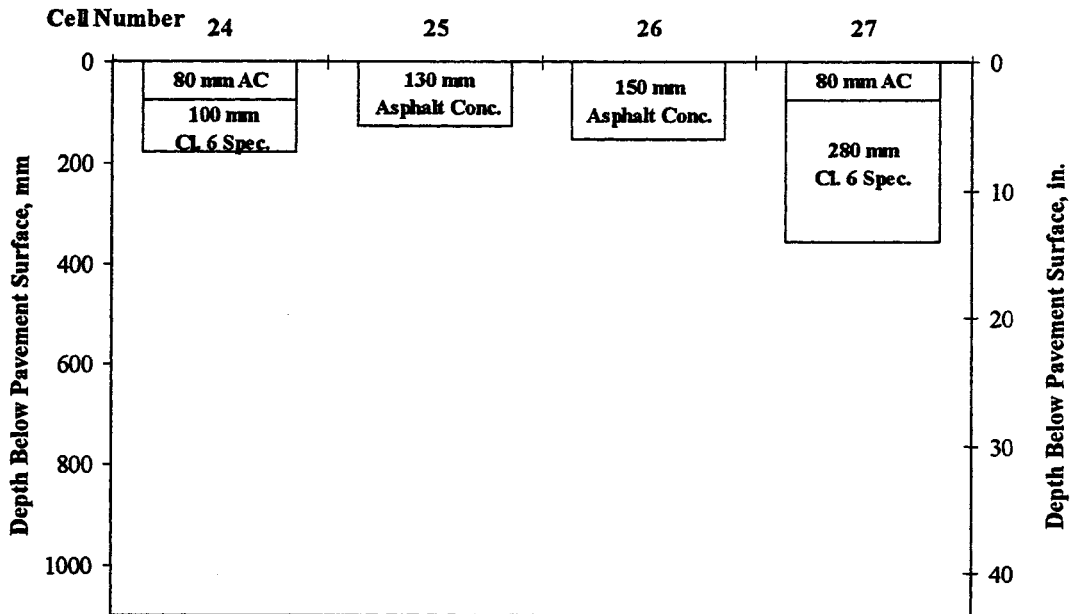
Fig. 2, cont. Mn/ROAD test section diagrams.

**10-Year Mainline Bituminous Test Sections
Cells 19 - 23**



(e)

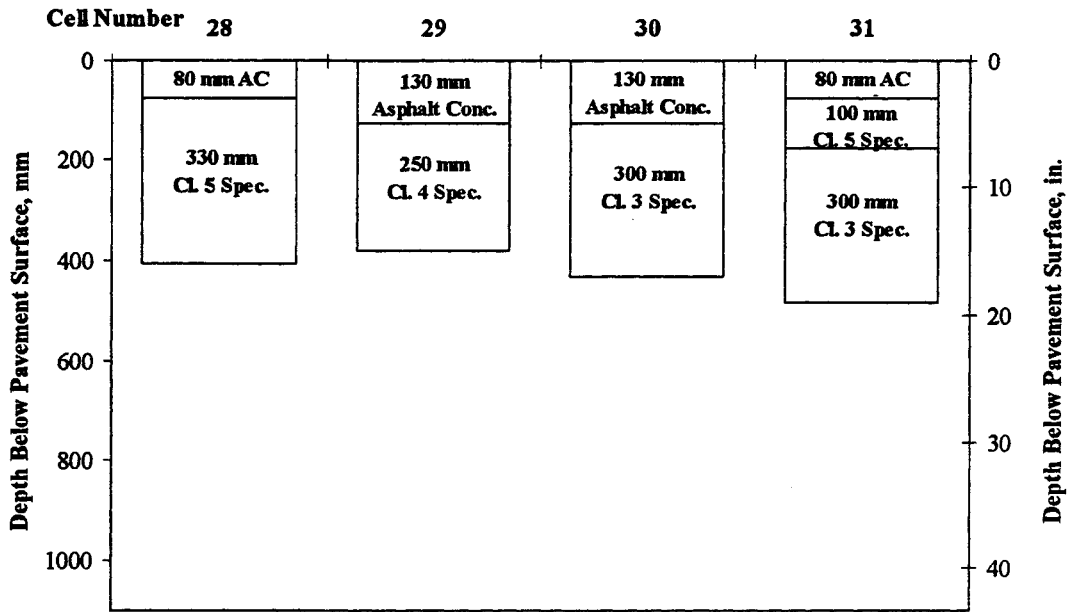
**Low Volume Road Bituminous Test Sections
Cells 24 - 27**



(f)

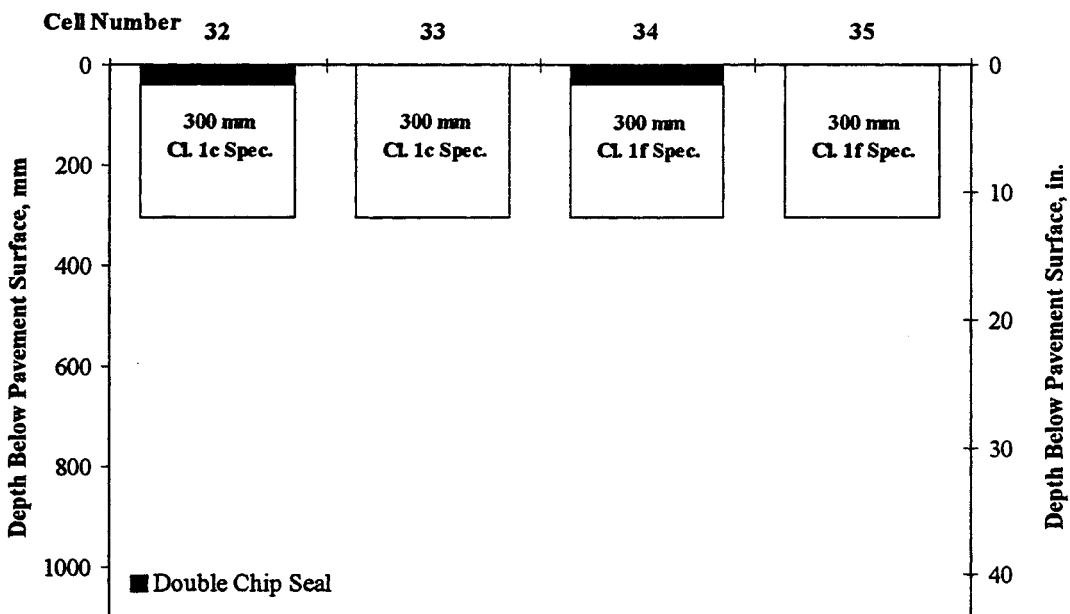
Fig. 2, cont. Mn/ROAD test section diagrams.

**Low Volume Road Bituminous Test Sections
Cells 28 - 31**



(g)

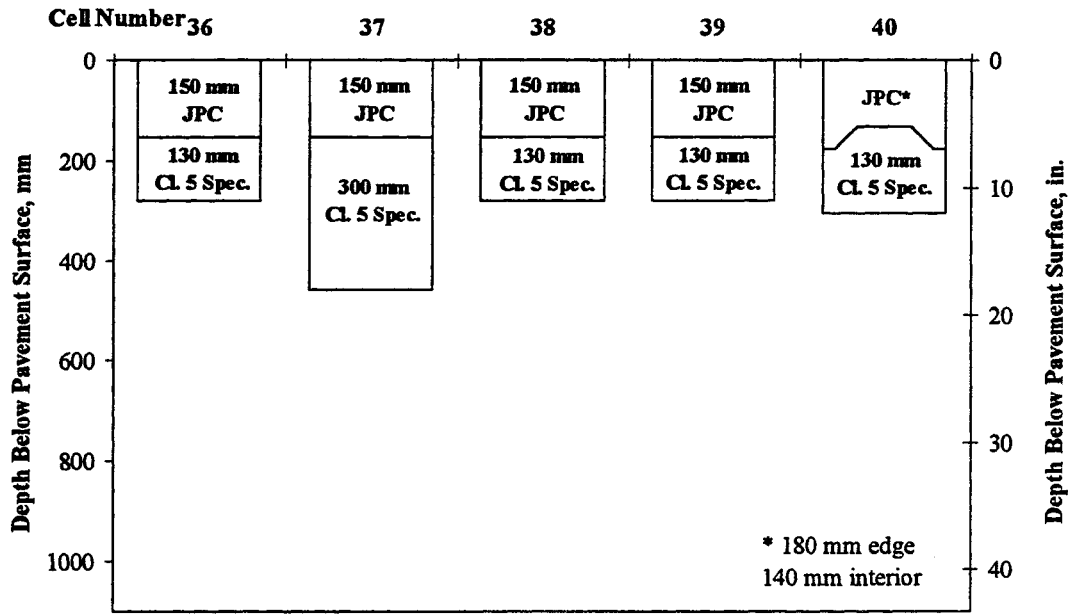
**Low Volume Road Aggregate Test Sections
Cells 32 - 35**



(h)

Fig. 2, cont. Mn/ROAD test section diagrams.

**Low Volume Road Concrete Test Sections
Cells 36 - 40**



(i)

Fig. 2, cont. Mn/ROAD test section diagrams.

COMPARISON OF FWD DEFLECTIONS

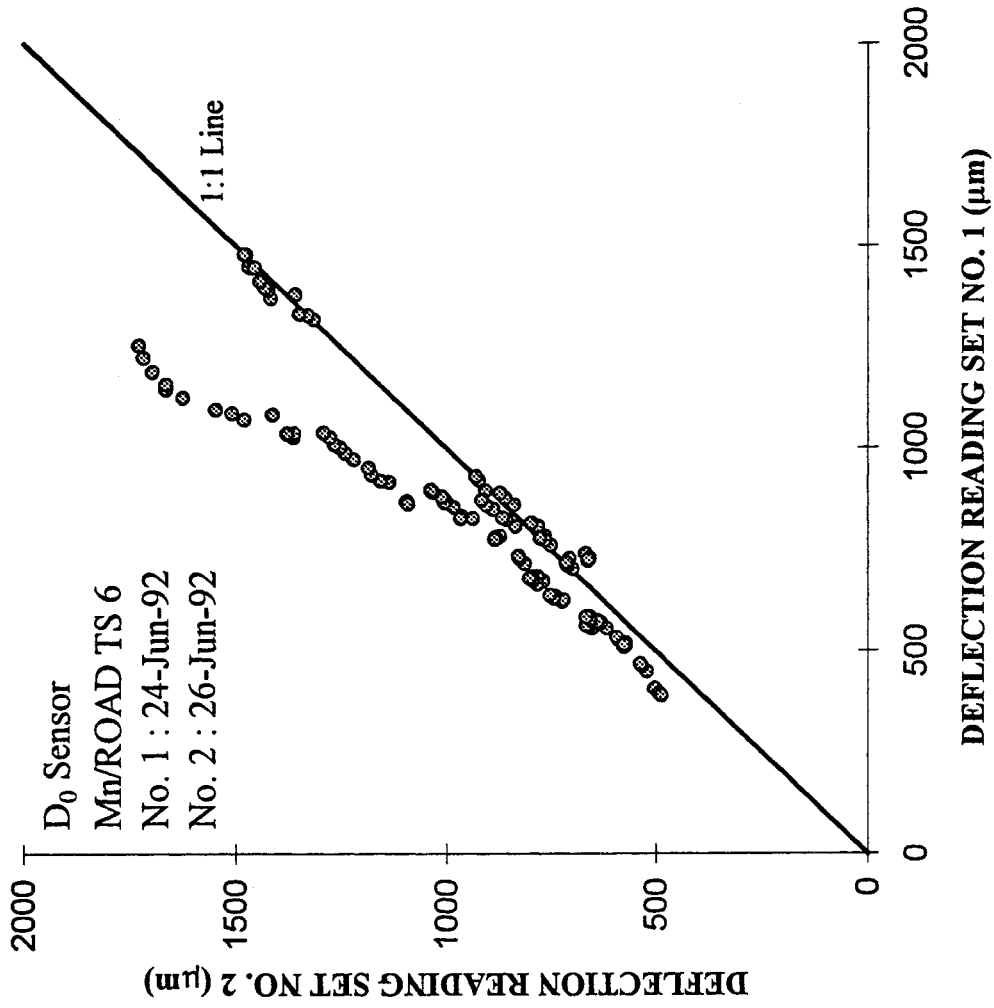


Fig. 3. Comparison of FWD deflections for TS 6, D₀ sensor, taken two days apart.

COMPARISON OF FWD DEFLECTIONS

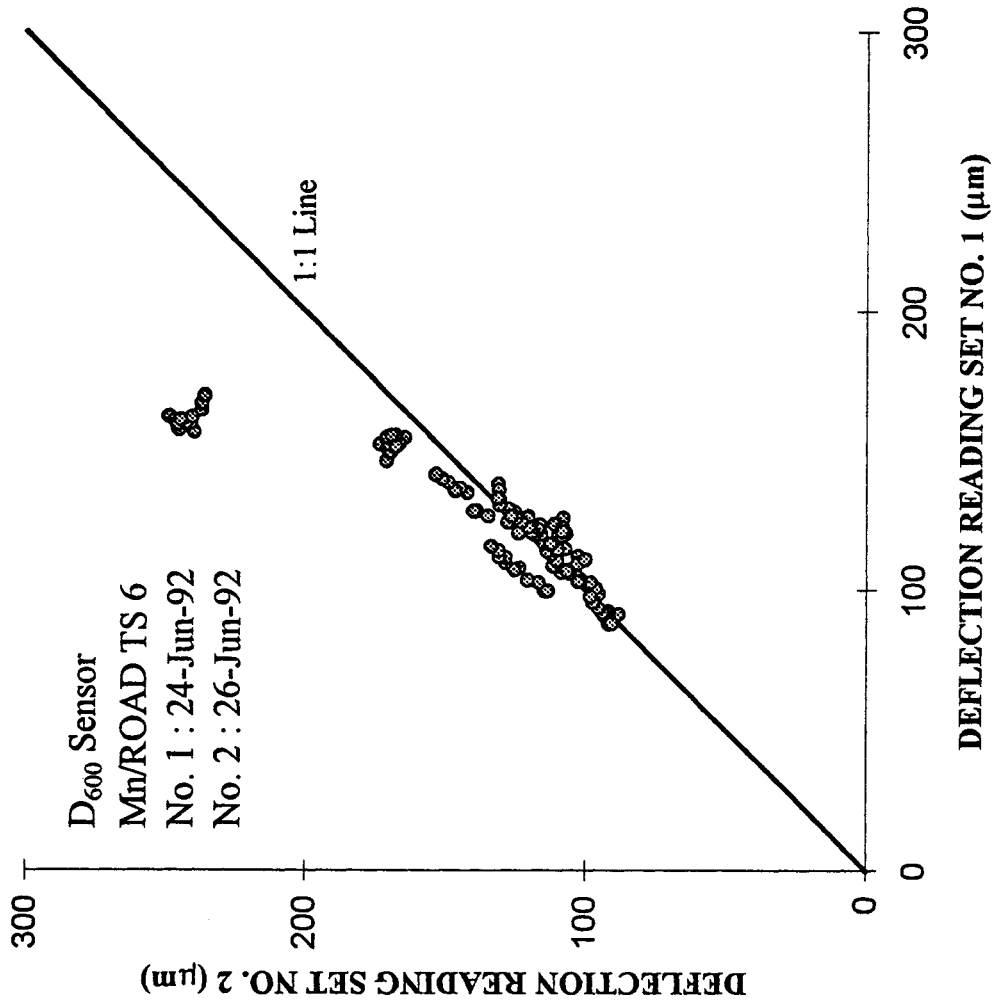


Fig. 4. Comparison of FWD deflections for TS 6, D₆₀₀ sensor, taken two days apart.

COMPARISON OF FWD DEFLECTIONS

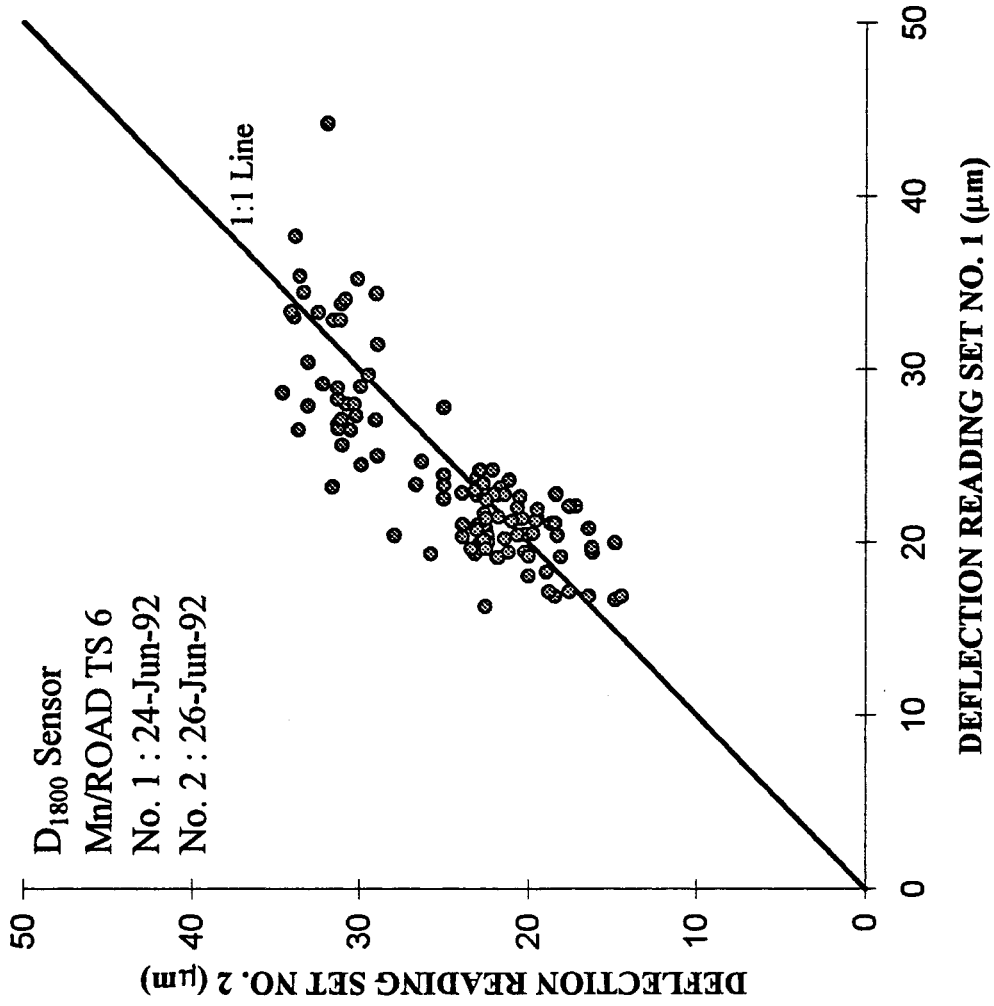


Fig. 5. Comparison of FWD deflections for TS 6, D₁₈₀₀ sensor, taken two days apart.

COMPARISON OF FWD DEFLECTIONS

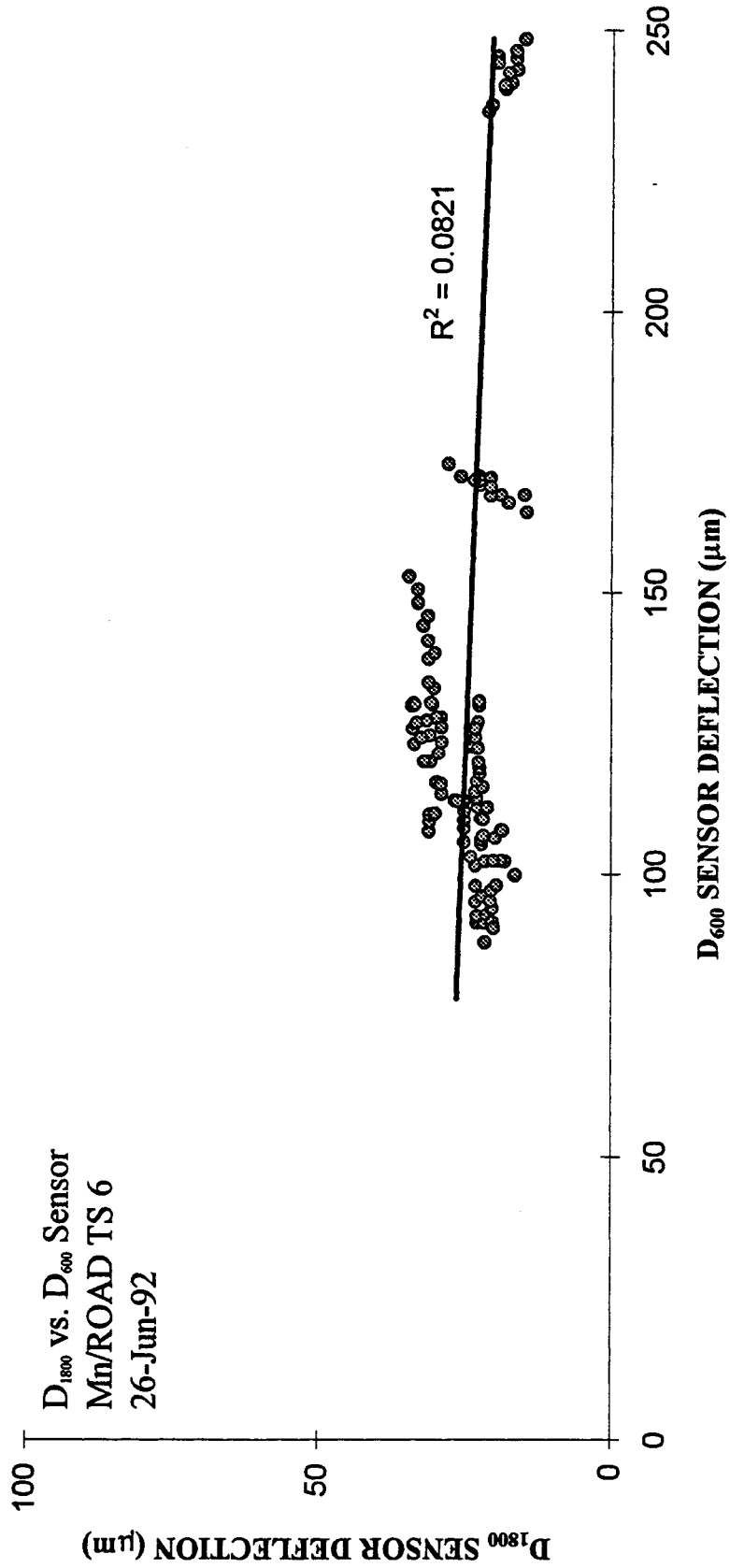


Fig. 6. Relationship between D_{1800} and D_{600} sensor deflections, TS 6 variability study.

COMPARISON OF FWD DEFLECTIONS

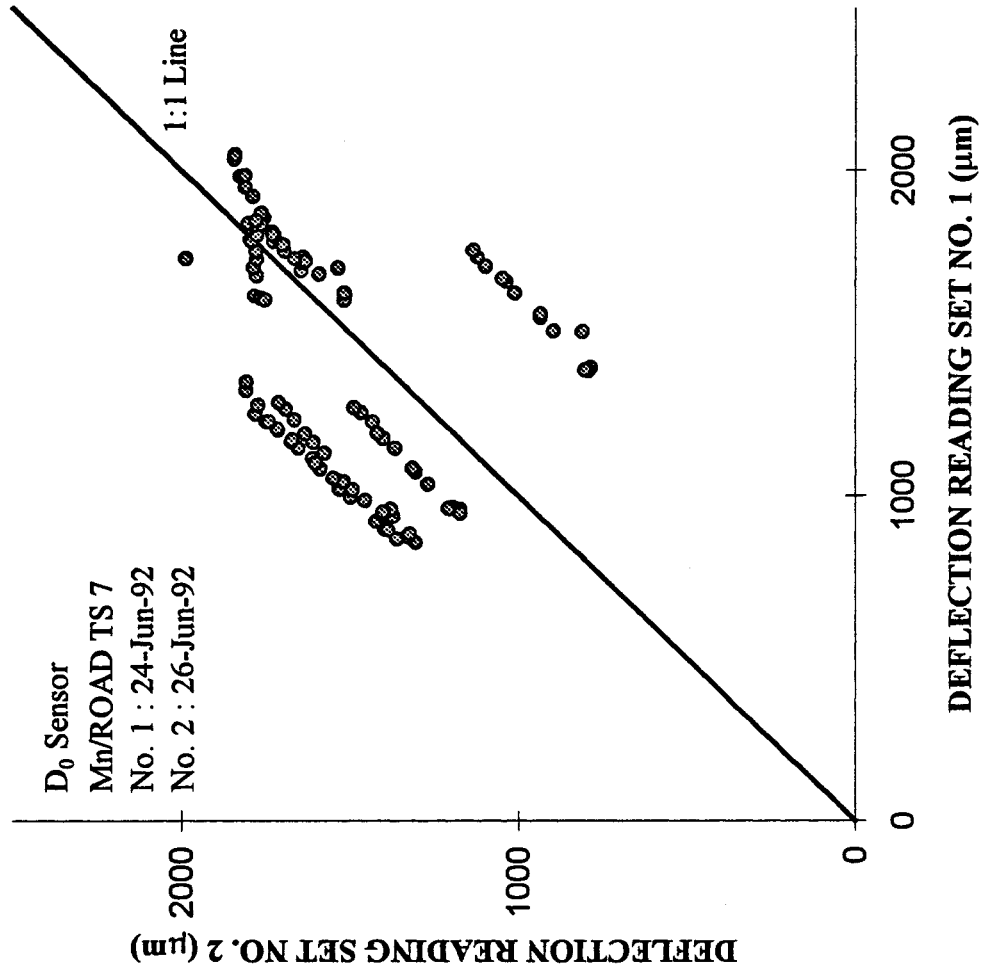


Fig. 7. Comparison of FWD deflections for TS 7, D₀ sensor, taken two days apart.

COMPARISON OF FWD DEFLECTIONS

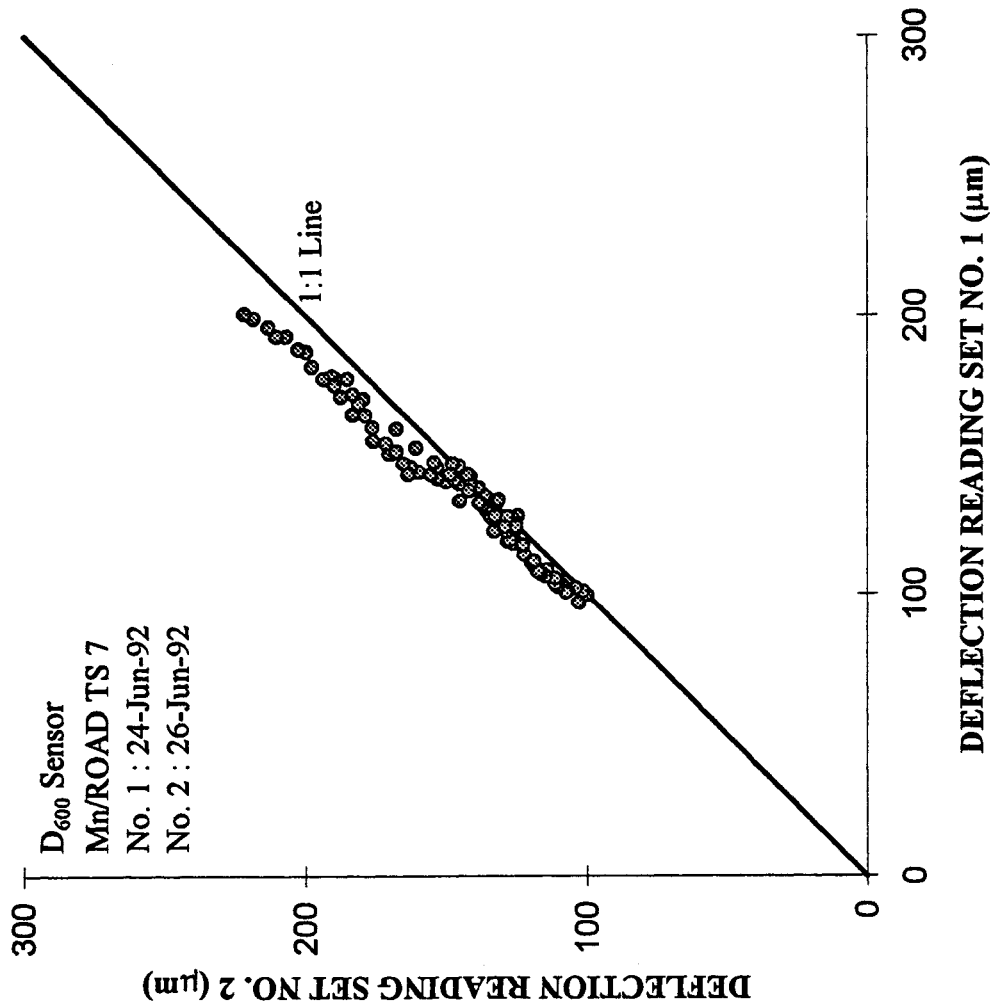


Fig. 8. Comparison of FWD deflections for TS 7, D₆₀₀ sensor, taken two days apart.

COMPARISON OF FWD DEFLECTIONS

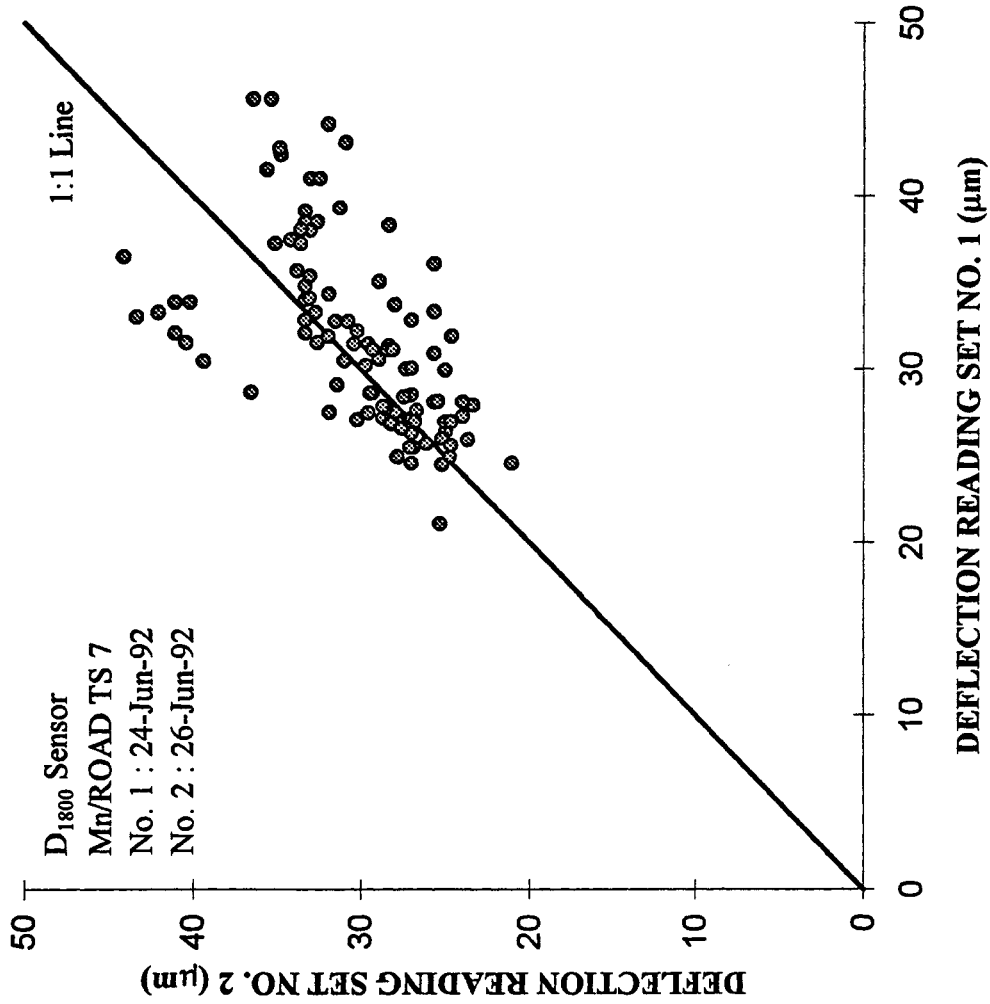


Fig. 9. Comparison of FWD deflections for TS 7, D₁₈₀₀ sensor, taken two days apart.

COMPARISON OF FWD DEFLECTIONS

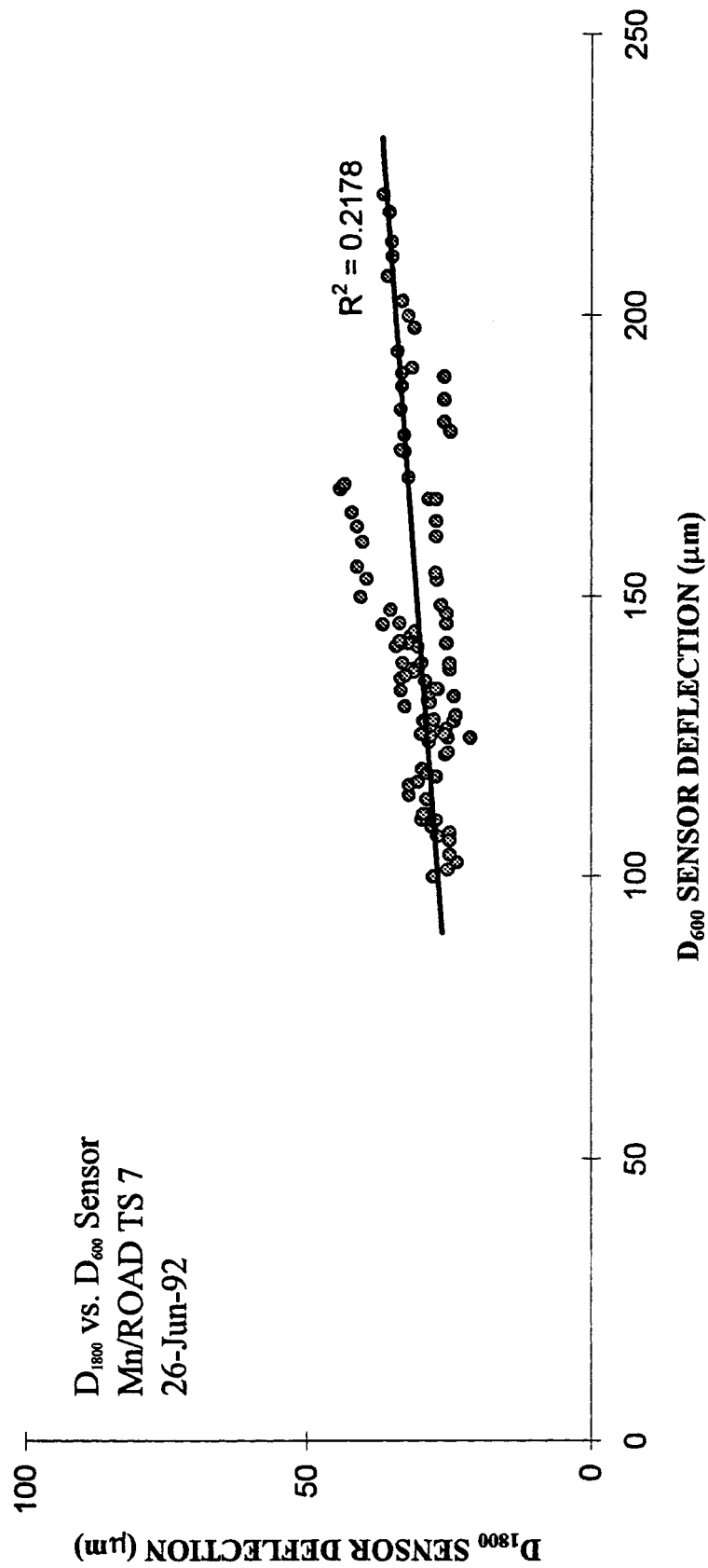


Fig. 10. Relationship between D_{1800} and D_{600} sensor deflections, TS 7 variability study.

APPARENT VARIATION IN MODULUS WITH DEPTH (SENSOR OFFSET)

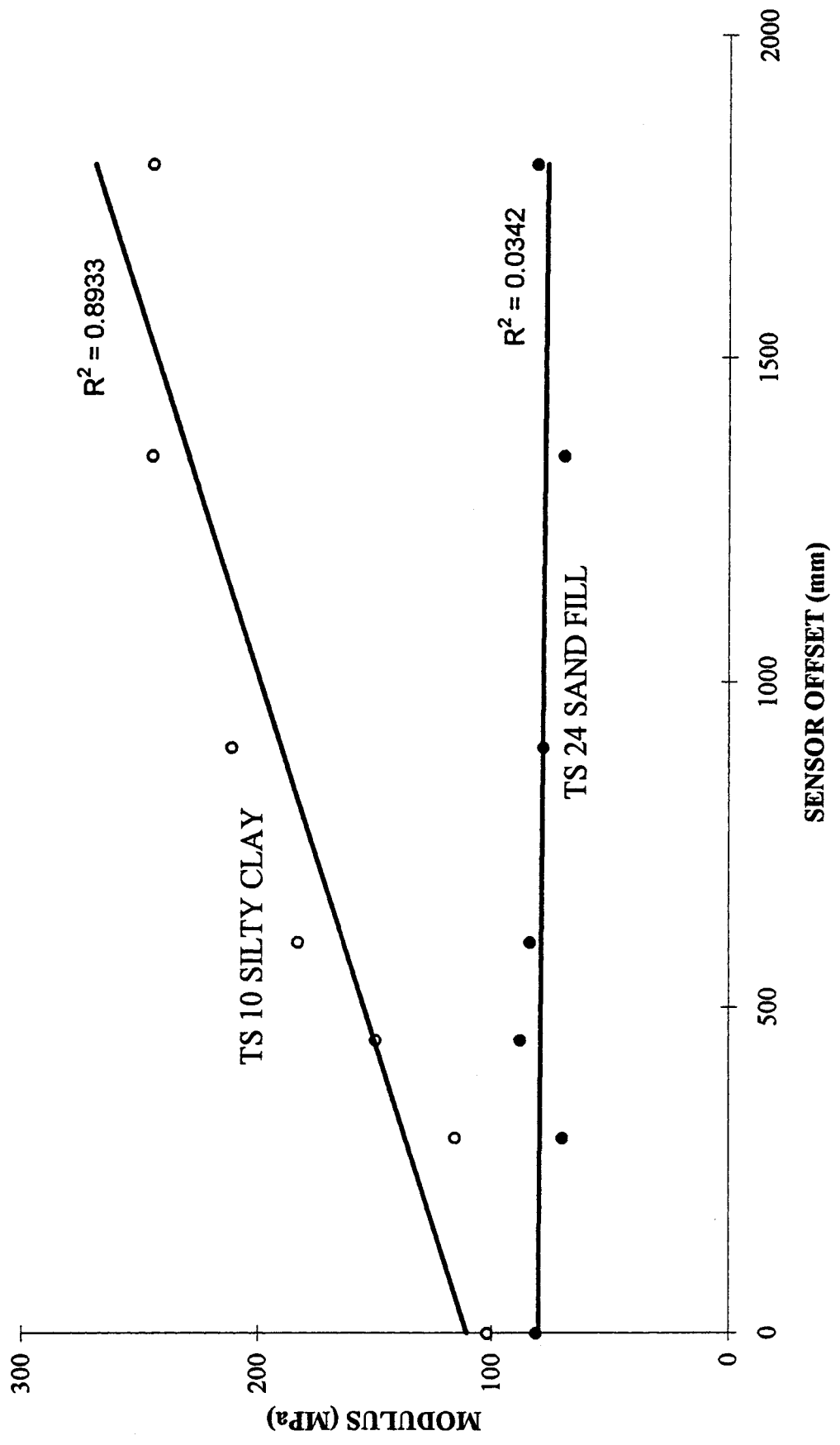


Fig. 11. Backcalculated moduli for all sensor offsets from TS 10 and 24.

VARIATION OF SUBGRADE MODULUS WITH STATION

MAINLINE TEST SECTIONS
LANE 1

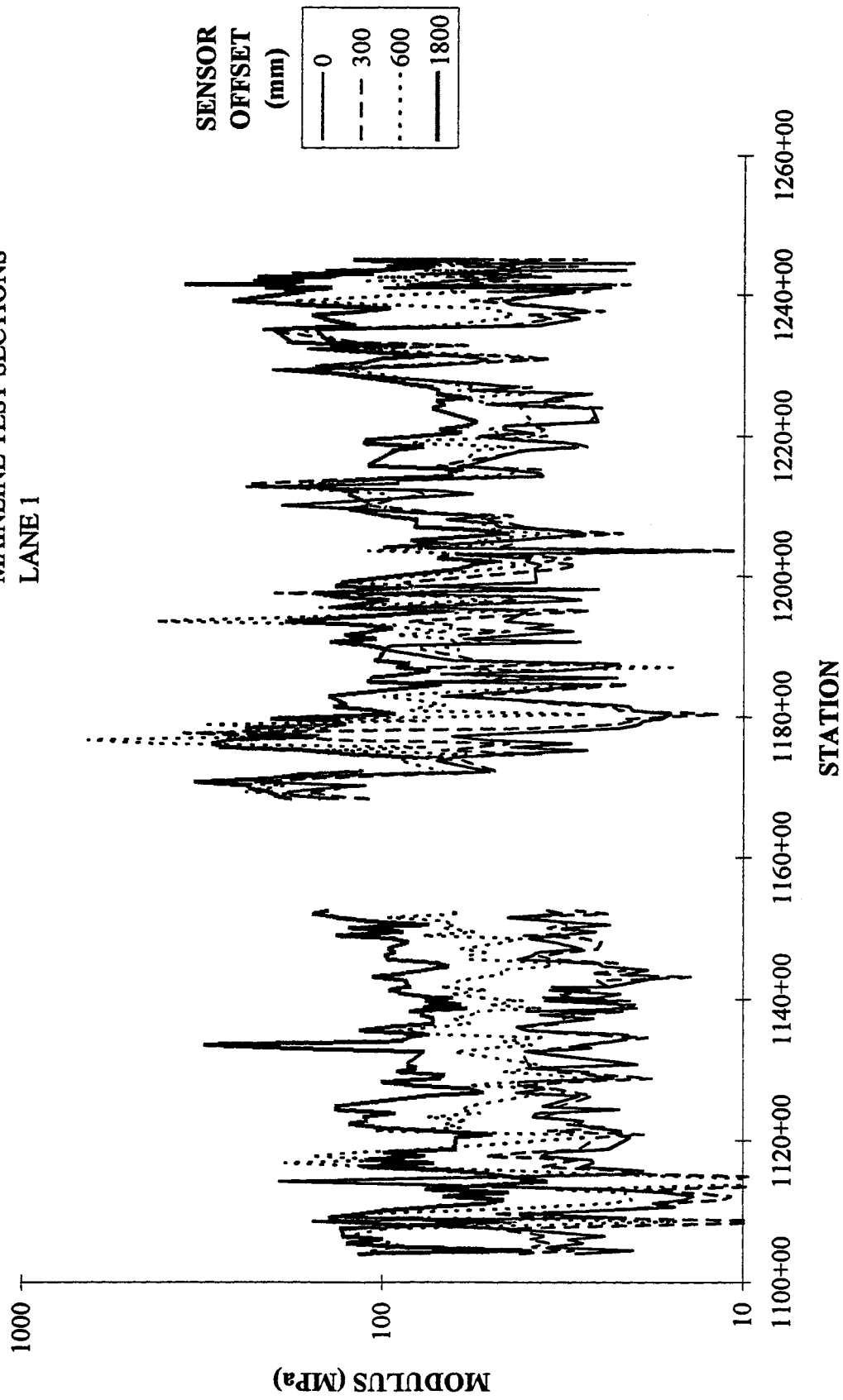


Fig. 12. Variation of backcalculated subgrade moduli for mainline test sections, lane 1.

VARIATION OF SUBGRADE MODULUS WITH STATION

MAINLINE TEST SECTIONS
LANE 4

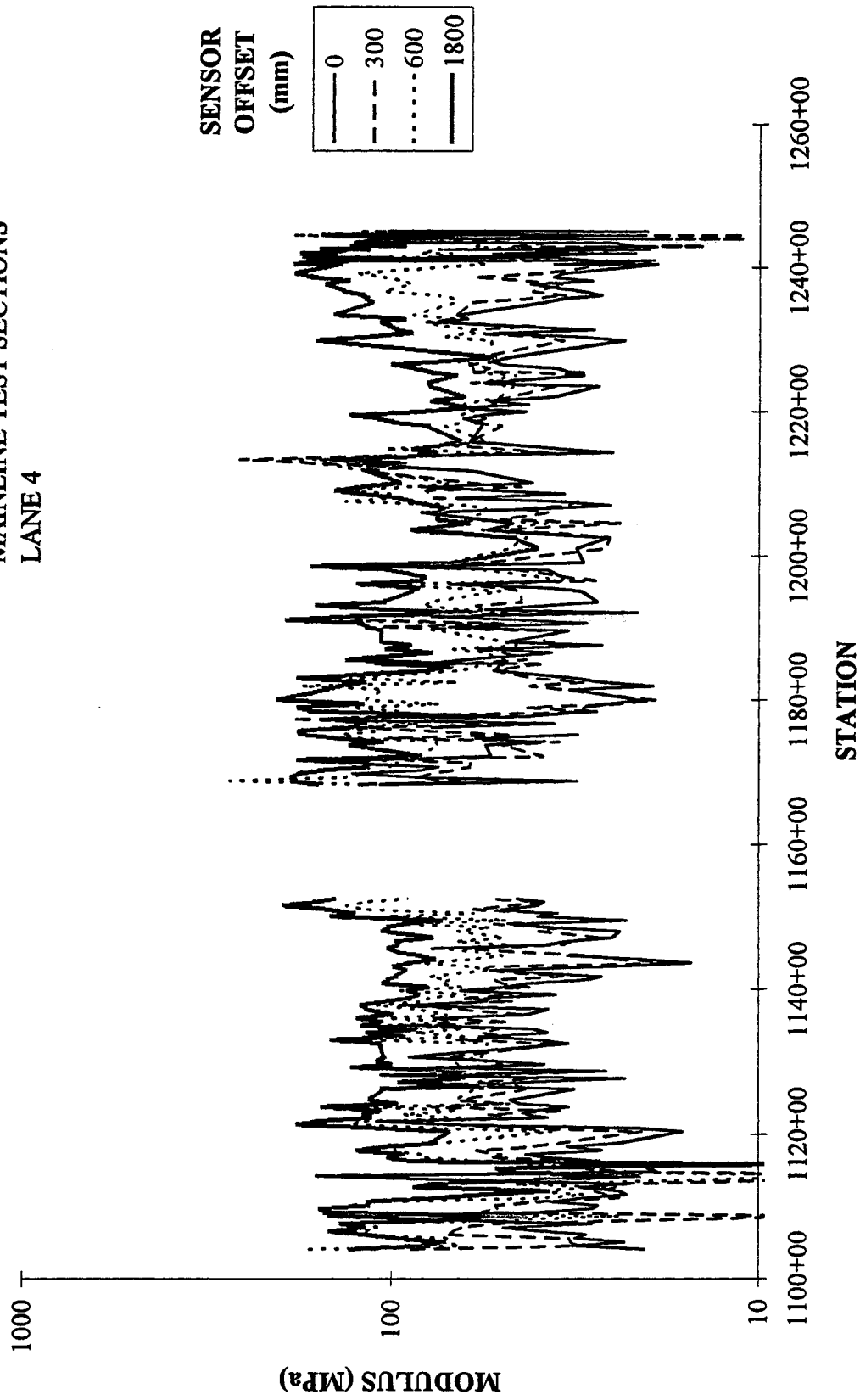


Fig. 13. Variation of backcalculated subgrade moduli for mainline test sections, lane 4.

VARIATION OF SUBGRADE MODULUS WITH STATION

MAINLINE TEST SECTIONS
LANE 7

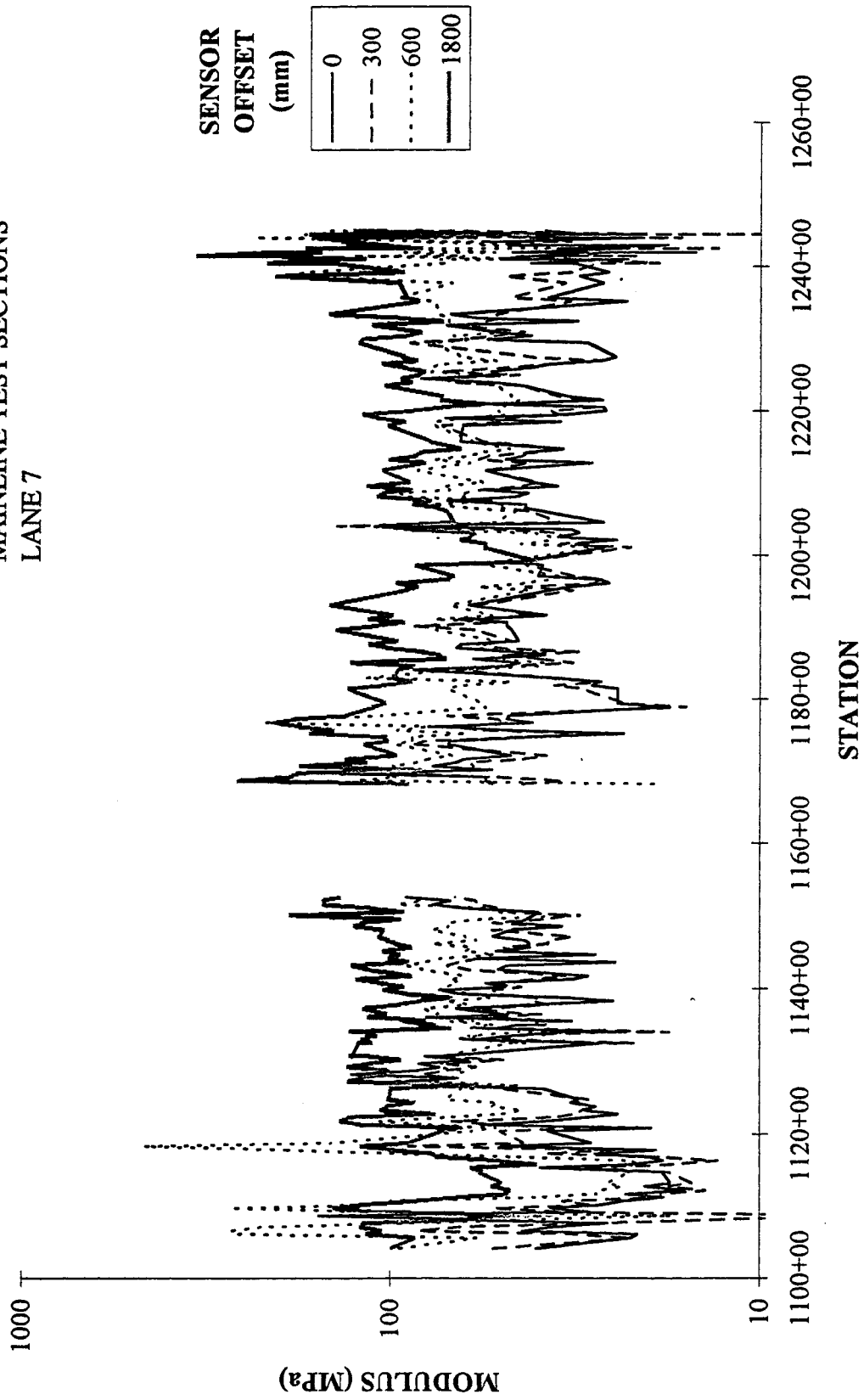


Fig. 14. Variation of backcalculated subgrade moduli for mainline test sections, lane 7.

VARIATION OF SUBGRADE MODULUS WITH STATION

LOW-VOLUME TEST SECTIONS
LANE 1

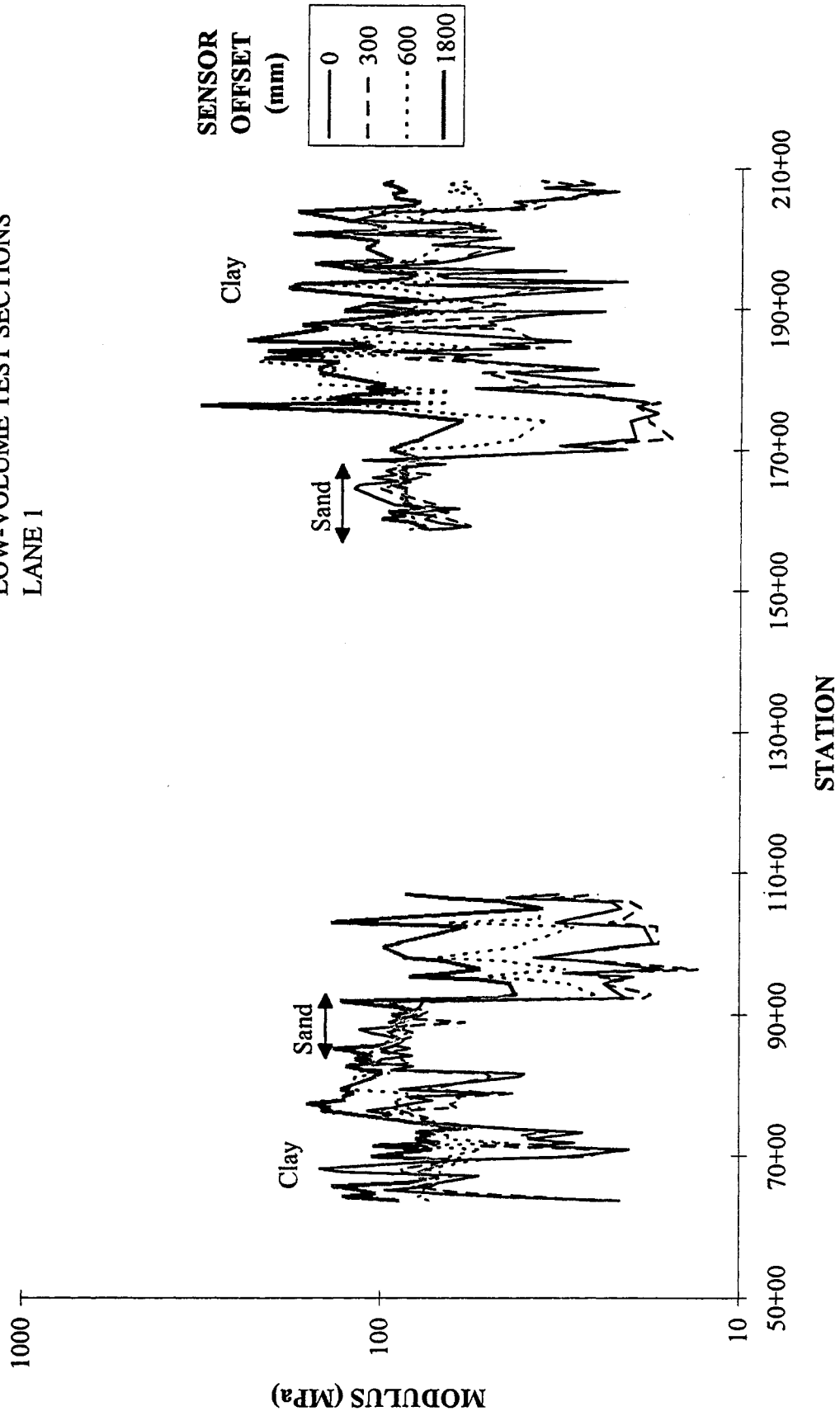


Fig. 15. Variation of backcalculated subgrade moduli for low-volume test sections, lane 1.

VARIATION OF SUBGRADE MODULUS WITH STATION

LOW-VOLUME TEST SECTIONS
LANE 4

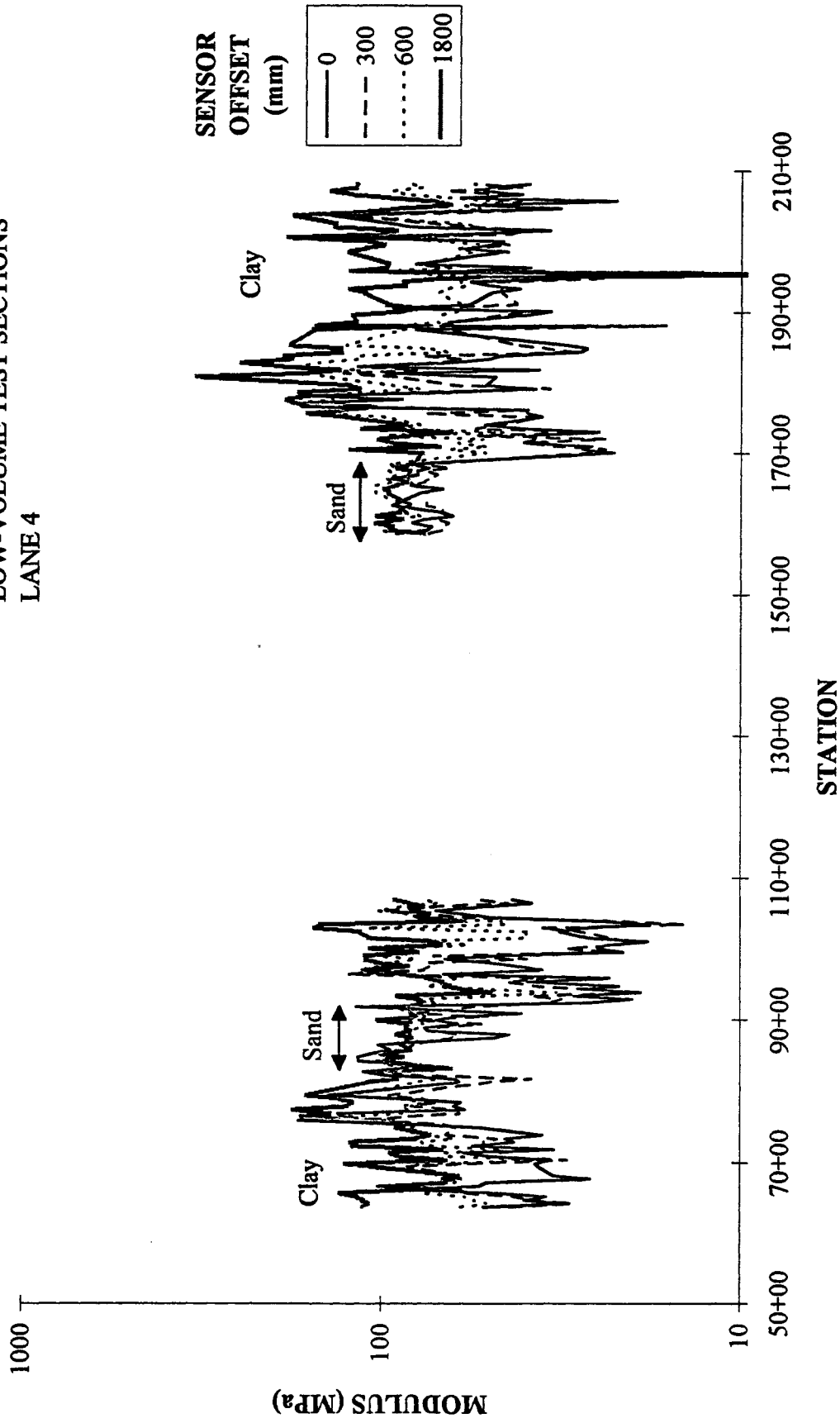


Fig. 16. Variation of backcalculated subgrade moduli for low-volume test sections, lane 4.

VARIATION OF SUBGRADE MODULUS WITH STATION

LOW-VOLUME TEST SECTIONS
LANE 7

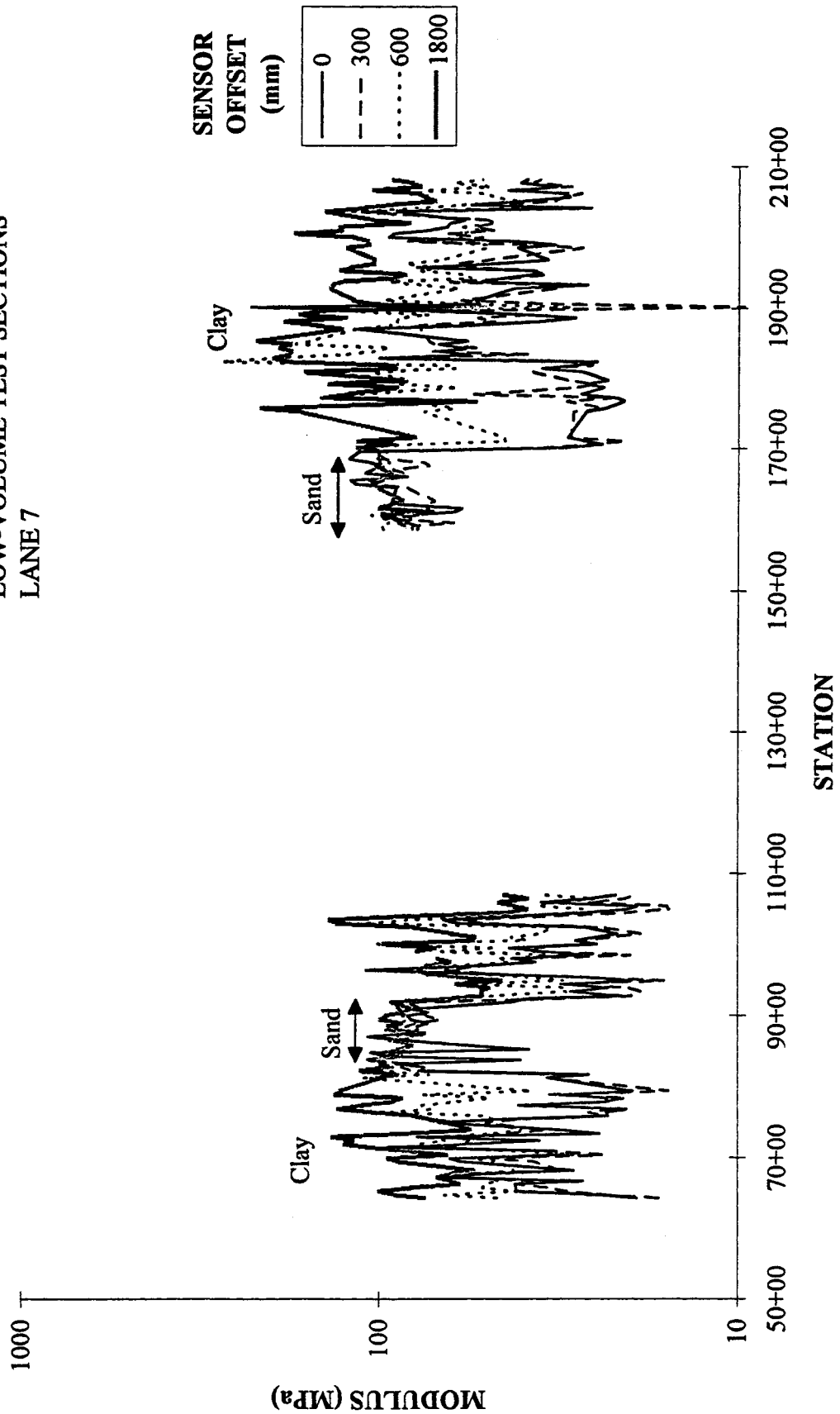


Fig. 17. Variation of backcalculated subgrade moduli for low-volume test sections, lane 7.

AVERAGE MODULUS FOR MAINLINE TEST SECTIONS

HOMOGENEOUS MODEL
LANE 1

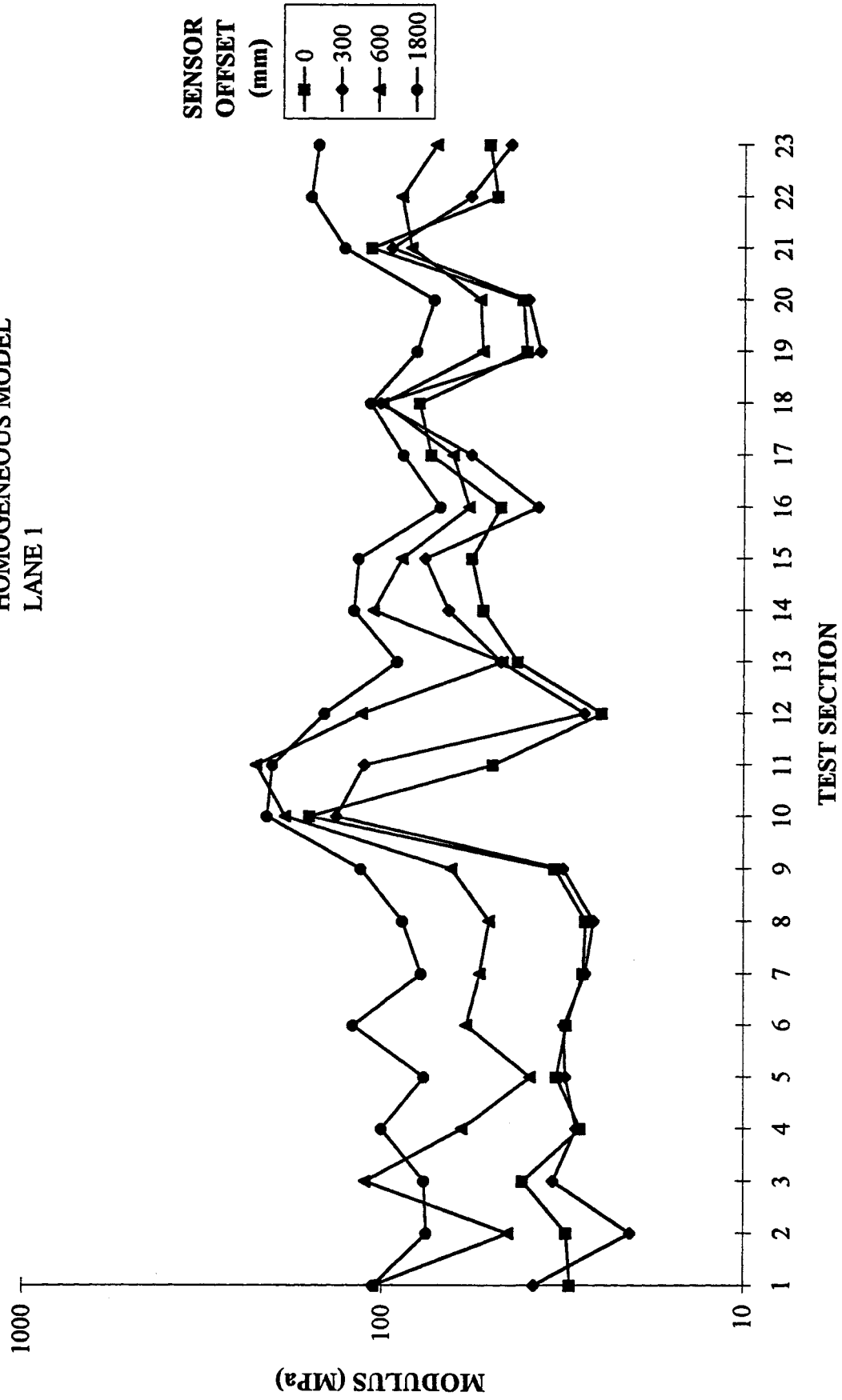


Fig. 18. Average backcalculated subgrade moduli for mainline test sections, lane 1.

AVERAGE MODULUS FOR MAINLINE TEST SECTIONS

**HOMOGENEOUS MODEL
LANE 4**

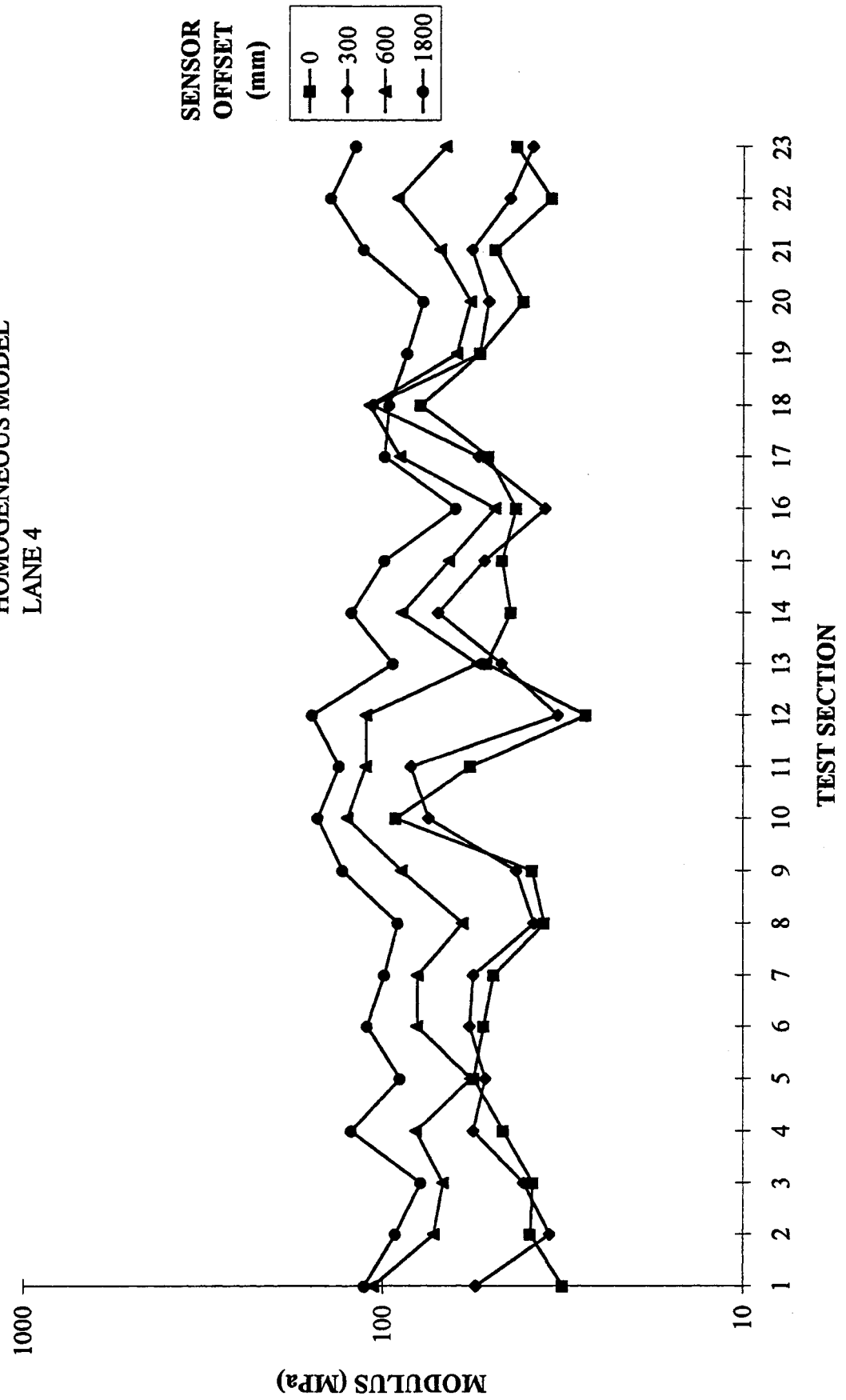


Fig. 19. Average backcalculated subgrade moduli for mainline test sections, lane 4.

AVERAGE MODULUS FOR MAINLINE TEST SECTIONS

**HOMOGENEOUS MODEL
LANE 7**

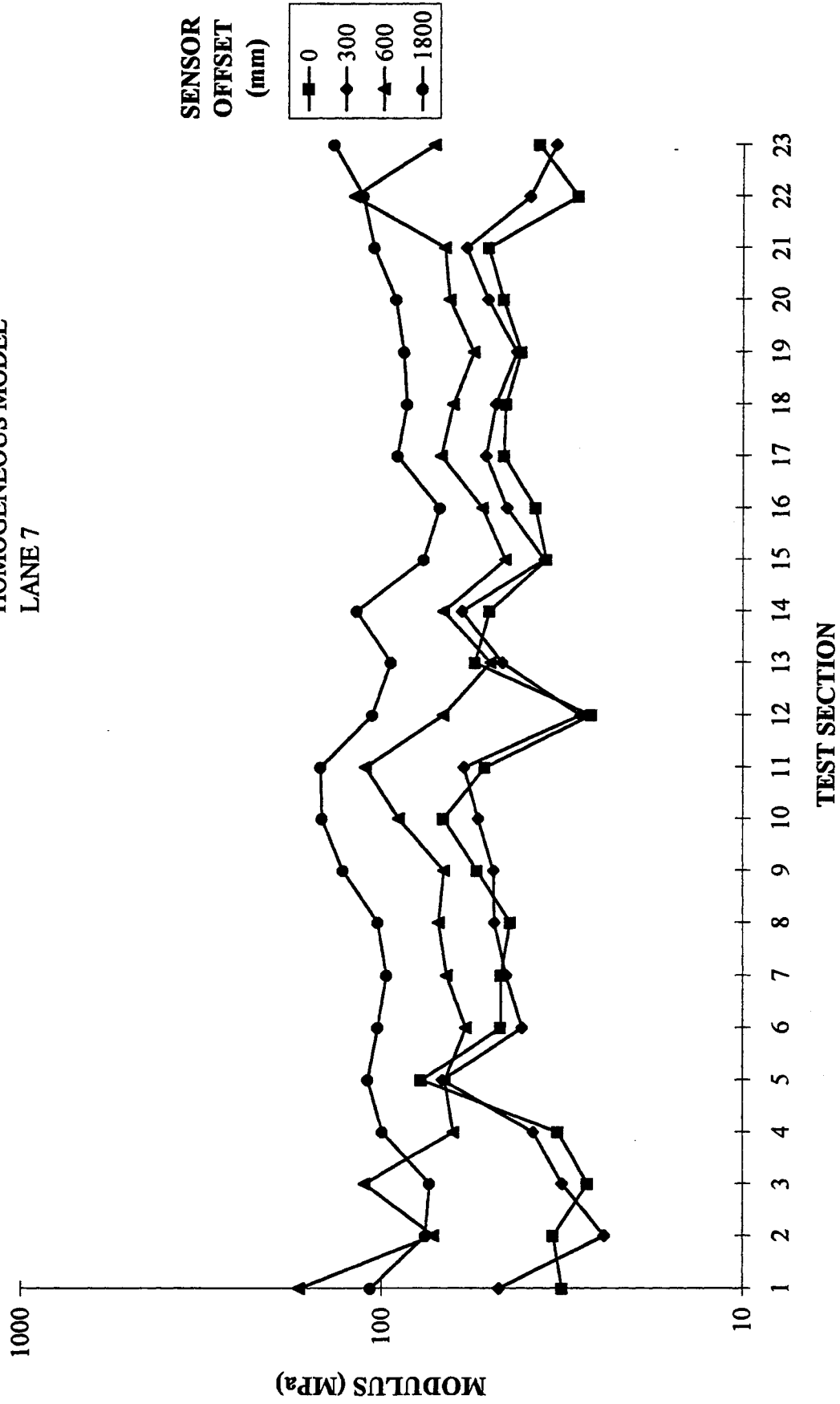


Fig. 20. Average backcalculated subgrade moduli for mainline test sections, lane 7.

AVERAGE MODULUS FOR LOW-VOLUME TEST SECTIONS
HOMOGENEOUS MODEL
LANE 1

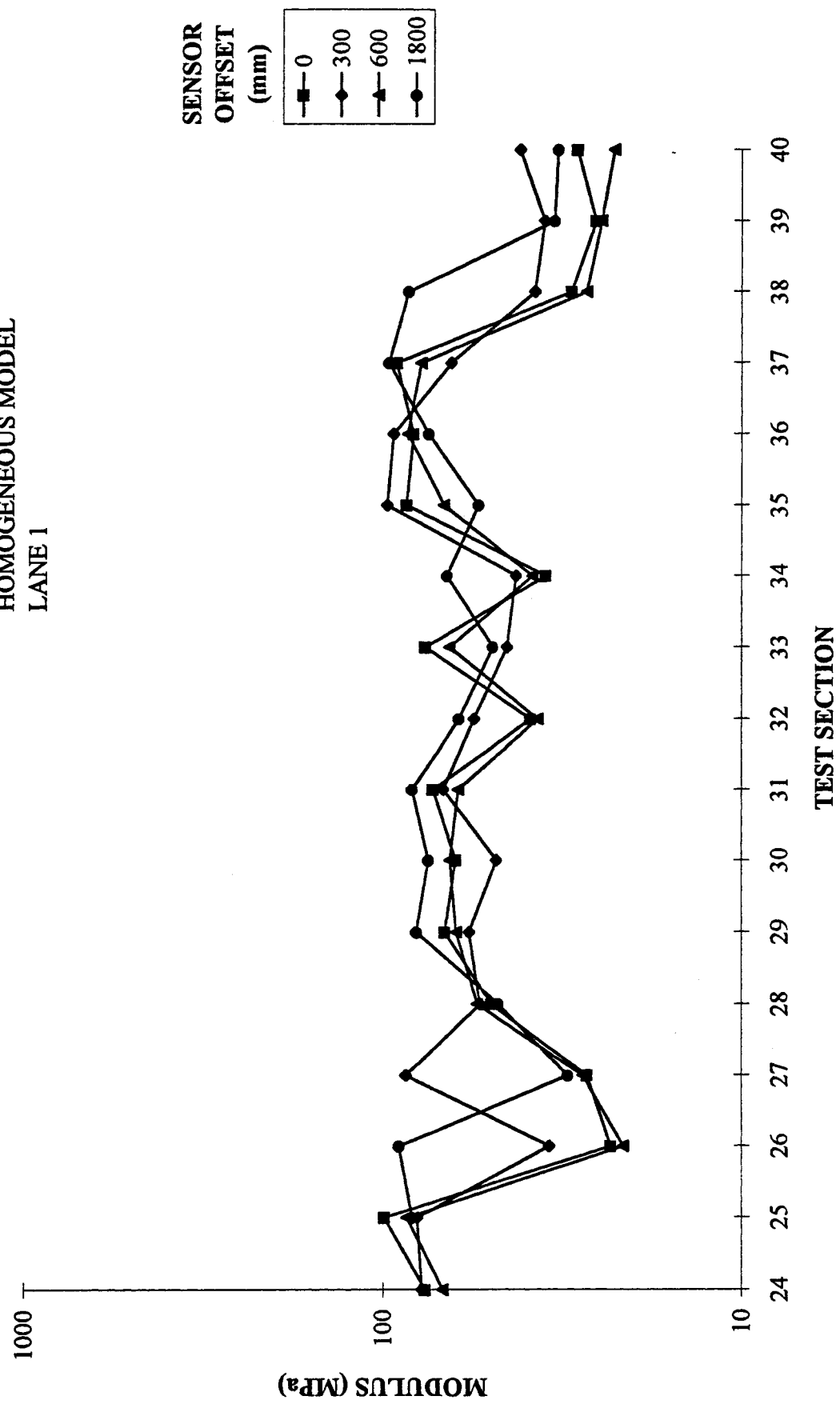


Fig. 21. Average backcalculated subgrade moduli for low-volume test sections, lane 1.

AVERAGE MODULUS FOR LOW-VOLUME TEST SECTIONS

**HOMOGENEOUS MODEL
LANE 4**

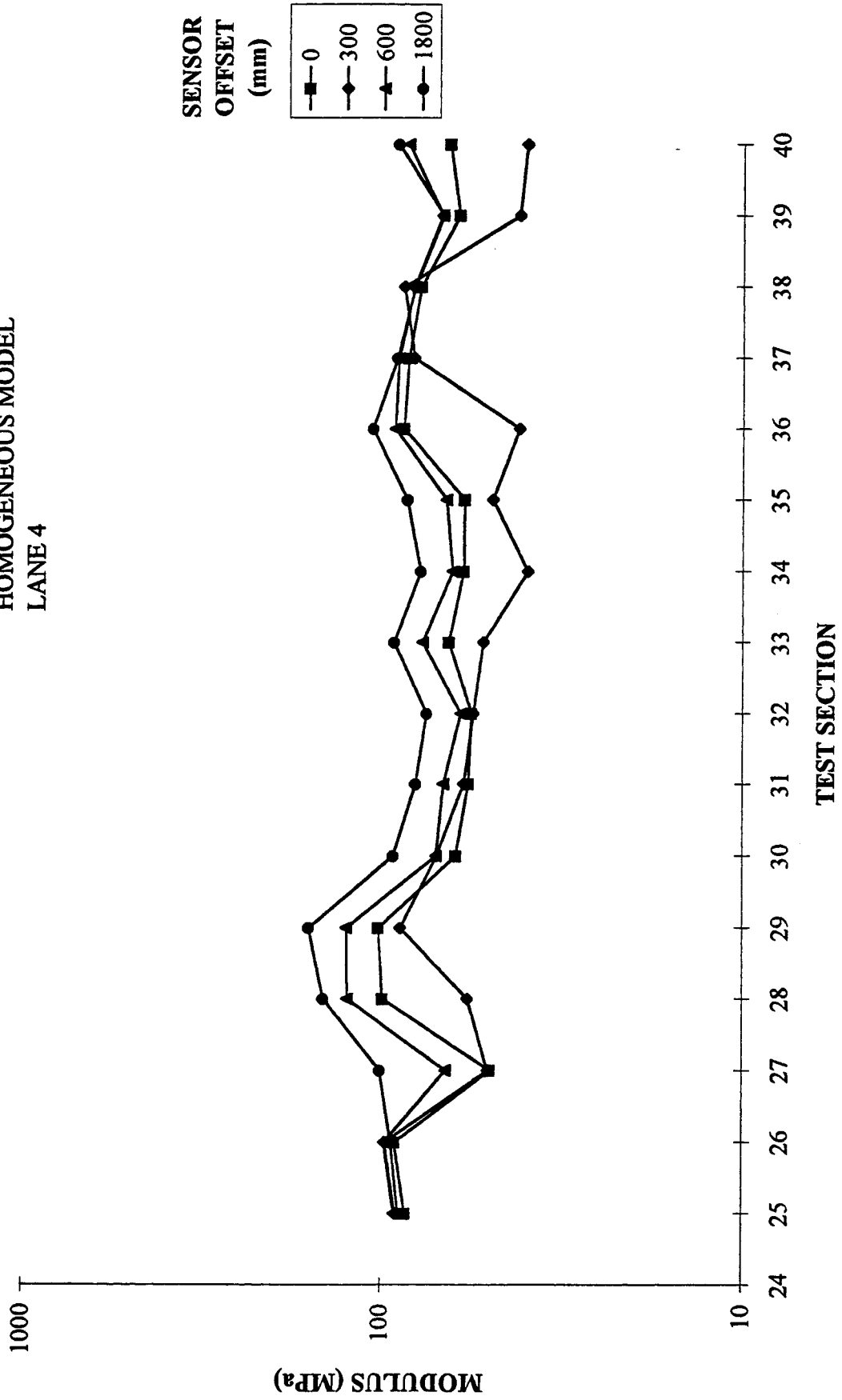


Fig. 22. Average backcalculated subgrade moduli for low-volume test sections, lane 4.

AVERAGE MODULUS FOR LOW-VOLUME TEST SECTIONS
HOMOGENEOUS MODEL
LANE 7

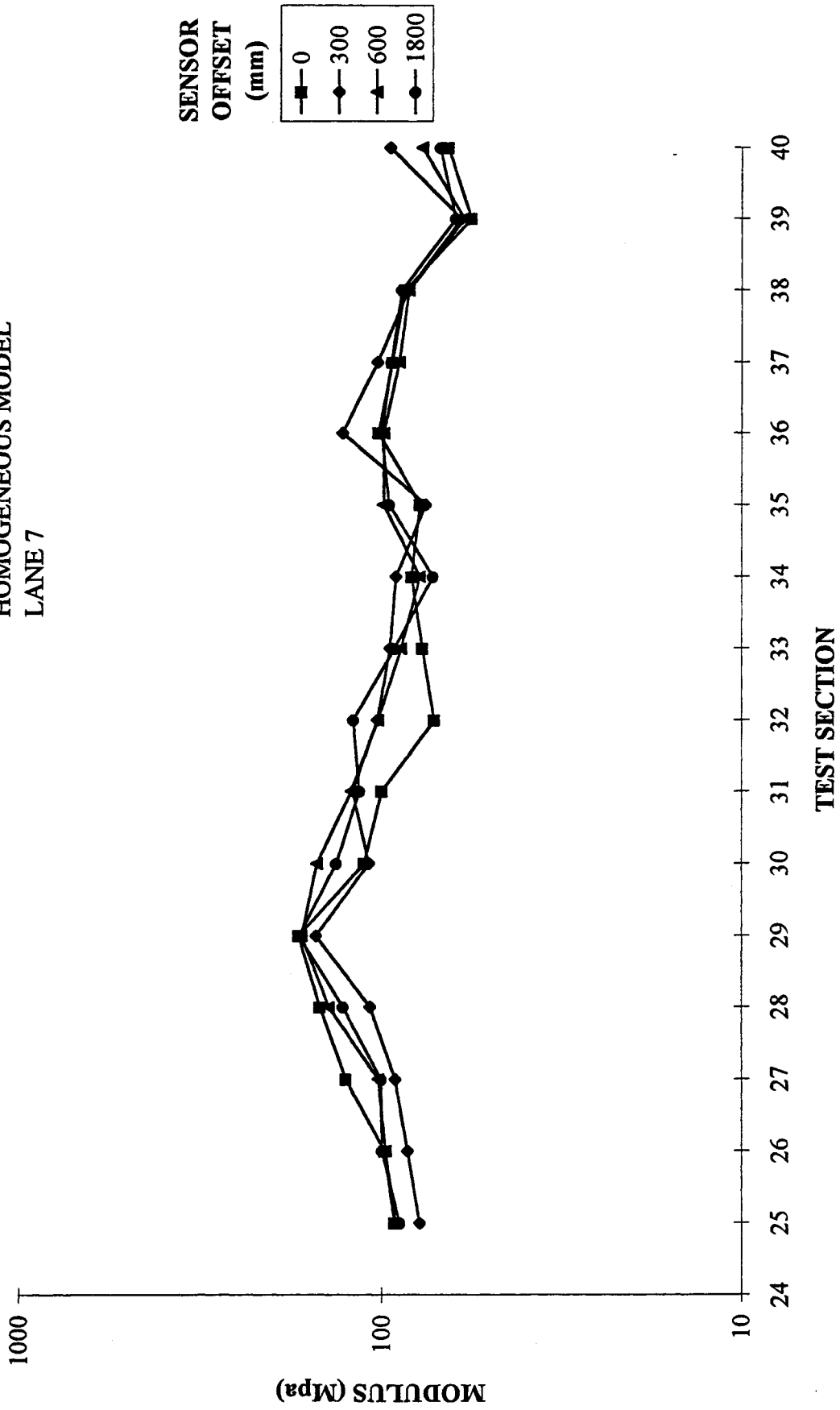


Fig. 23. Average backcalculated subgrade moduli for low-volume test sections, lane 7.

VARIATION OF SUBGRADE MODULUS WITH STATION

MAINLINE TEST SECTIONS
POST-BASE TESTING
LANE 1

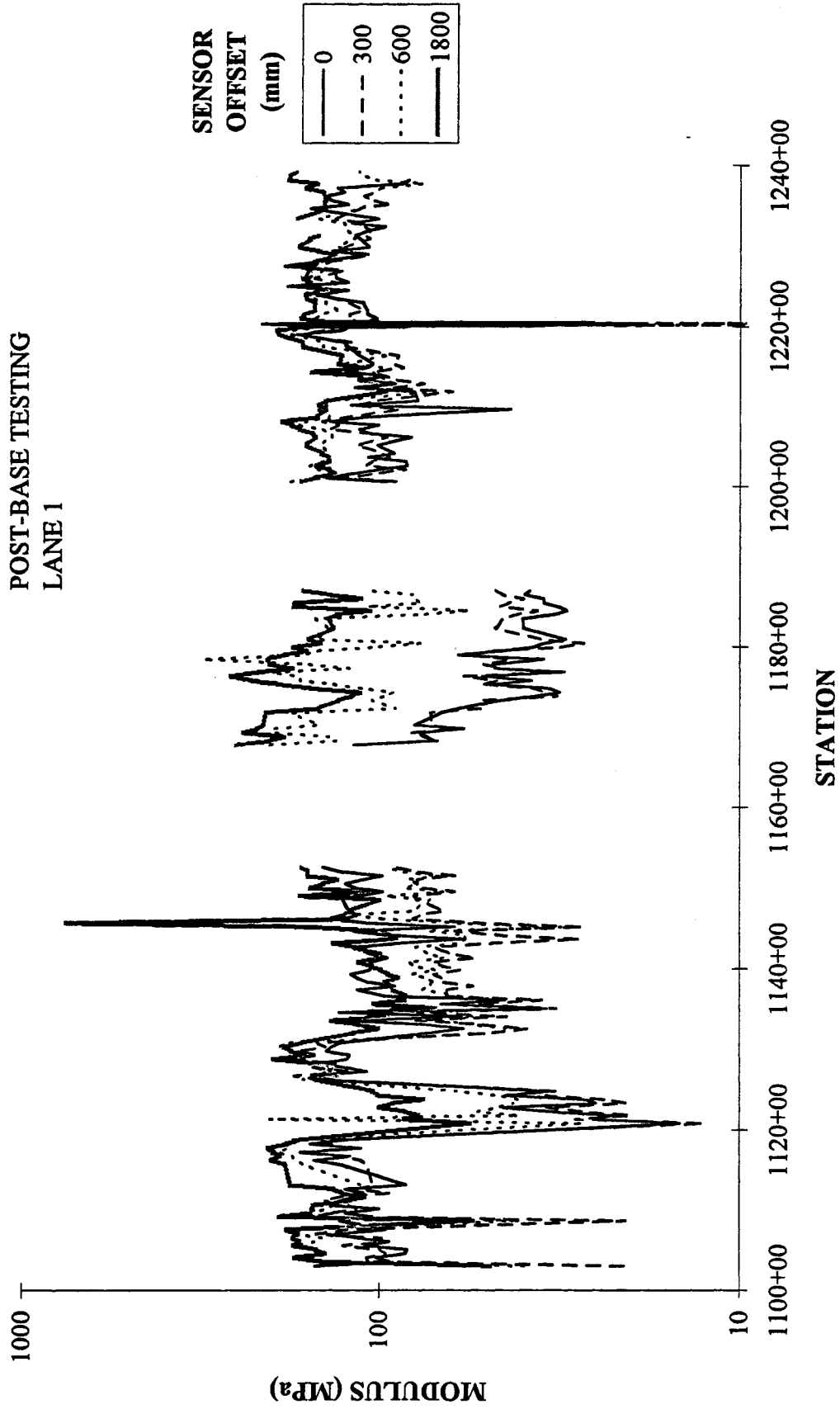


Fig. 24. Variation of backcalculated post-base subgrade moduli for mainline test sections, lane 1.

VARIATION OF SUBGRADE MODULUS WITH STATION

**MAINLINE TEST SECTIONS
POST-BASE TESTING
LANE 4**

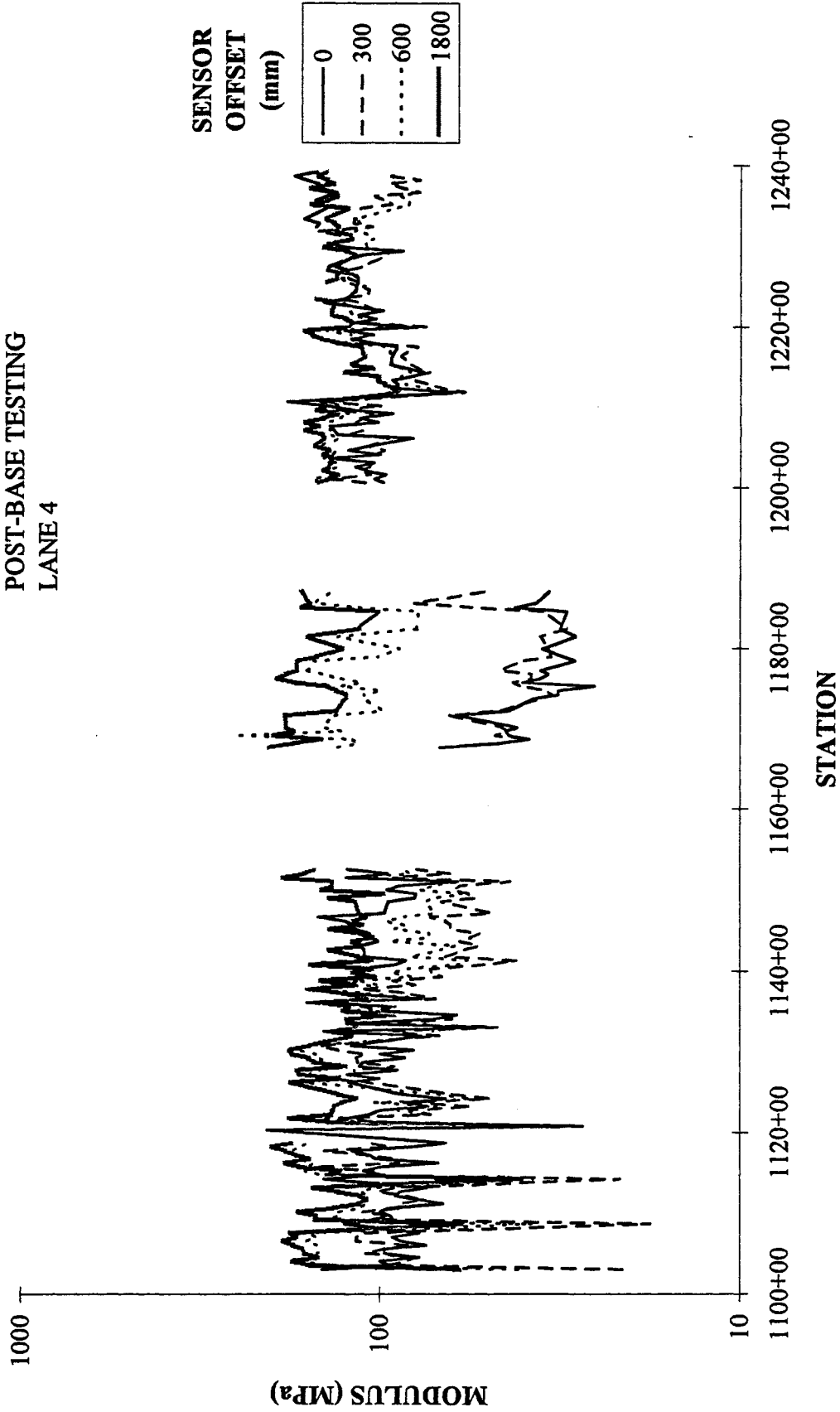


Fig. 25. Variation of backcalculated post-base subgrade moduli for mainline test sections, lane 4.

VARIATION OF SUBGRADE MODULUS WITH STATION

MAINLINE TEST SECTIONS
POST-BASE TESTING
LANE 7

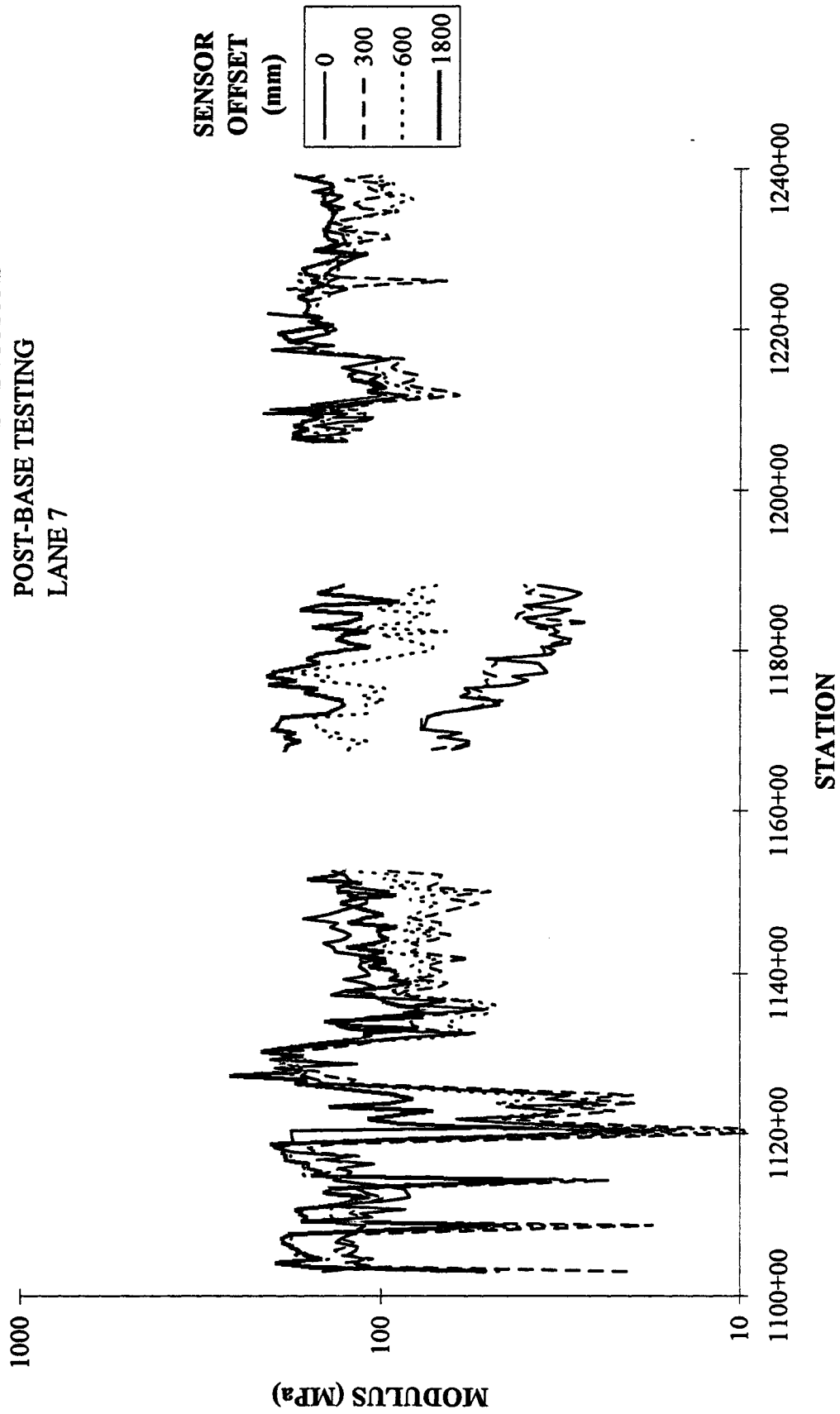


Fig. 26. Variation of backcalculated post-base subgrade moduli for mainline test sections, lane 7.

VARIATION OF SUBGRADE MODULUS WITH STATION

**LOW-VOLUME TEST SECTIONS
POST-BASE TESTING
LANE 1**

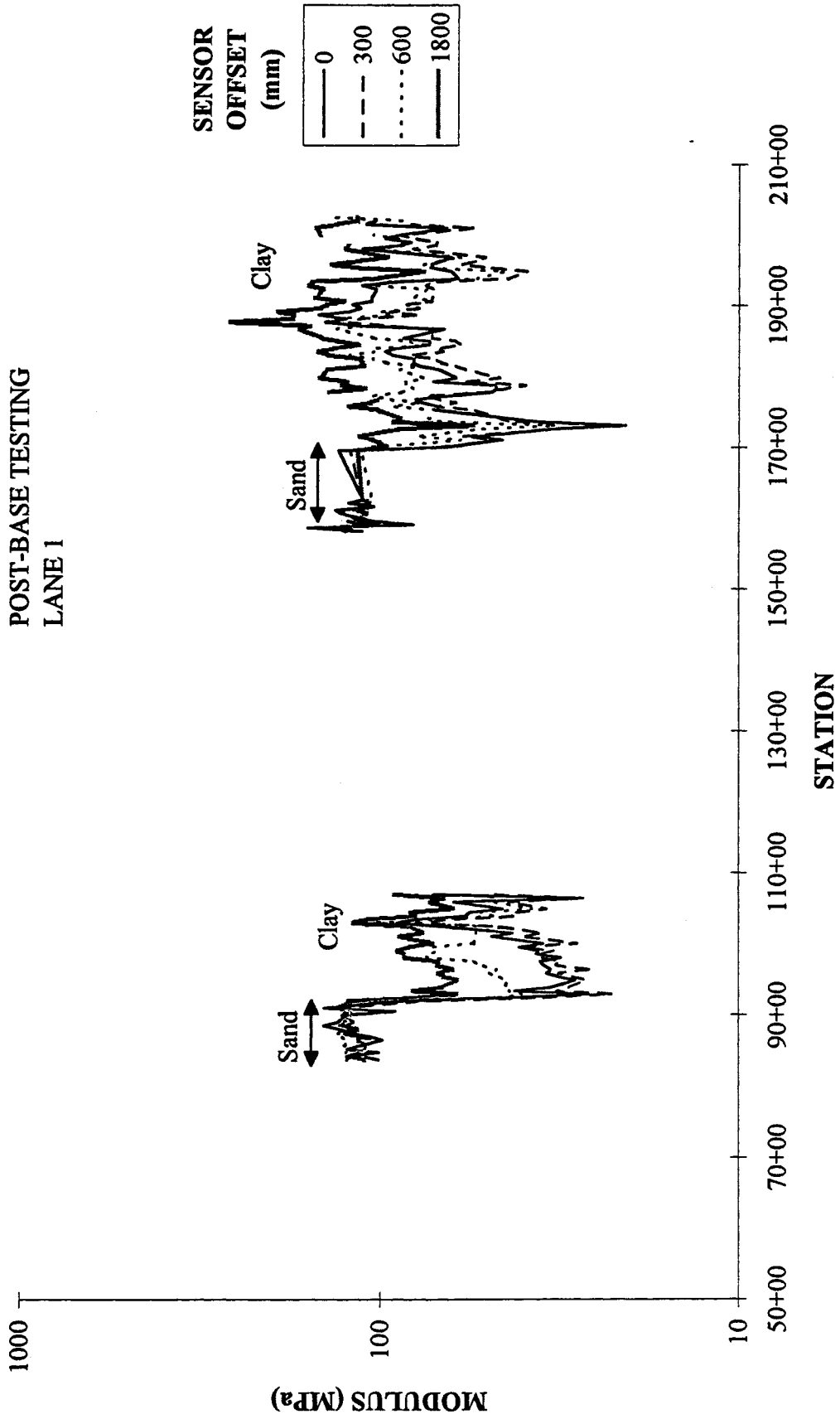


Fig. 27. Variation of backcalculated post-base subgrade moduli for low-volume test sections, lane 1.

VARIATION OF SUBGRADE MODULUS WITH STATION

**LOW-VOLUME TEST SECTIONS
POST-BASE TESTING
LANE 4**

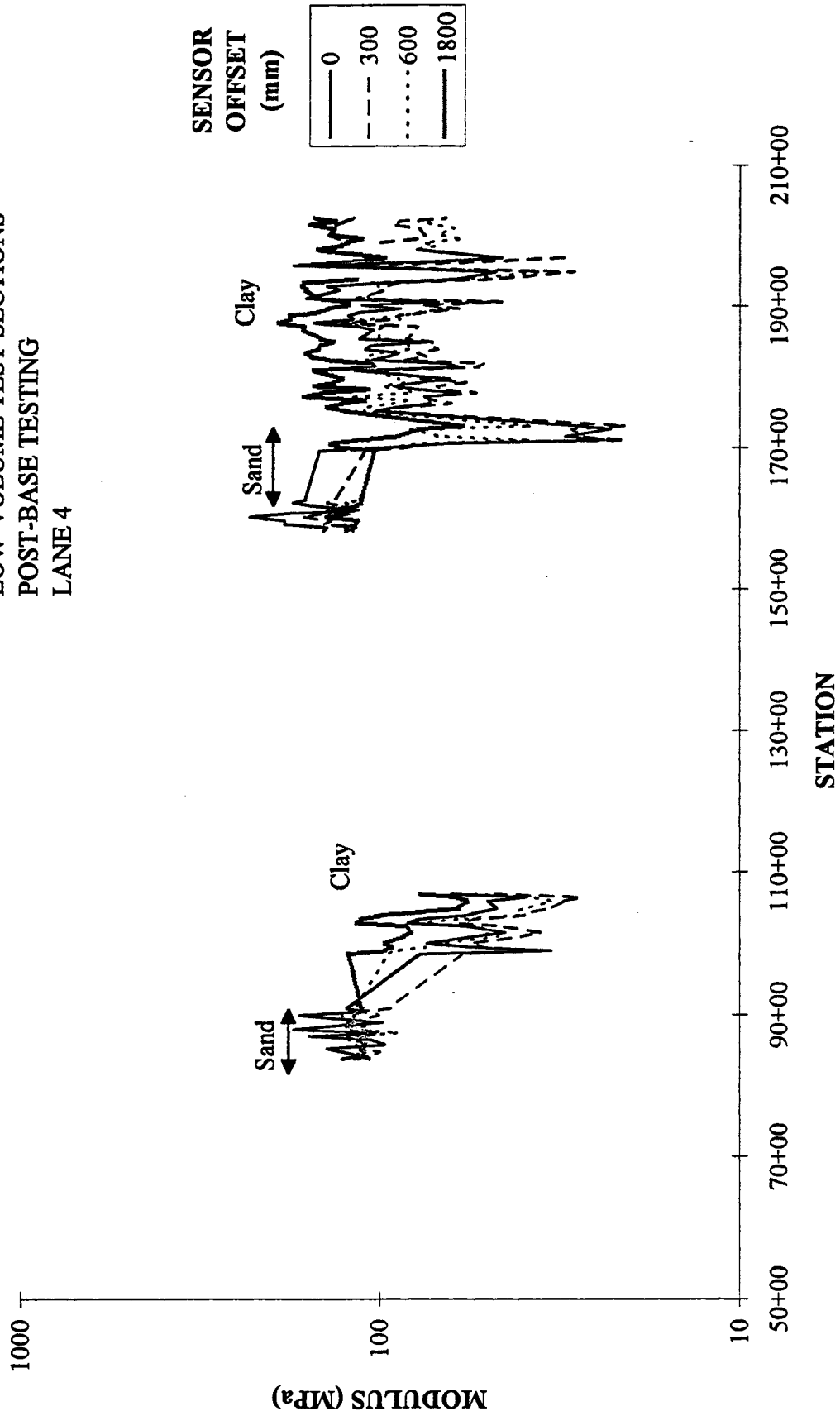


Fig. 28. Variation of backcalculated post-base subgrade moduli for low-volume test sections, lane 4.

VARIATION OF SUBGRADE MODULUS WITH STATION
LOW-VOLUME TEST SECTIONS
POST-BASE TESTING
LANE 7

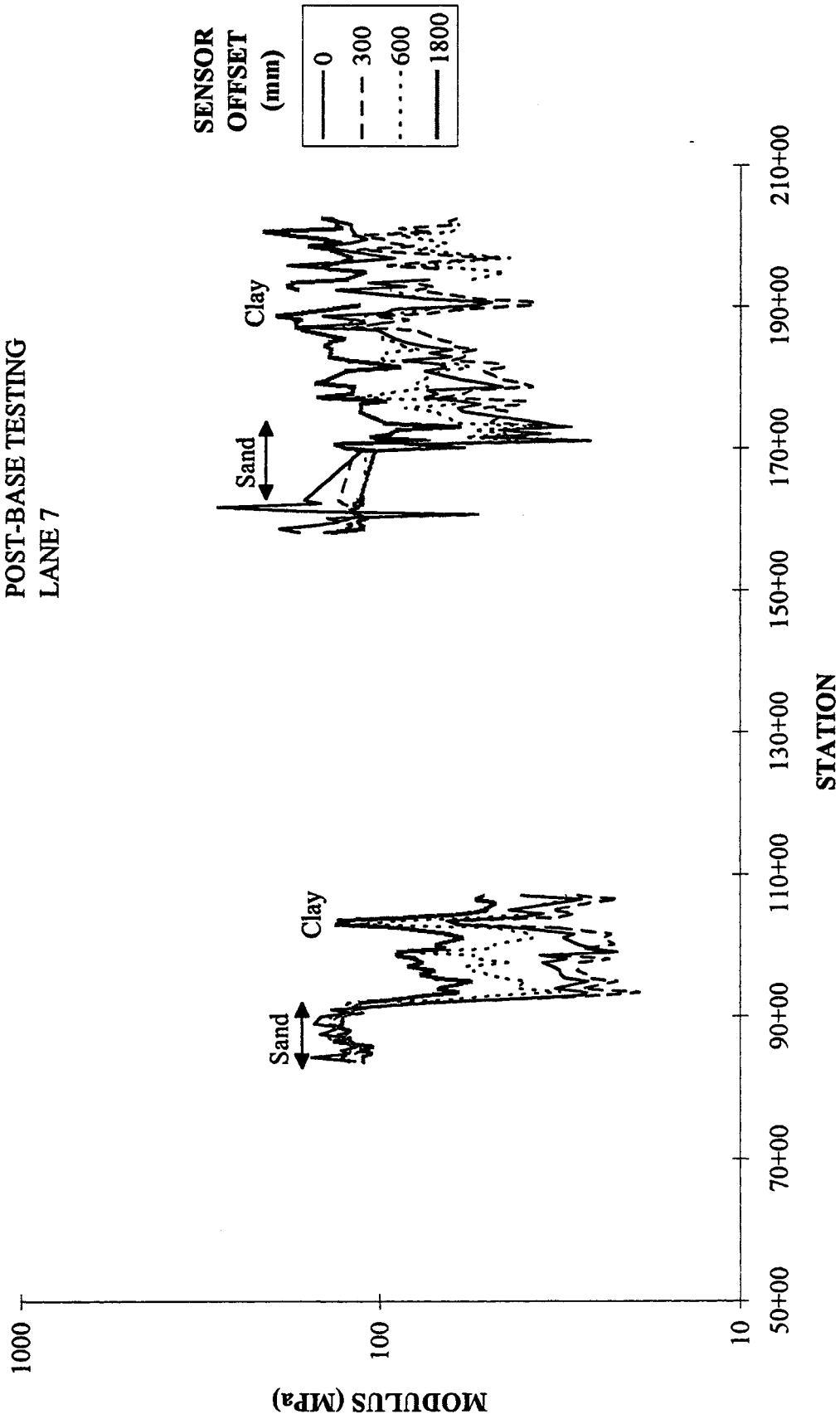


Fig. 29. Variation of backcalculated post-base subgrade moduli for low-volume test sections, lane 7.

**AVERAGE MODULUS FOR MAINLINE TEST SECTIONS
HOMOGENEOUS MODEL
POST-BASE TESTING
LANE 1**

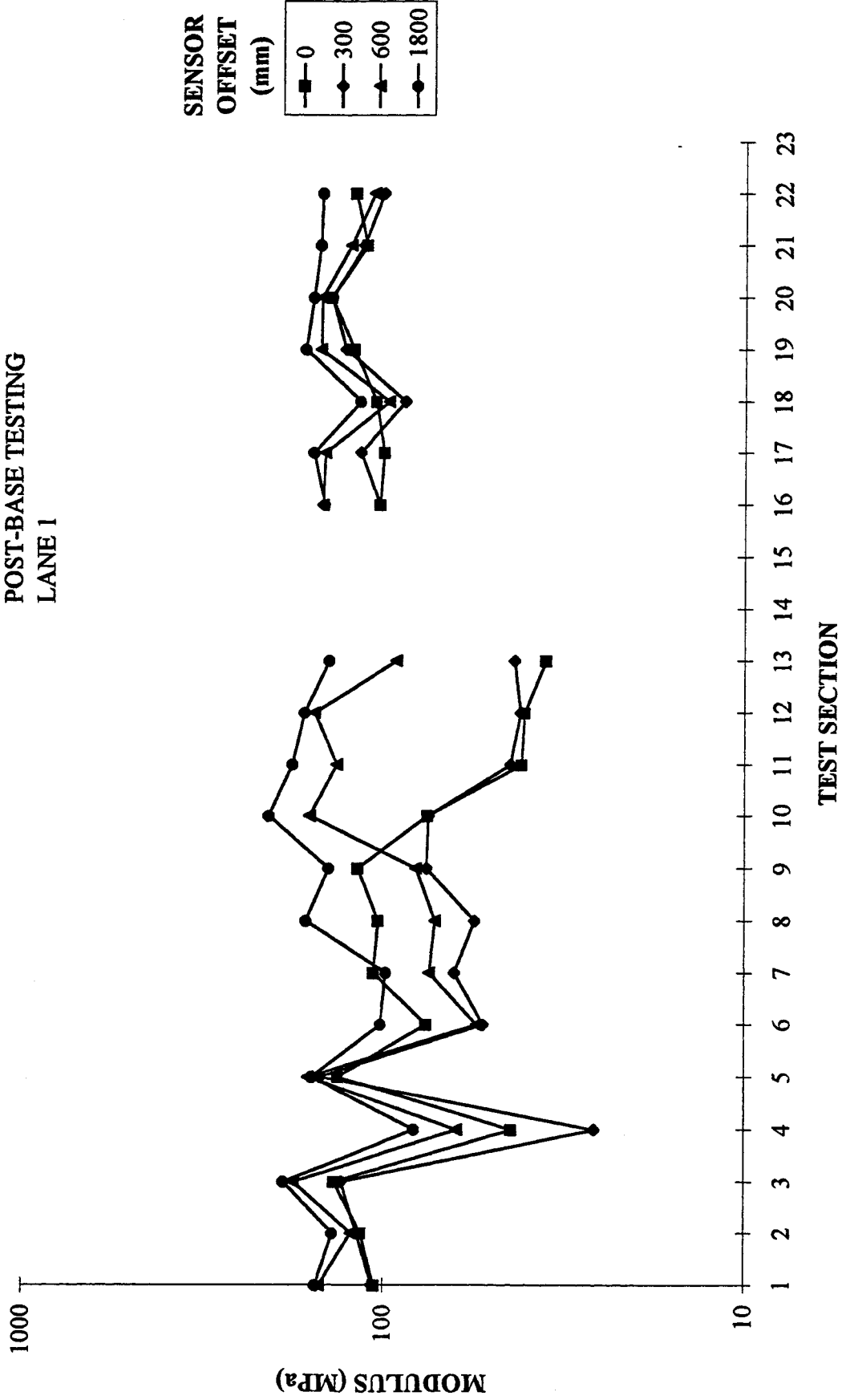


Fig. 30. Average backcalculated post-base subgrade moduli for mainline test sections, lane 1.

AVERAGE MODULUS FOR MAINLINE TEST SECTIONS
HOMOGENEOUS MODEL
POST-BASE TESTING
LANE 4

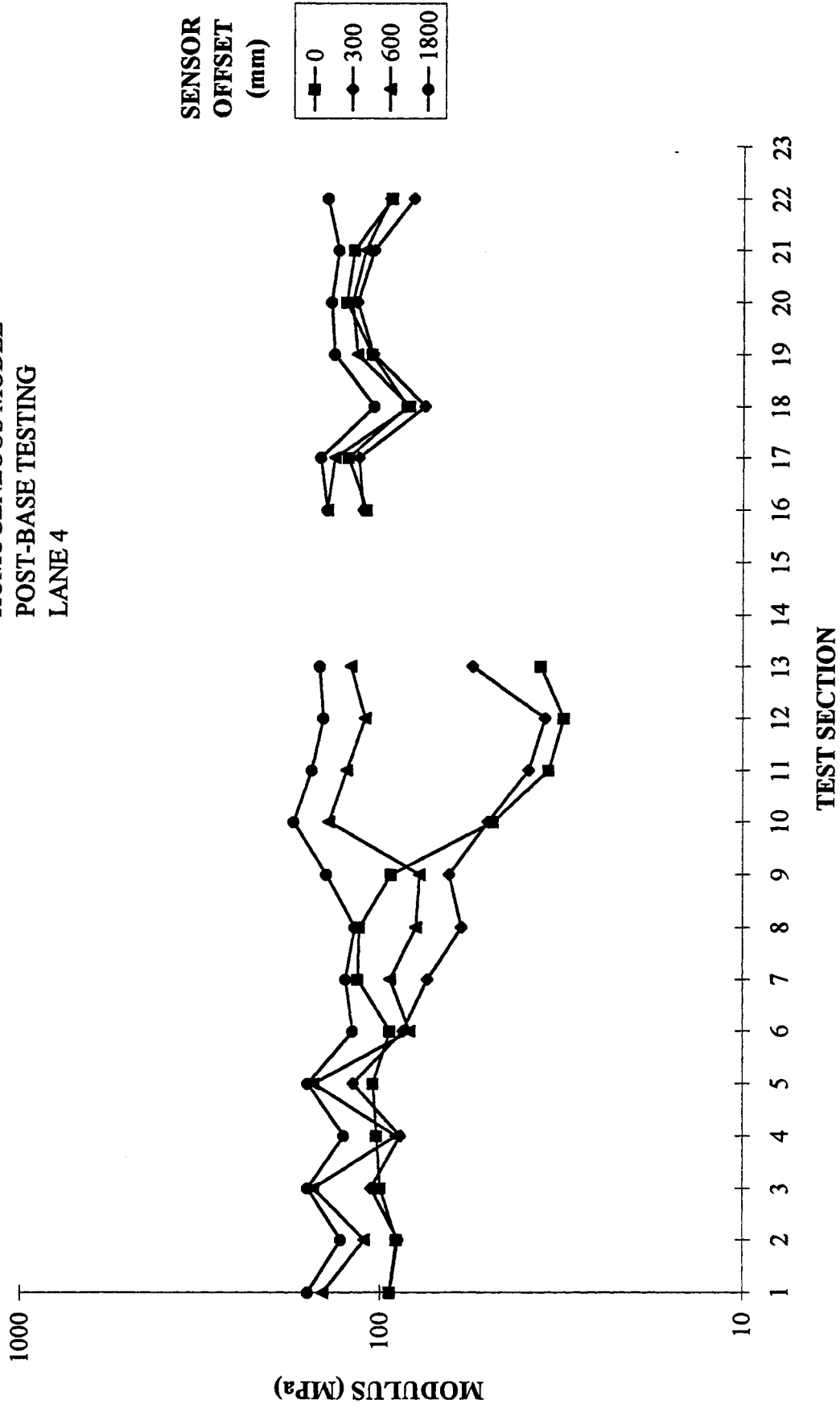


Fig. 31. Average backcalculated post-base subgrade moduli for mainline test sections, lane 4.

AVERAGE MODULUS FOR MAINLINE TEST SECTIONS

**HOMOGENEOUS MODEL
POST-BASE TESTING
LANE 7**

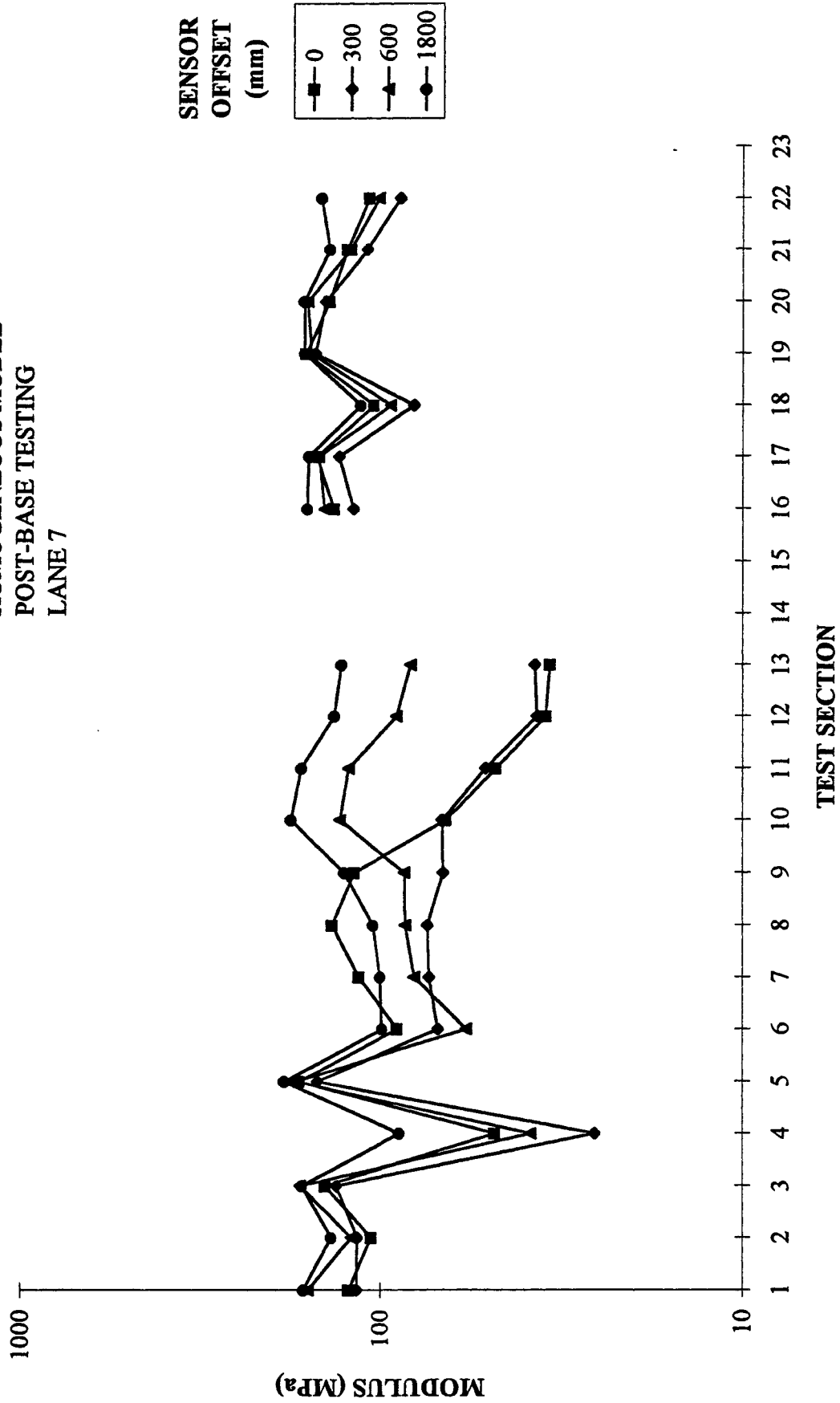


Fig. 32. Average backcalculated post-base subgrade moduli for mainline test sections, lane 7.

AVERAGE MODULUS FOR MAINLINE TEST SECTIONS

**HOMOGENEOUS MODEL
POST-BASE TESTING
LANE 1**

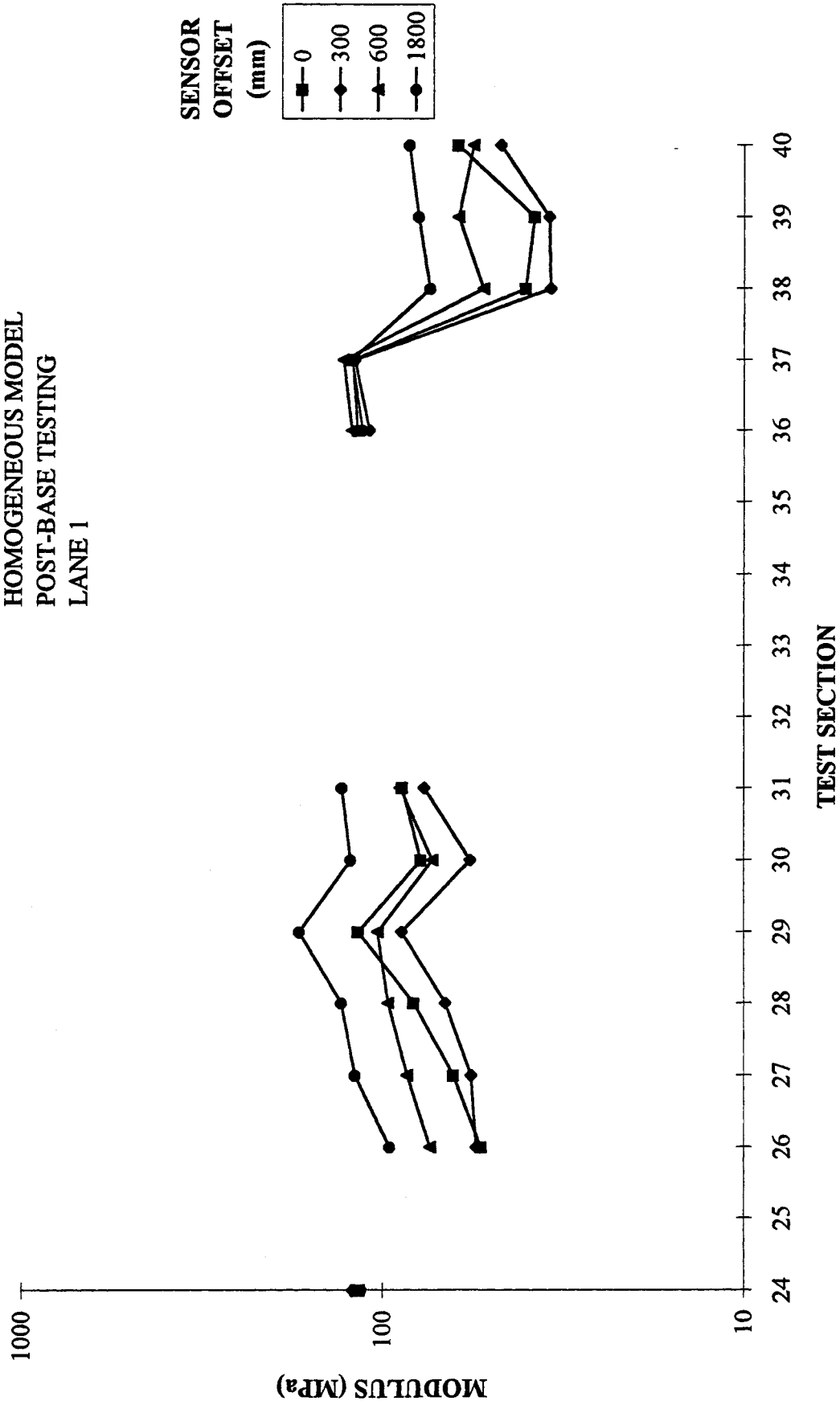


Fig. 33. Average backcalculated post-base subgrade moduli for low-volume test sections, lane 1.

AVERAGE MODULUS FOR MAINLINE TEST SECTIONS

**HOMOGENEOUS MODEL
POST-BASE TESTING
LANE 4**

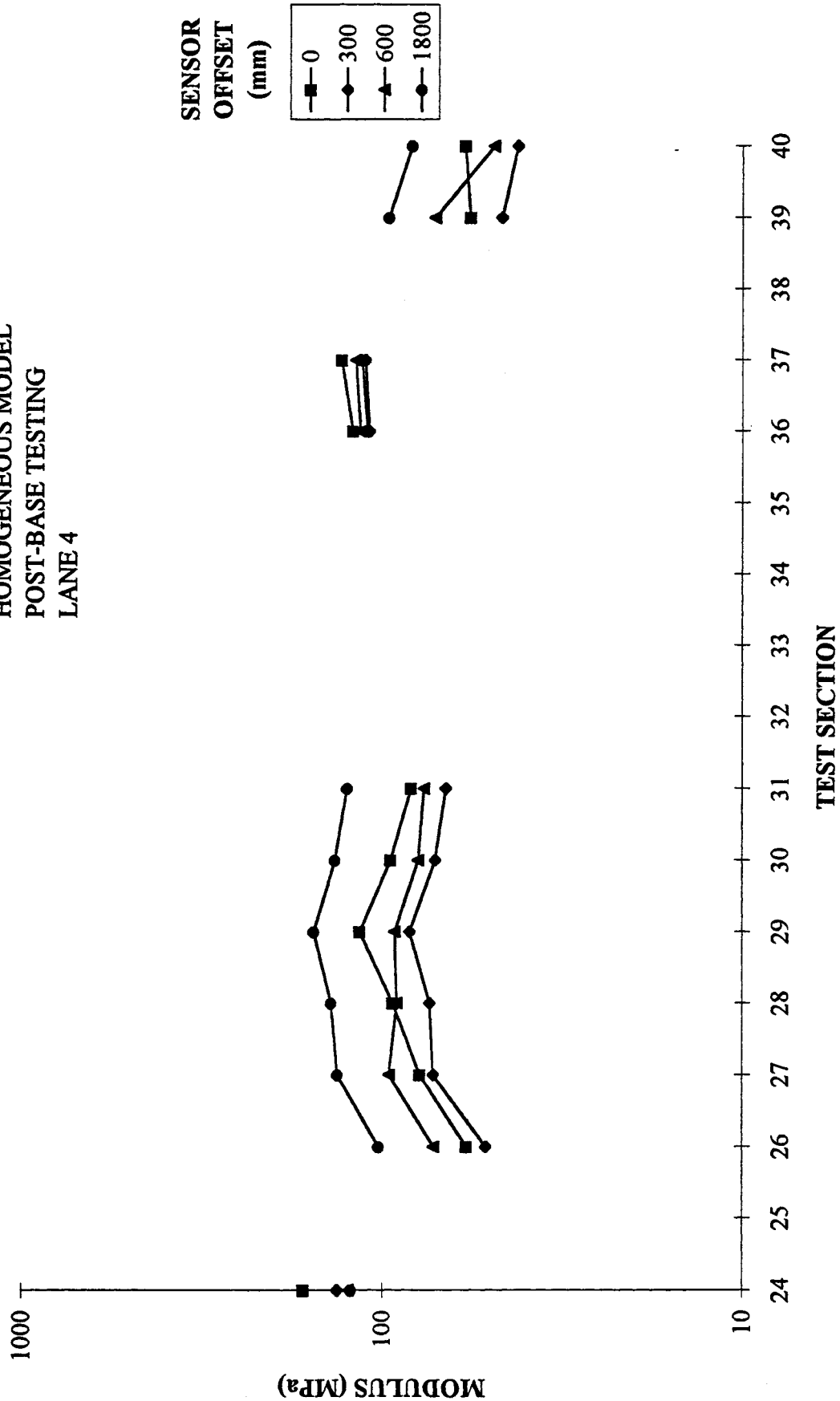


Fig. 34. Average backcalculated post-base subgrade moduli for low-volume test sections, lane 4.

AVERAGE MODULUS FOR MAINLINE TEST SECTIONS

**HOMOGENEOUS MODEL
POST-BASE TESTING
LANE 7**

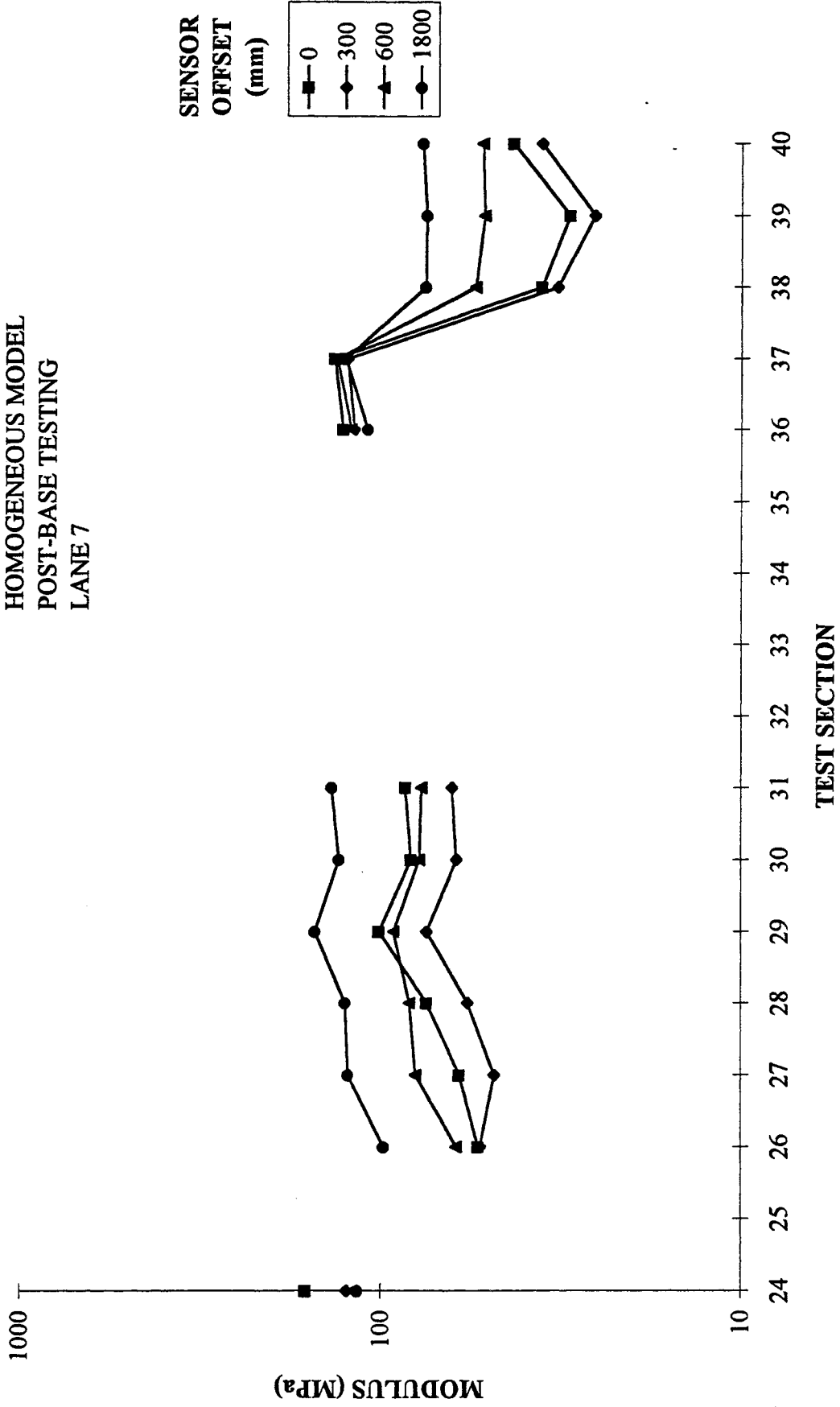


Fig. 35. Average backcalculated post-base subgrade moduli for low-volume test sections, lane 7.

COMPARISON OF BACKCALCULATED PRE-AND POST-BASE SUBGRADE MODULI

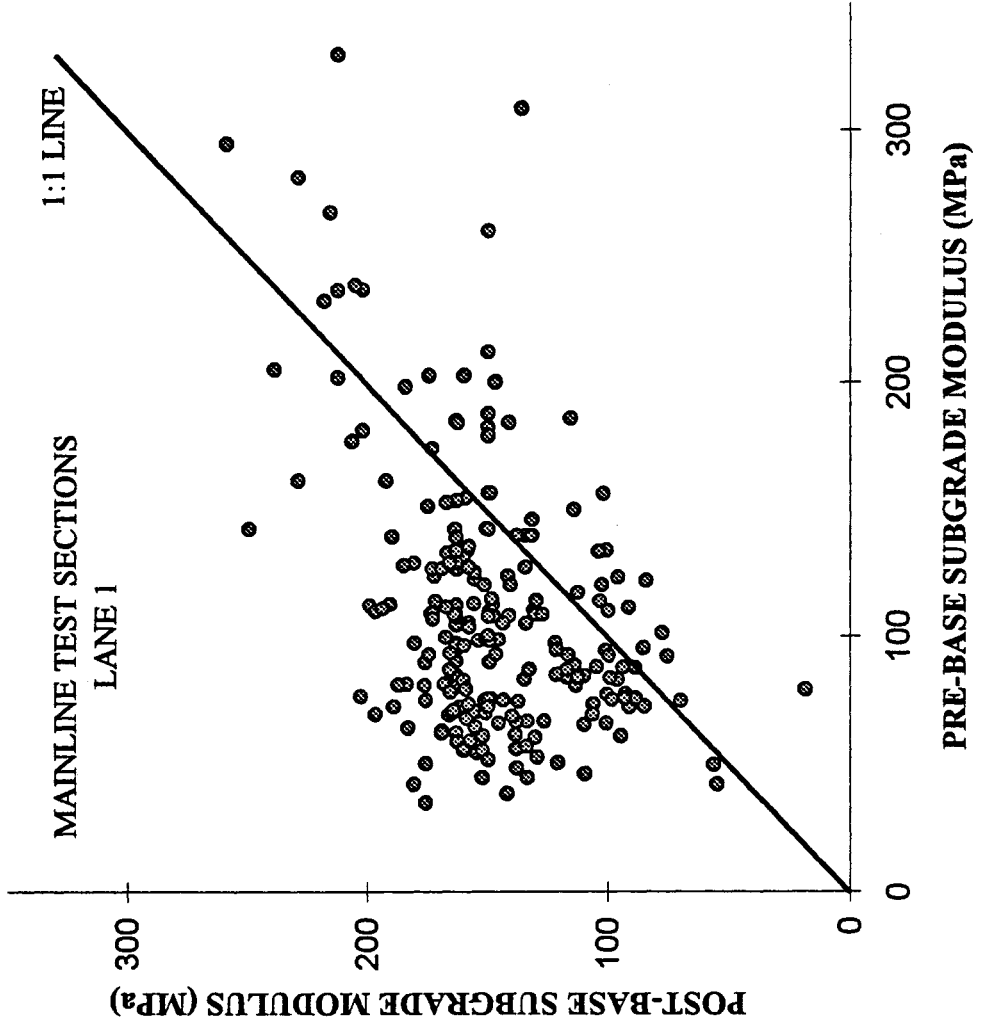


Fig. 36. Comparison of backcalculated moduli obtained from pre- and post-base tests on the mainline sections.

COMPARISON OF BACKCALCULATED PRE-AND POST-BASE SUBGRADE MODULI

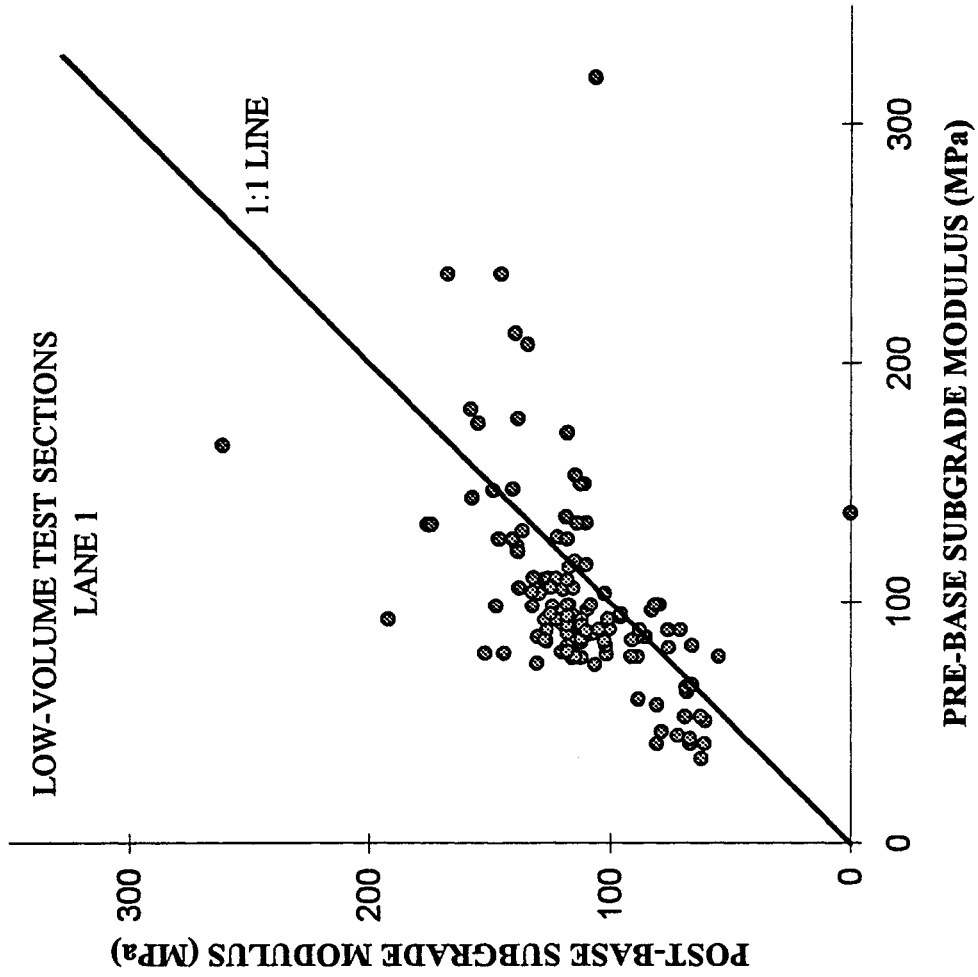


Fig. 37. Comparison of backcalculated moduli obtained from pre- and post-base tests on the low-volume sections.

**COMPARISON OF HOMOGENEOUS AND MULTI-LAYERED SYSTEM
BACKCALCULATED MODULI**

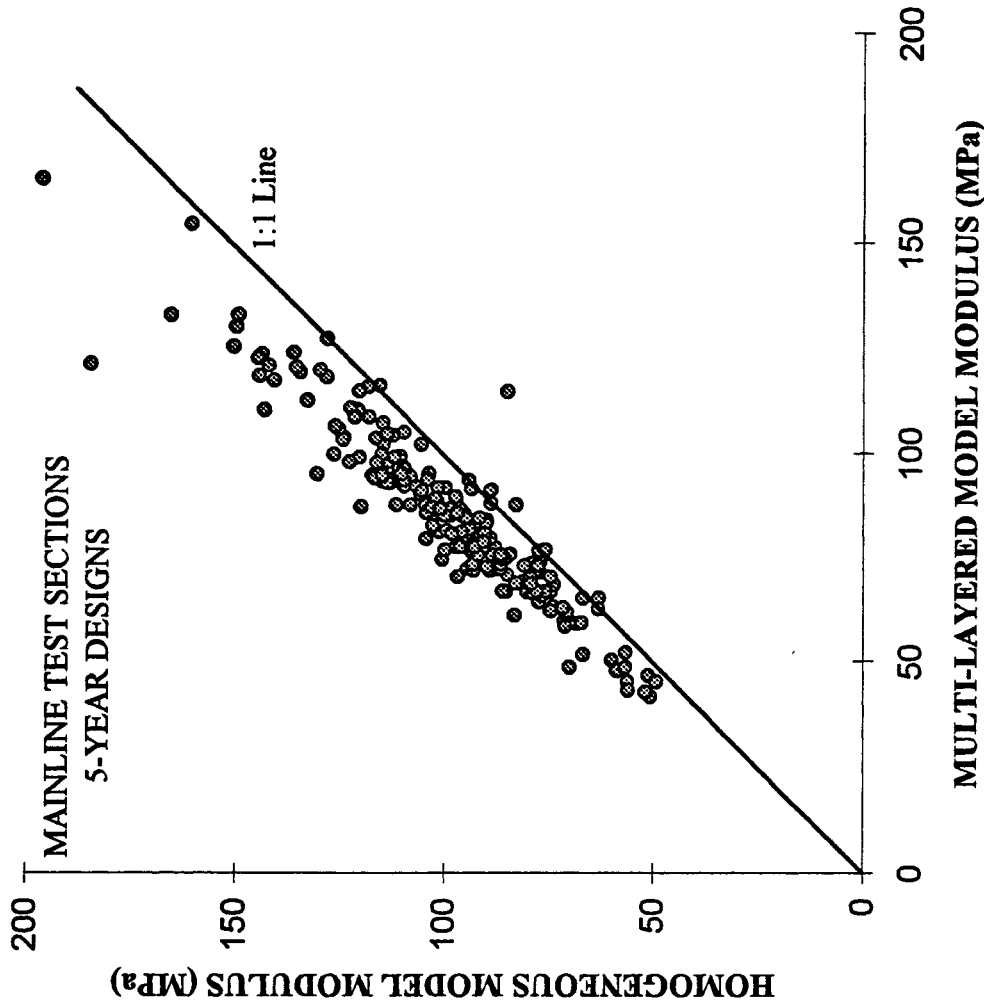


Fig. 38. Comparison of moduli obtained from homogeneous and multi-layered approaches: 5-year designs.

**COMPARISON OF HOMOGENEOUS AND MULTI-LAYERED SYSTEM
BACKCALCULATED MODULI**

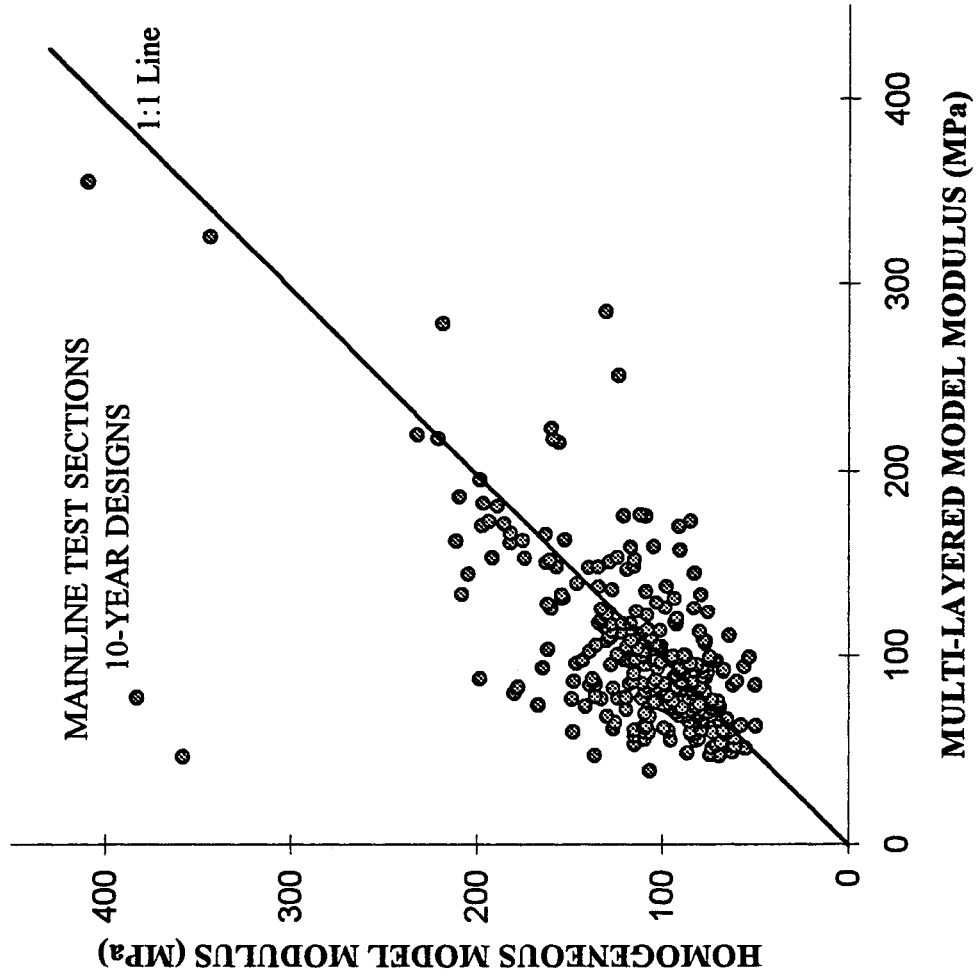


Fig. 39. Comparison of moduli obtained from homogeneous and multi-layered approaches: 10-year designs.

VARIATION OF SOIL MOISTURE CONTENT

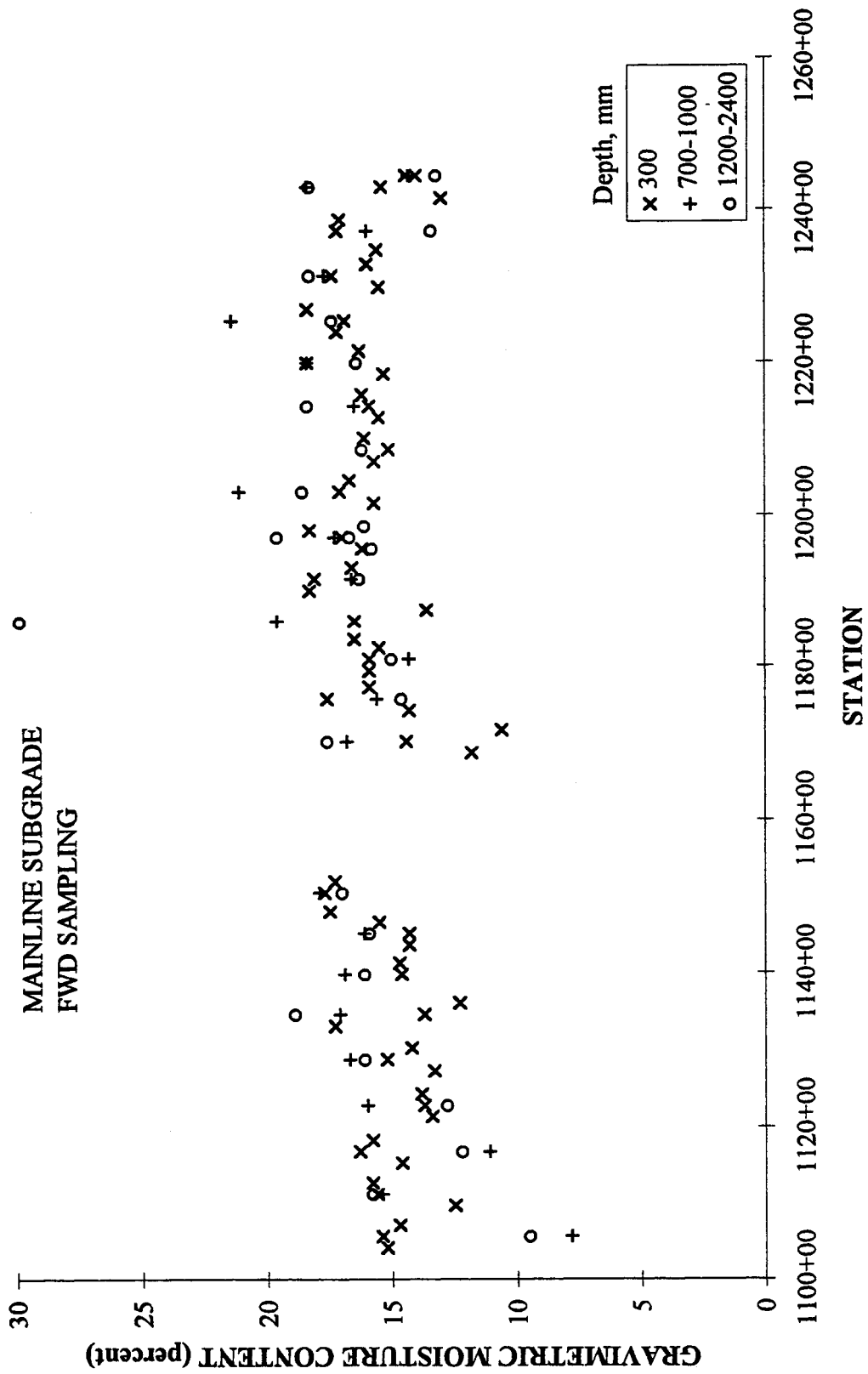


Fig. 40. Variation of laboratory soil moisture content obtained during subgrade FWD testing, mainline test sections.

VARIATION OF SOIL MOISTURE CONTENT

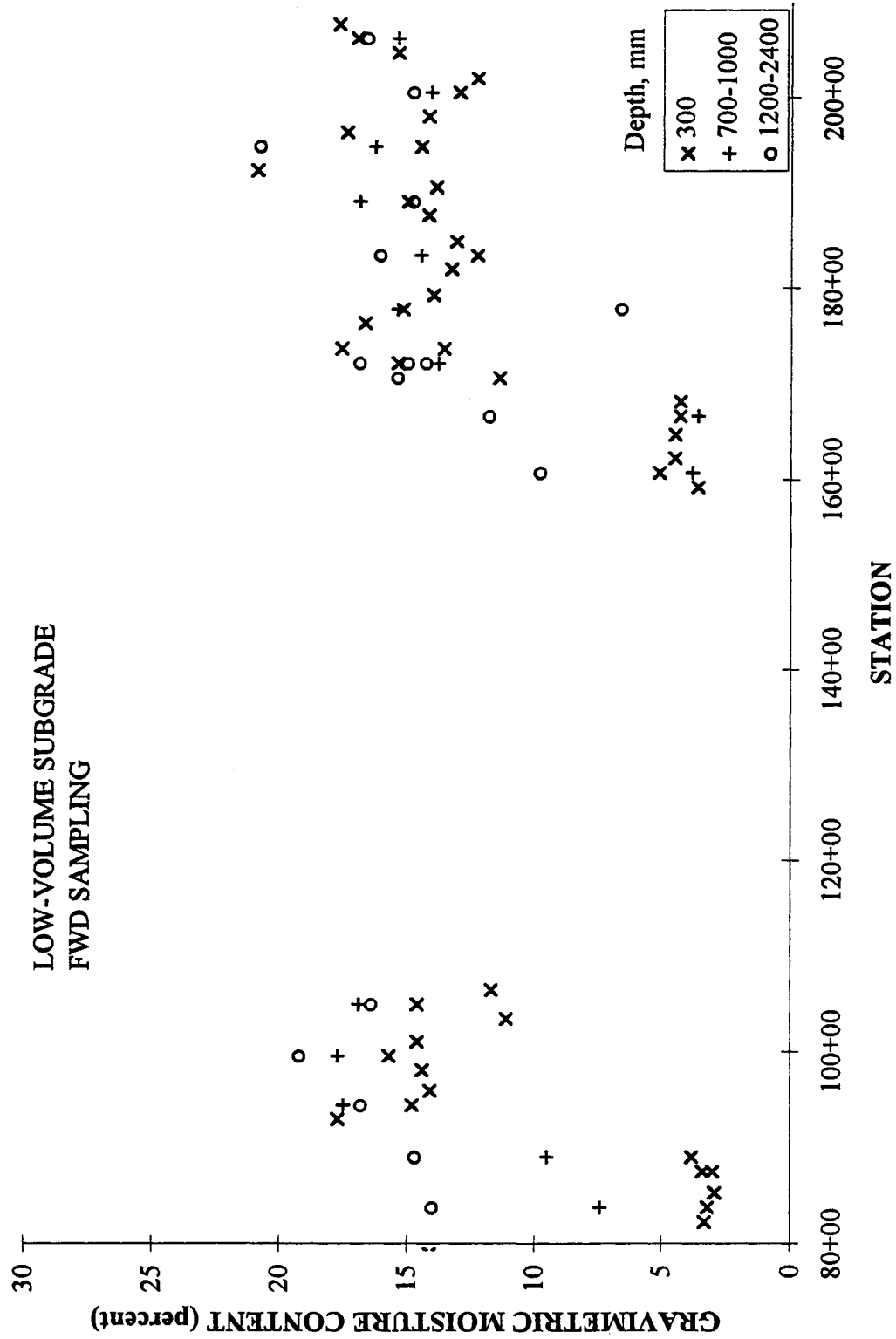


Fig. 41. Variation of laboratory soil moisture content obtained during subgrade FWD testing, low-volume test sections.

VARIATION OF SOIL MOISTURE CONTENT

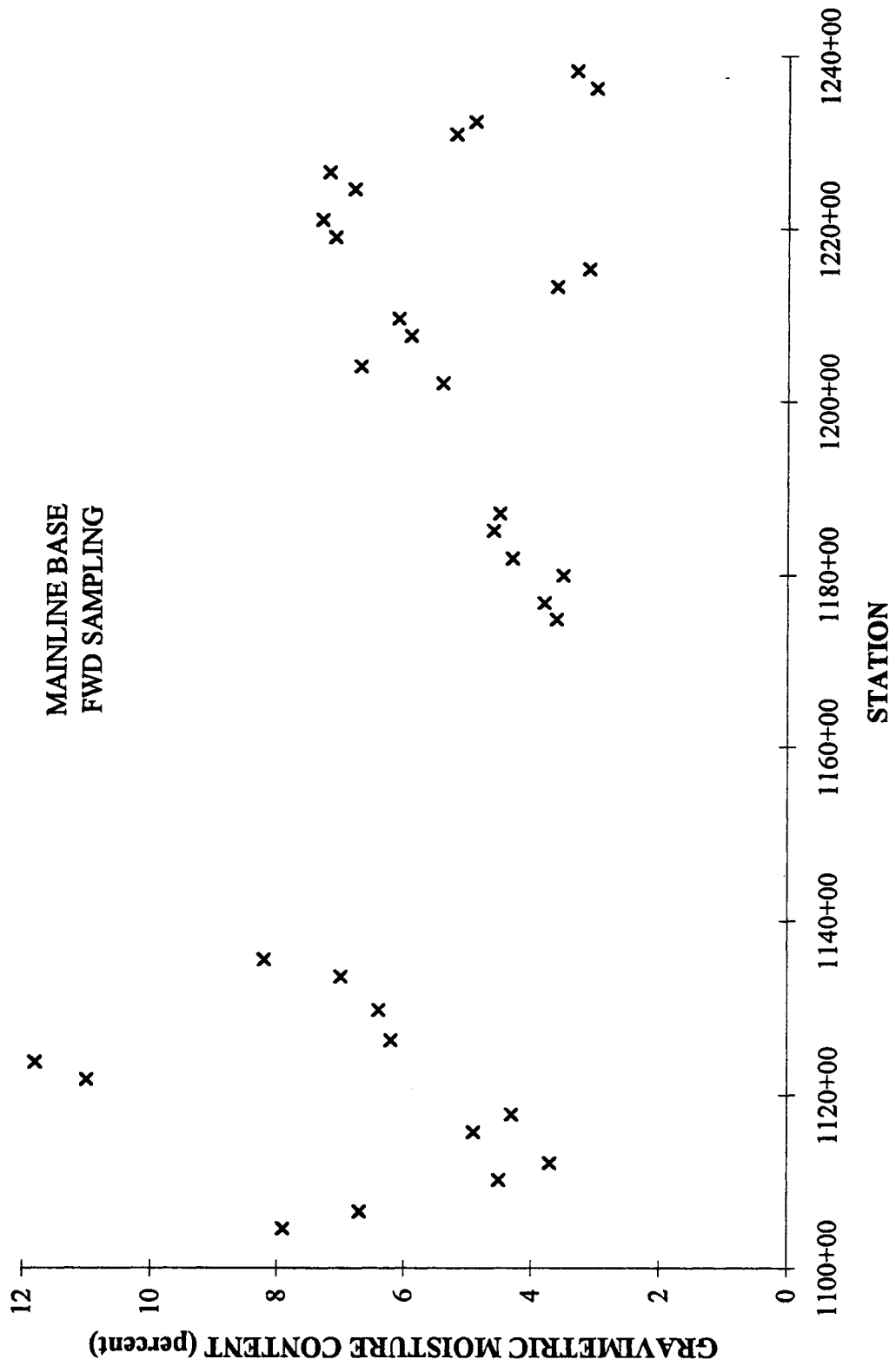
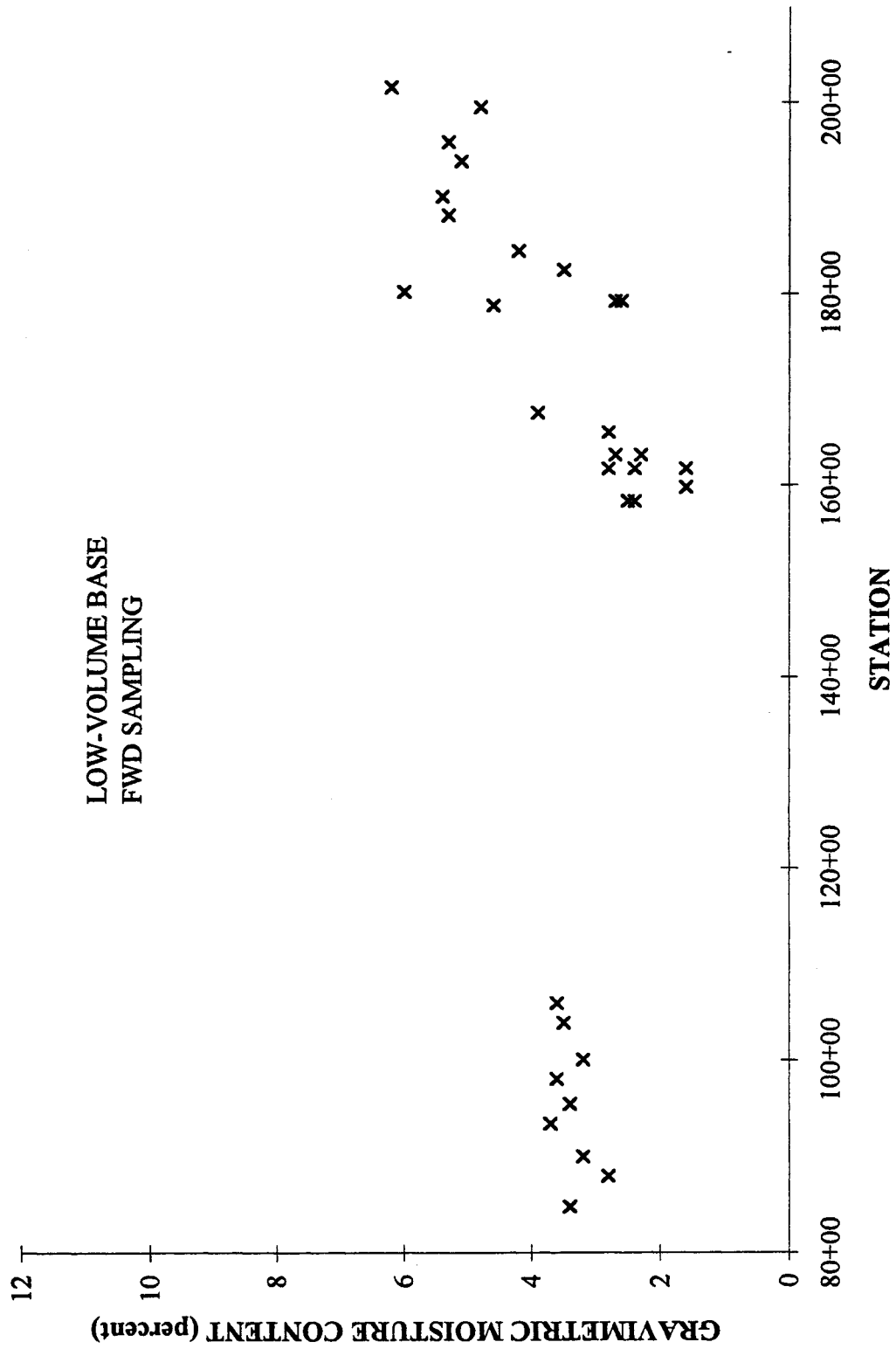


Fig. 42. Variation of laboratory granular base moisture content obtained during subgrade FWD testing, mainline test sections.

VARIATION OF SOIL MOISTURE CONTENT



RESILIENT MODULUS VS. DEGREE OF SATURATION

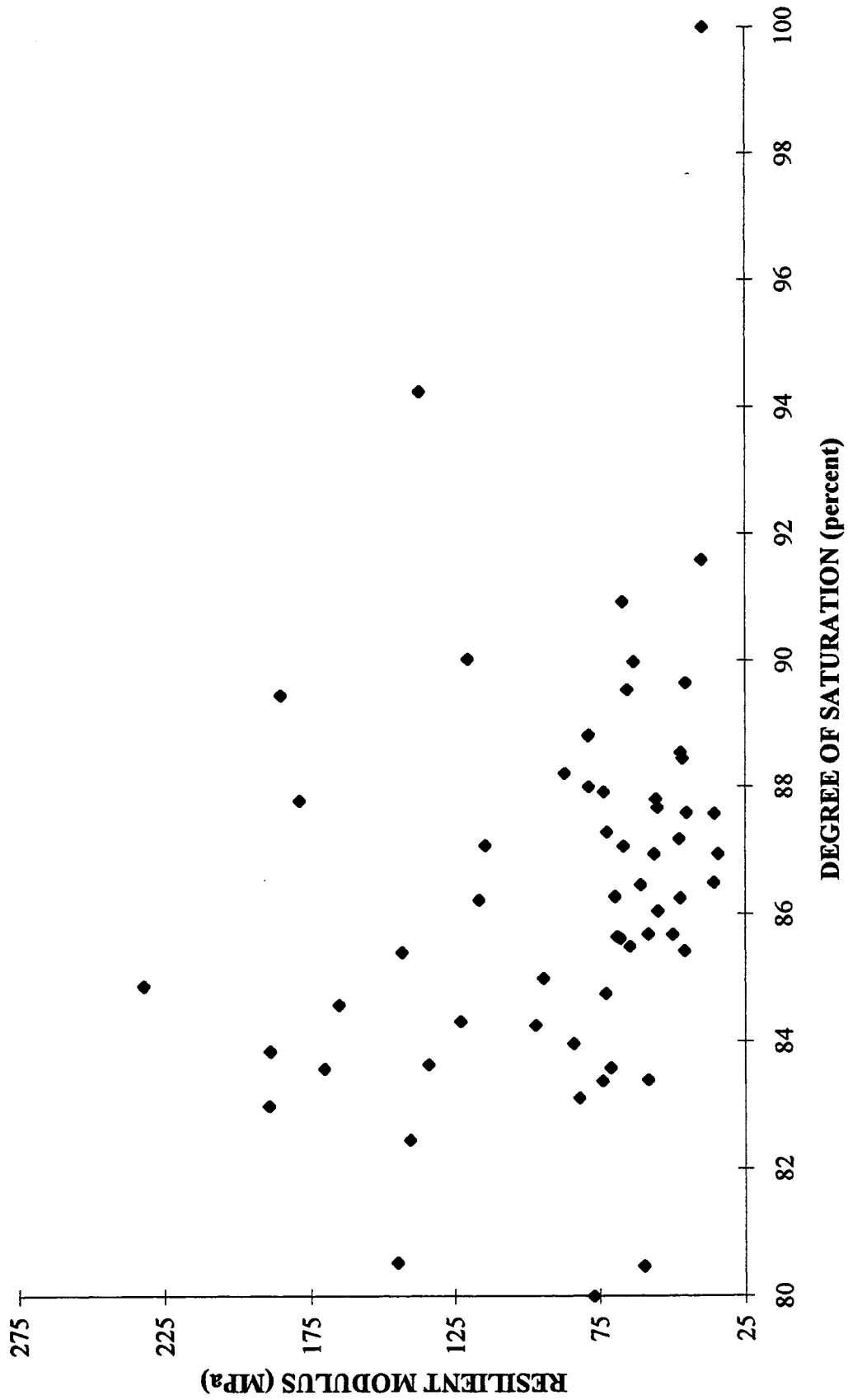


Fig. 44. Effect of saturation level on resilient modulus of thin-walled (undisturbed) samples.

RESILIENT MODULUS VS. UNCONFINED COMPRESSIVE STRENGTH

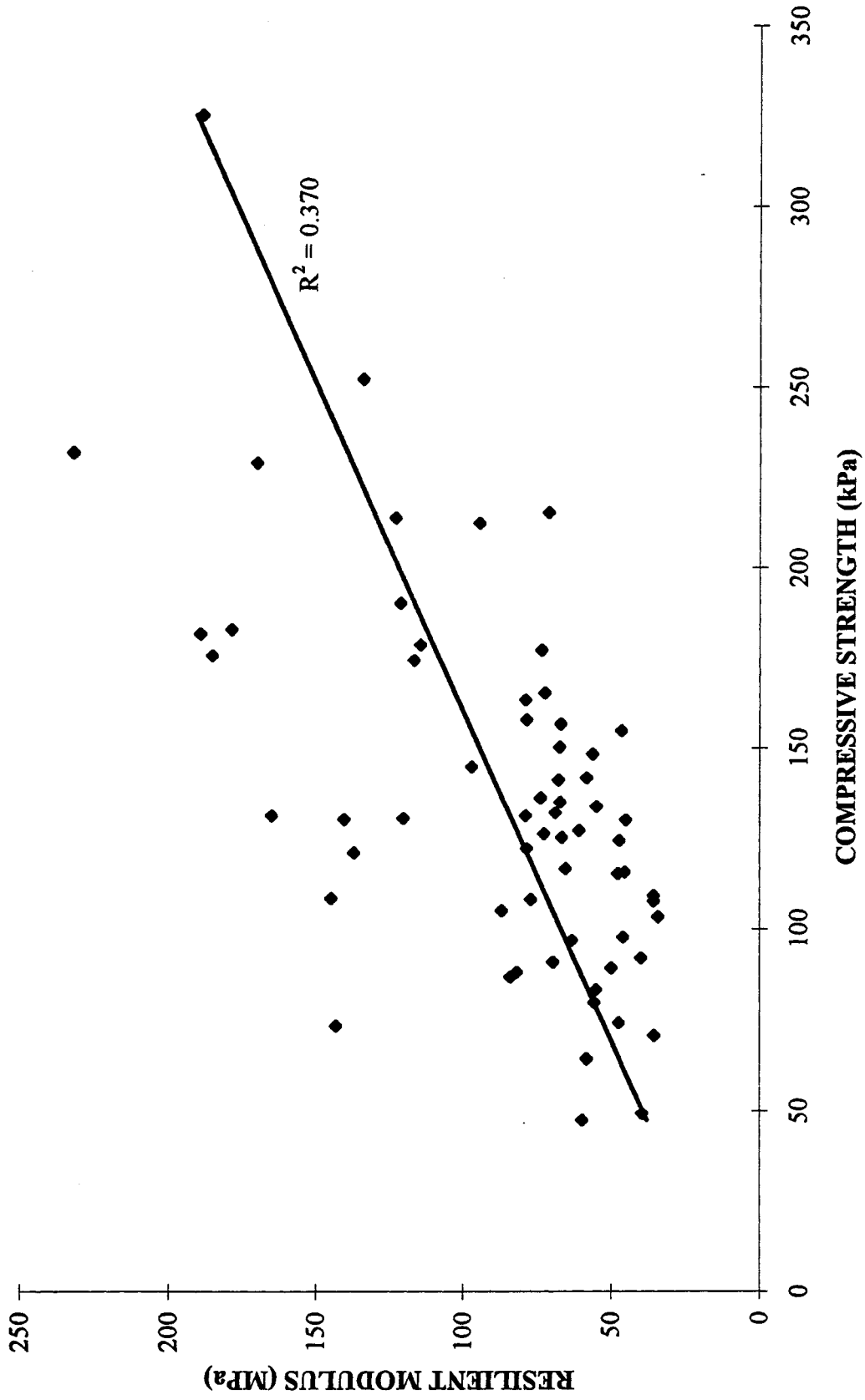


Fig. 45. Comparison of resilient moduli and compressive strength of thin-walled (undisturbed) samples.

DISTRIBUTION OF STRESS DIFFERENCES IN HALF-SPACE

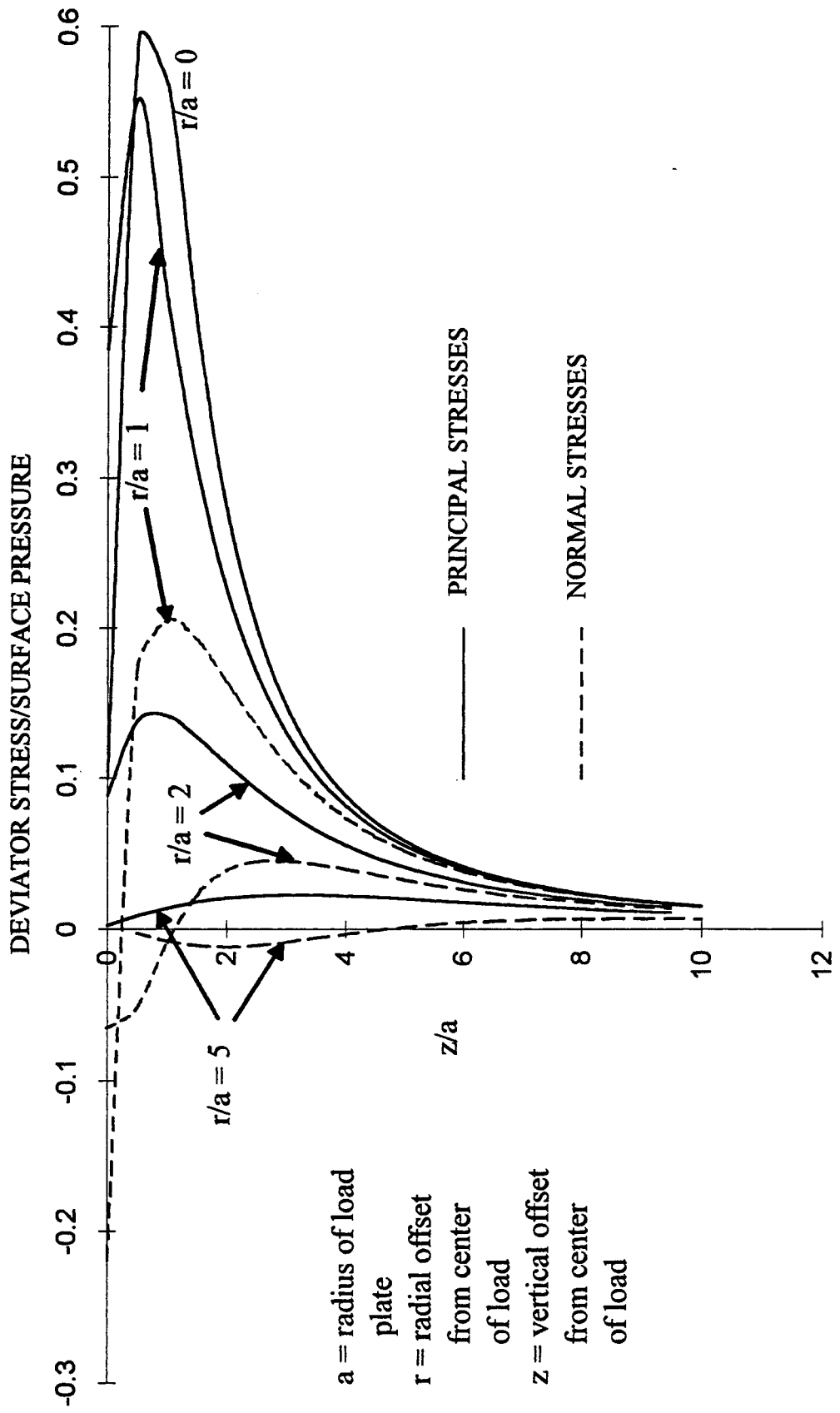


Fig. 46. Distribution of deviator stresses in half-space: normal and principal stress differences.

COMPARISON OF PRE- AND POST-BASE SUBGRADE MODULI

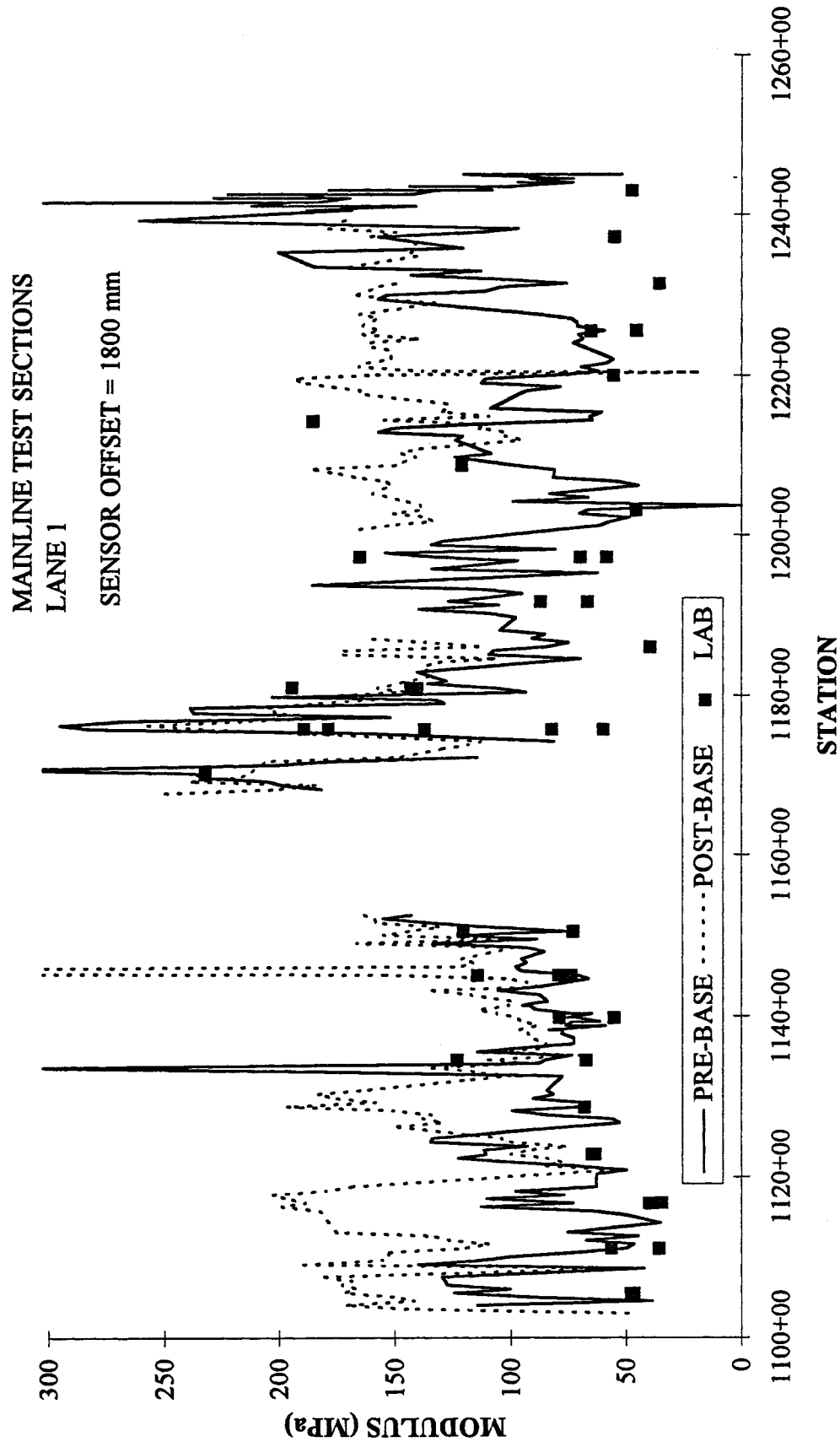


Fig. 47. Variation of backcalculated and laboratory subgrade moduli.

**COMPARISON OF BACKCALCULATED AND
LABORATORY MODULI**

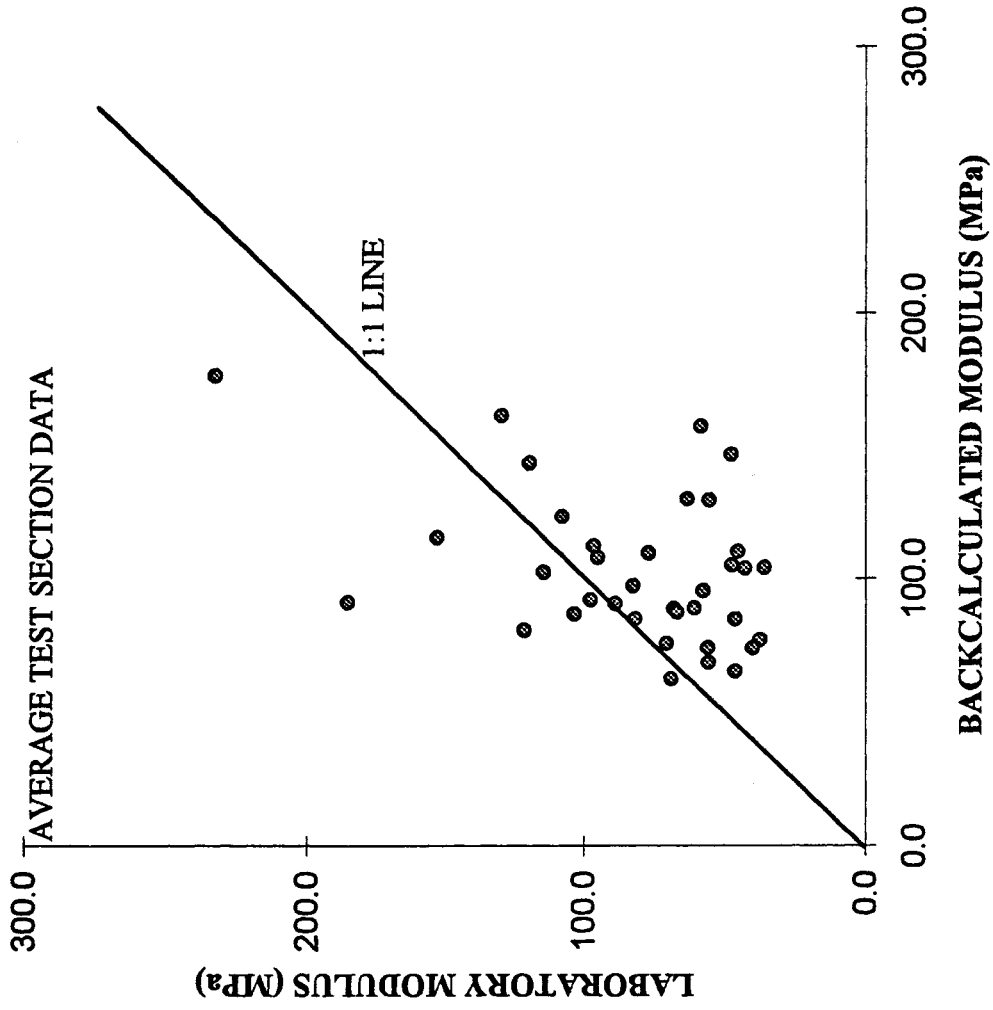


Fig. 48. Comparison of backcalculated and thin-walled (undisturbed) laboratory resilient moduli: average test section data.

VARIATION OF PENETRATION INDEX FOR MAINLINE TEST SECTIONS

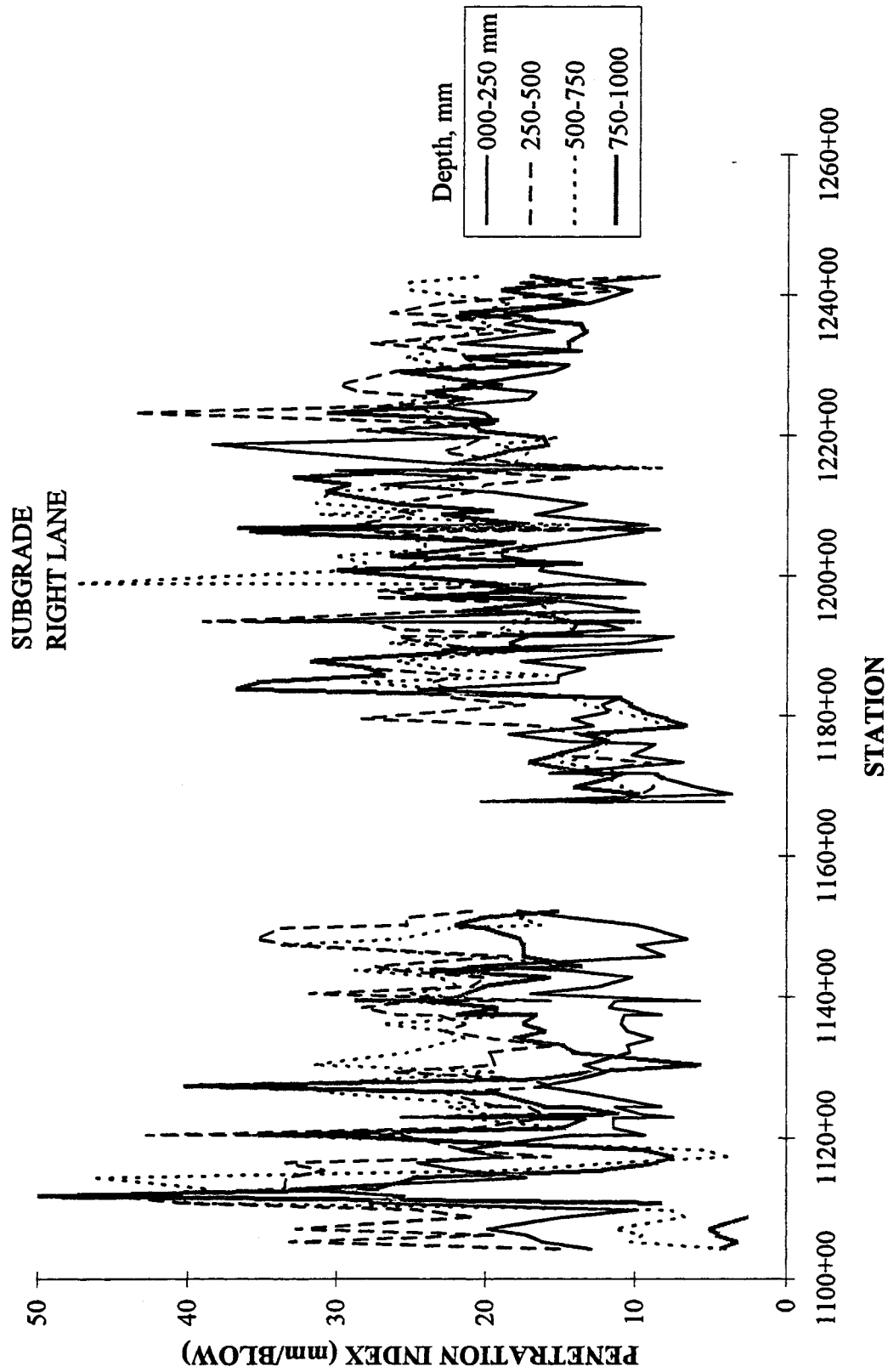


Fig. 49. Variation of sub-layer penetration index values for the mainline test sections, subgrade testing (right lane).

VARIATION OF PENETRATION INDEX FOR MAINLINE TEST SECTIONS

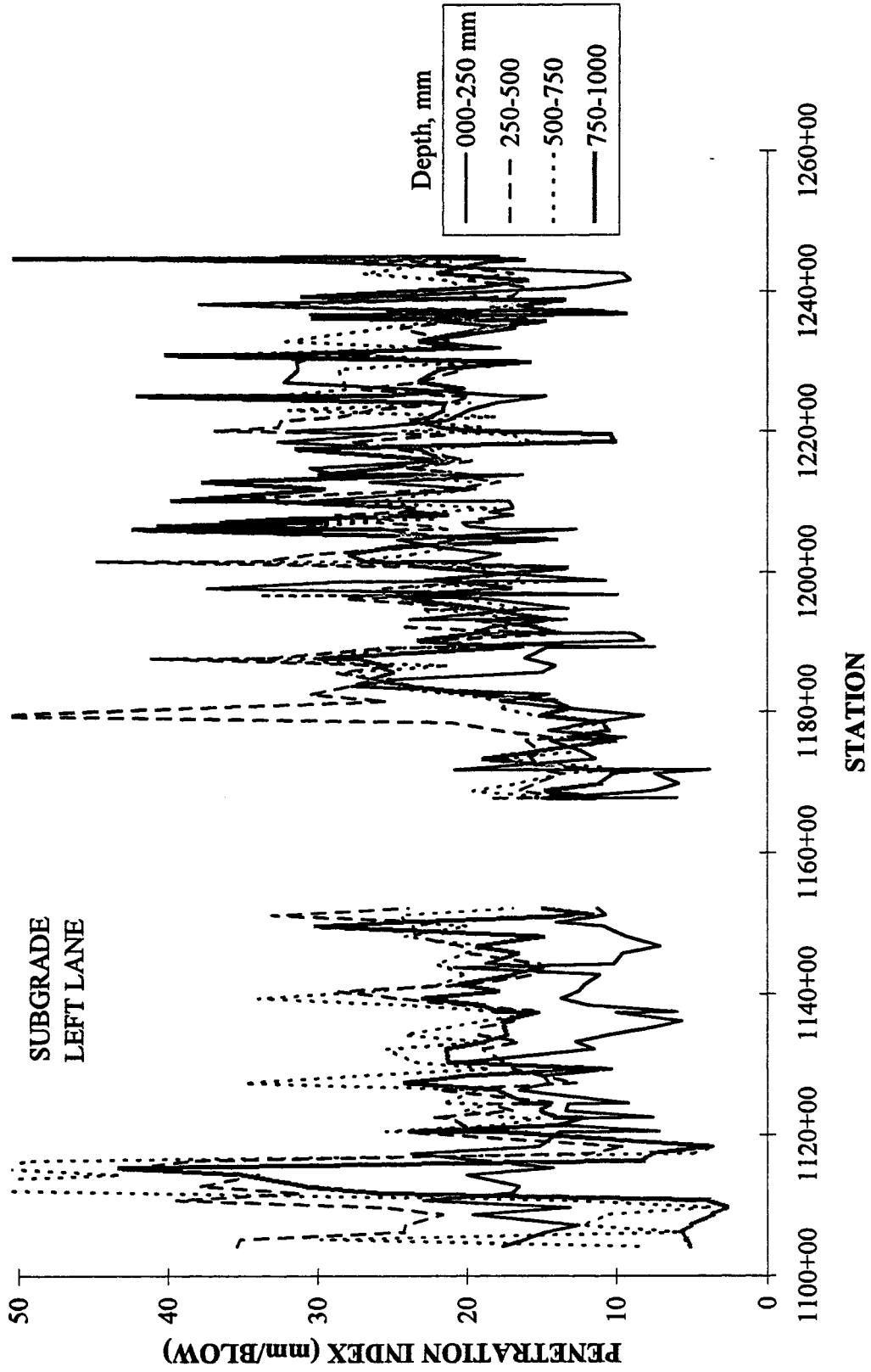


Fig. 50. Variation of sub-layer penetration index values for the mainline test sections, subgrade testing (left lane).

VARIATION OF PENETRATION INDEX FOR MAINLINE TEST SECTIONS

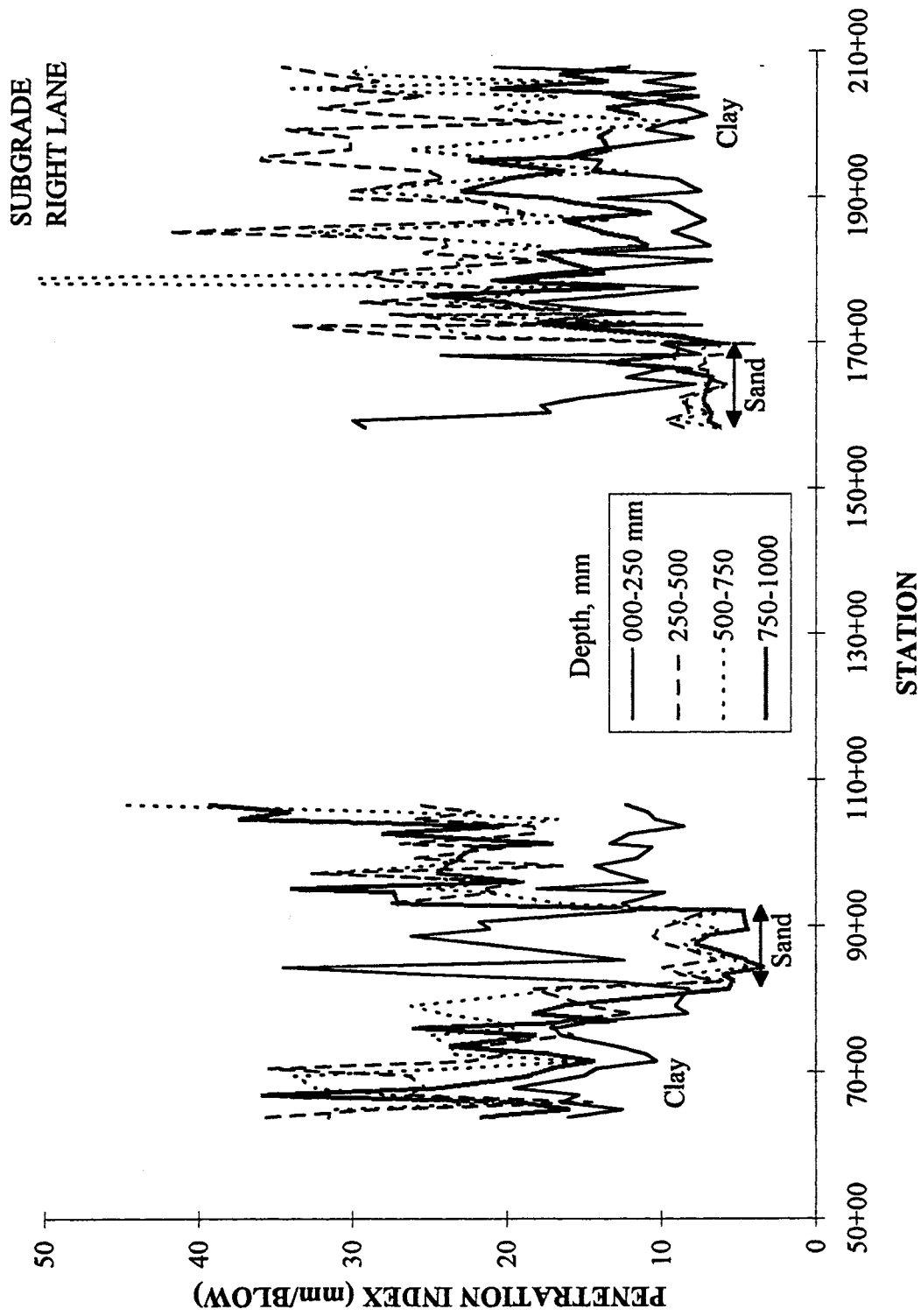


Fig. 51. Variation of sub-layer penetration index values for the low-volume test sections, subgrade testing (right lane).

VARIATION OF PENETRATION INDEX FOR MAINLINE TEST SECTIONS

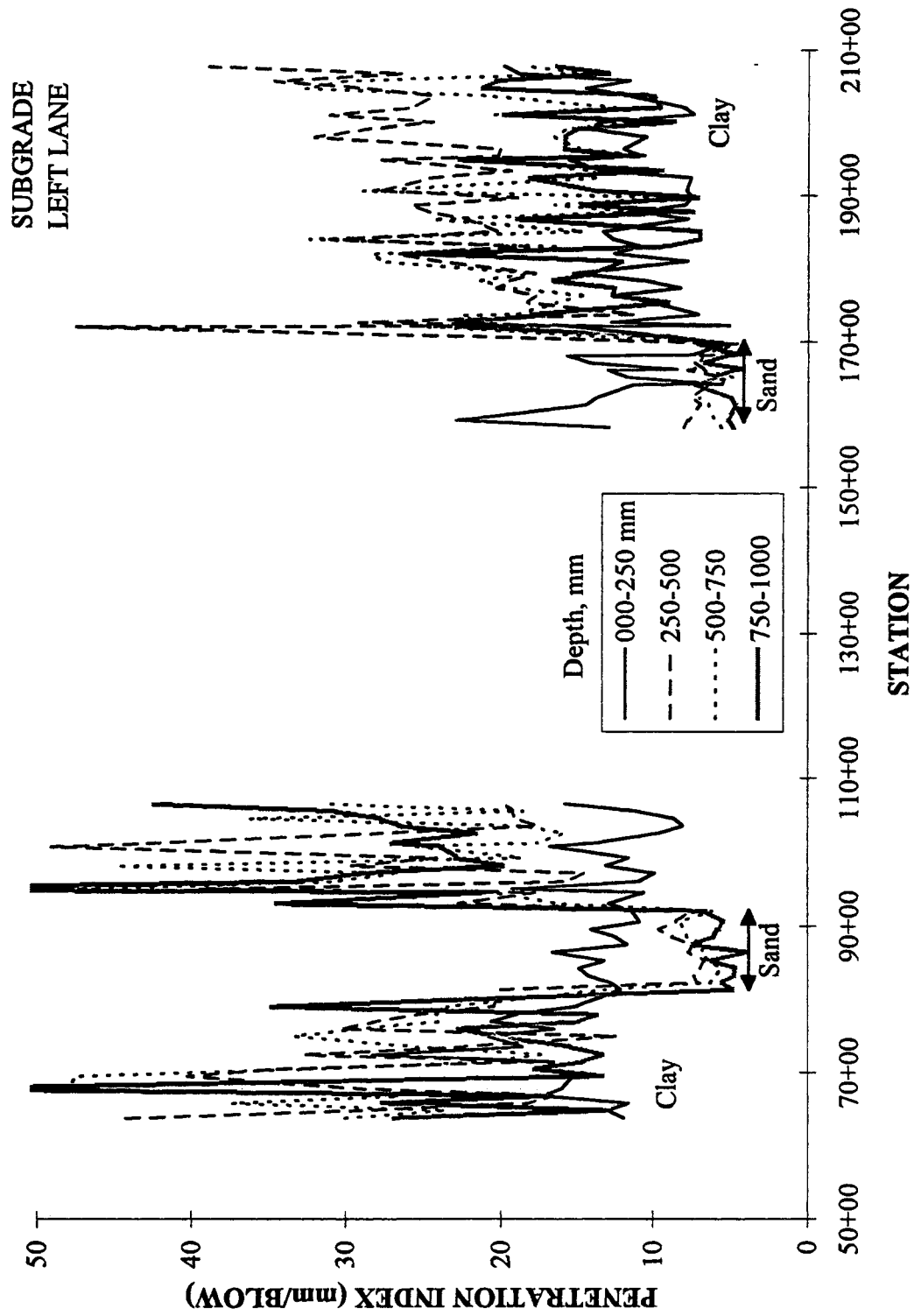


Fig. 52. Variation of sub-layer penetration index values for the low-volume test sections, subgrade testing (left lane).

VARIATION OF PENETRATION INDEX FOR MAINLINE TEST SECTIONS

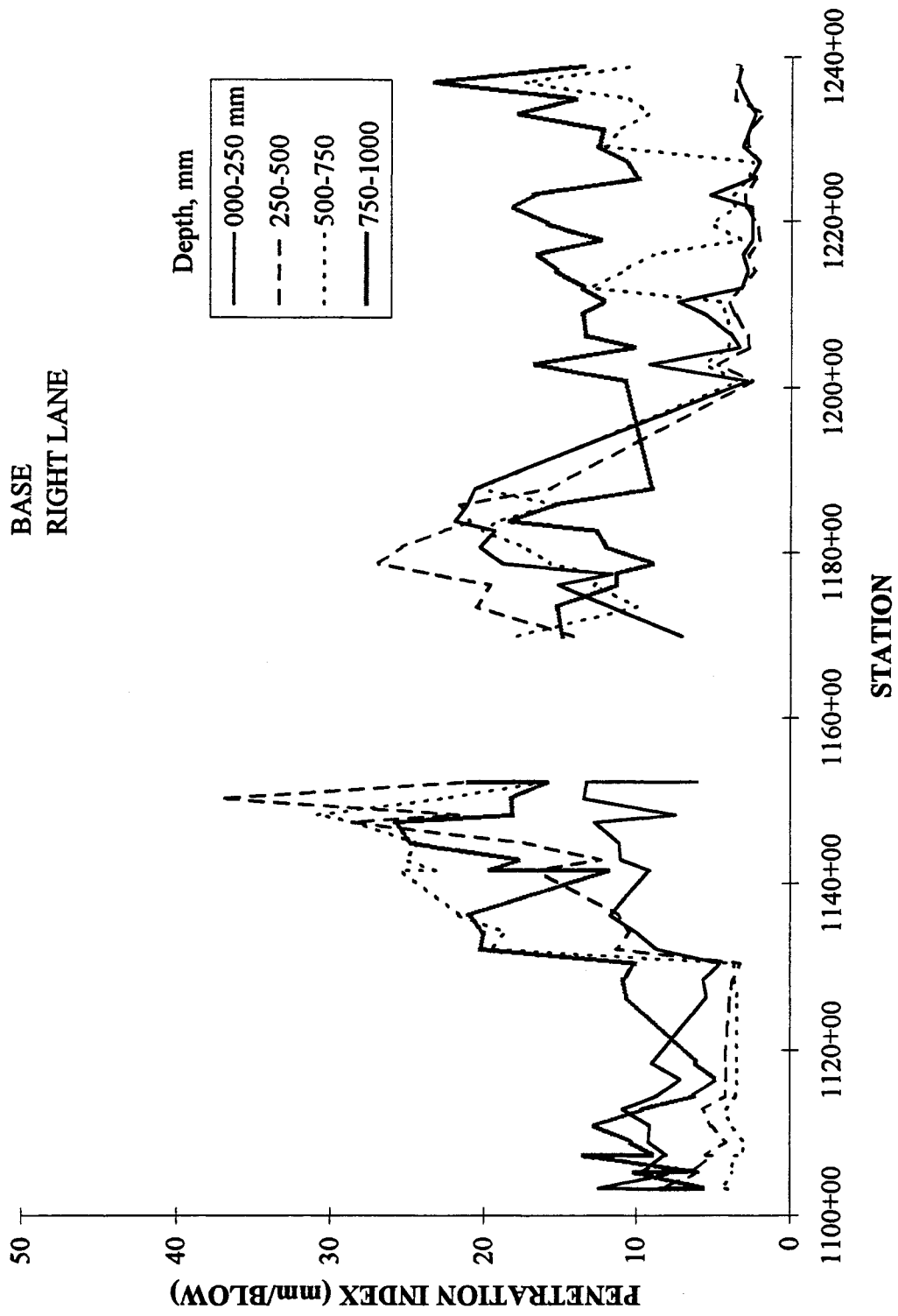


Fig. 53. Variation of sub-layer penetration index values for the mainline test sections, base testing (right lane).

VARIATION OF PENETRATION INDEX FOR MAINLINE TEST SECTIONS

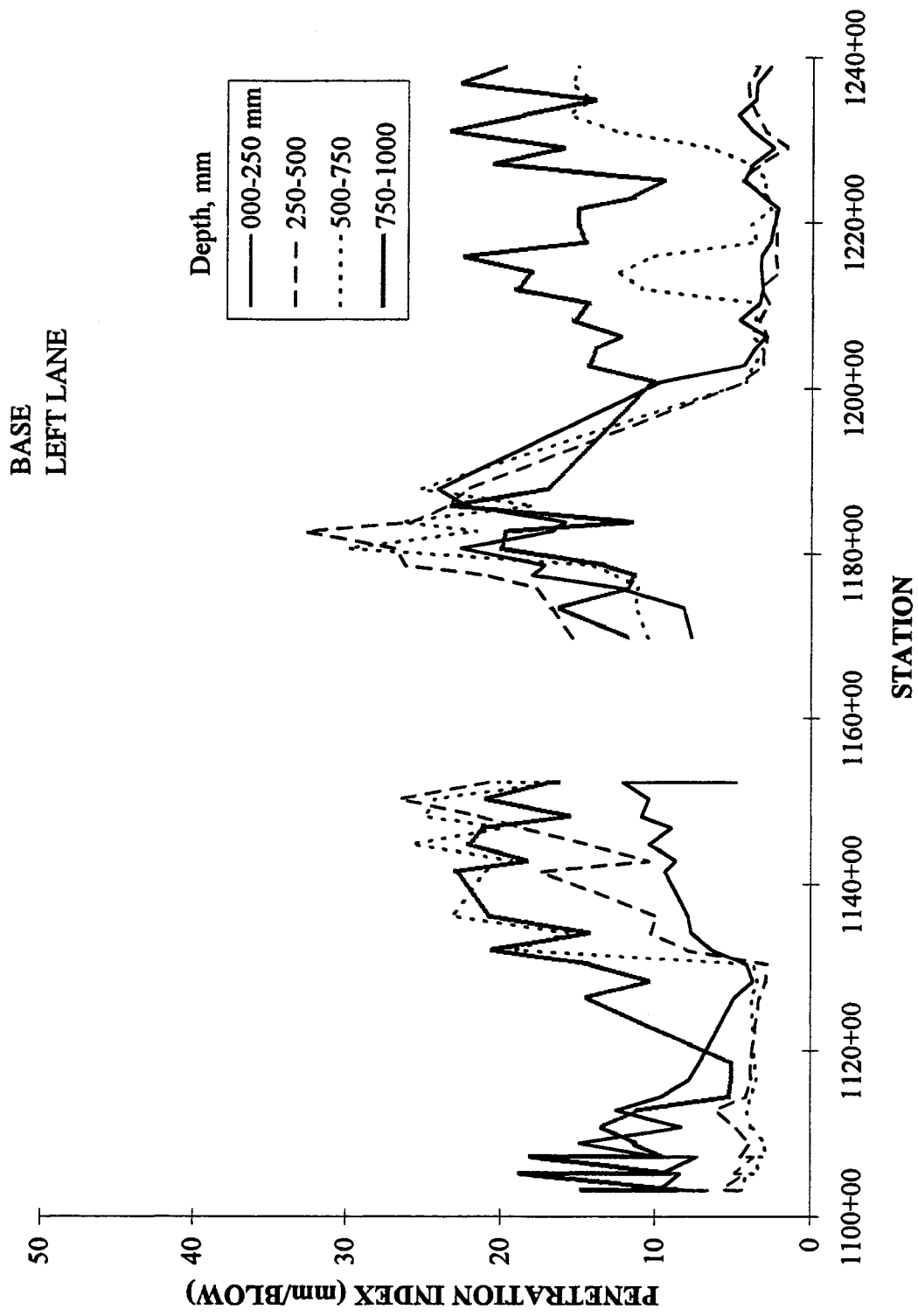


Fig. 54. Variation of sub-layer penetration index values for the mainline test sections, base testing (left lane).

VARIATION OF PENETRATION INDEX FOR MAINLINE TEST SECTIONS

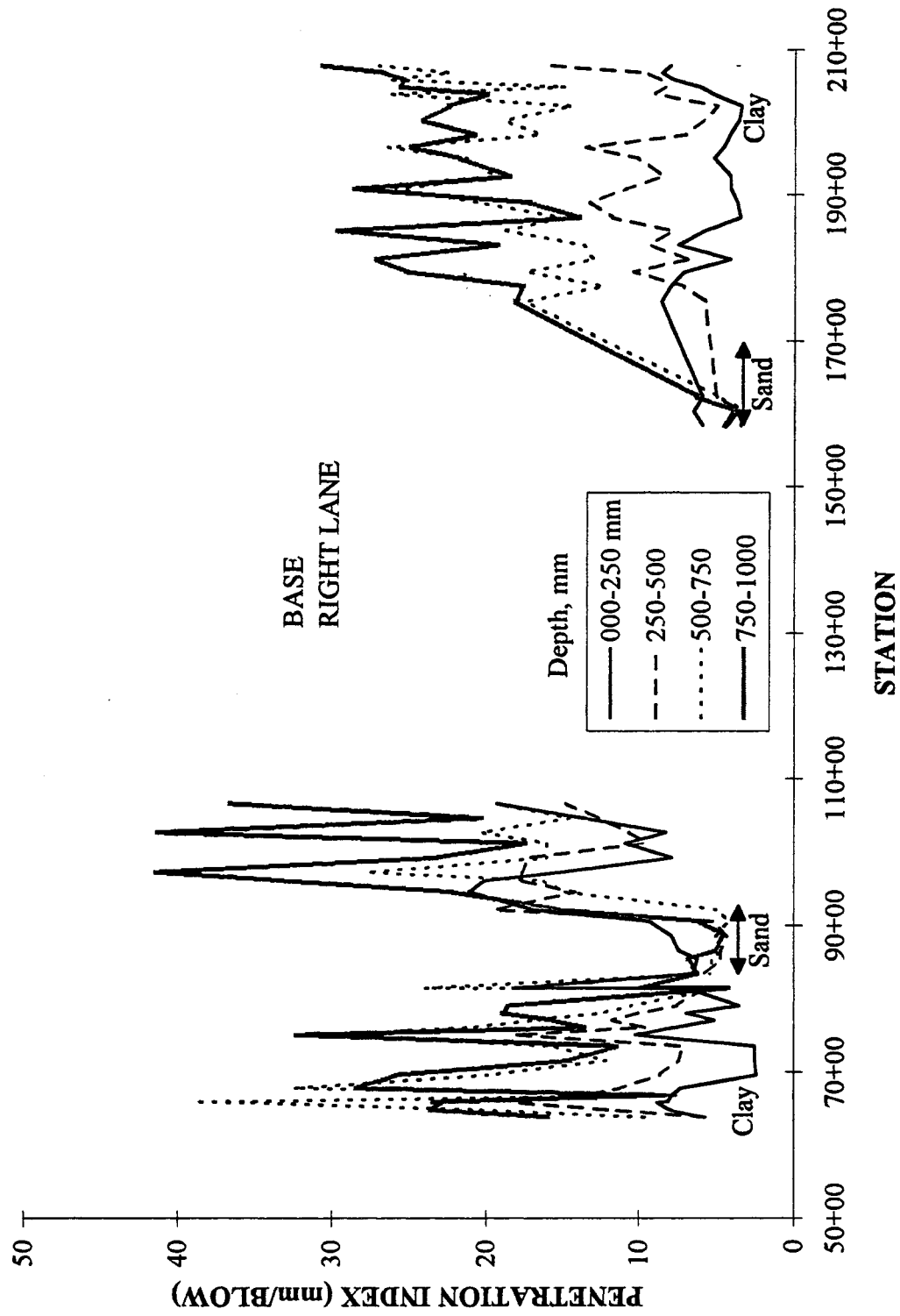


Fig. 55. Variation of sub-layer penetration index values for the low-volume test sections, base testing (right lane).

VARIATION OF PENETRATION INDEX FOR MAINLINE TEST SECTIONS

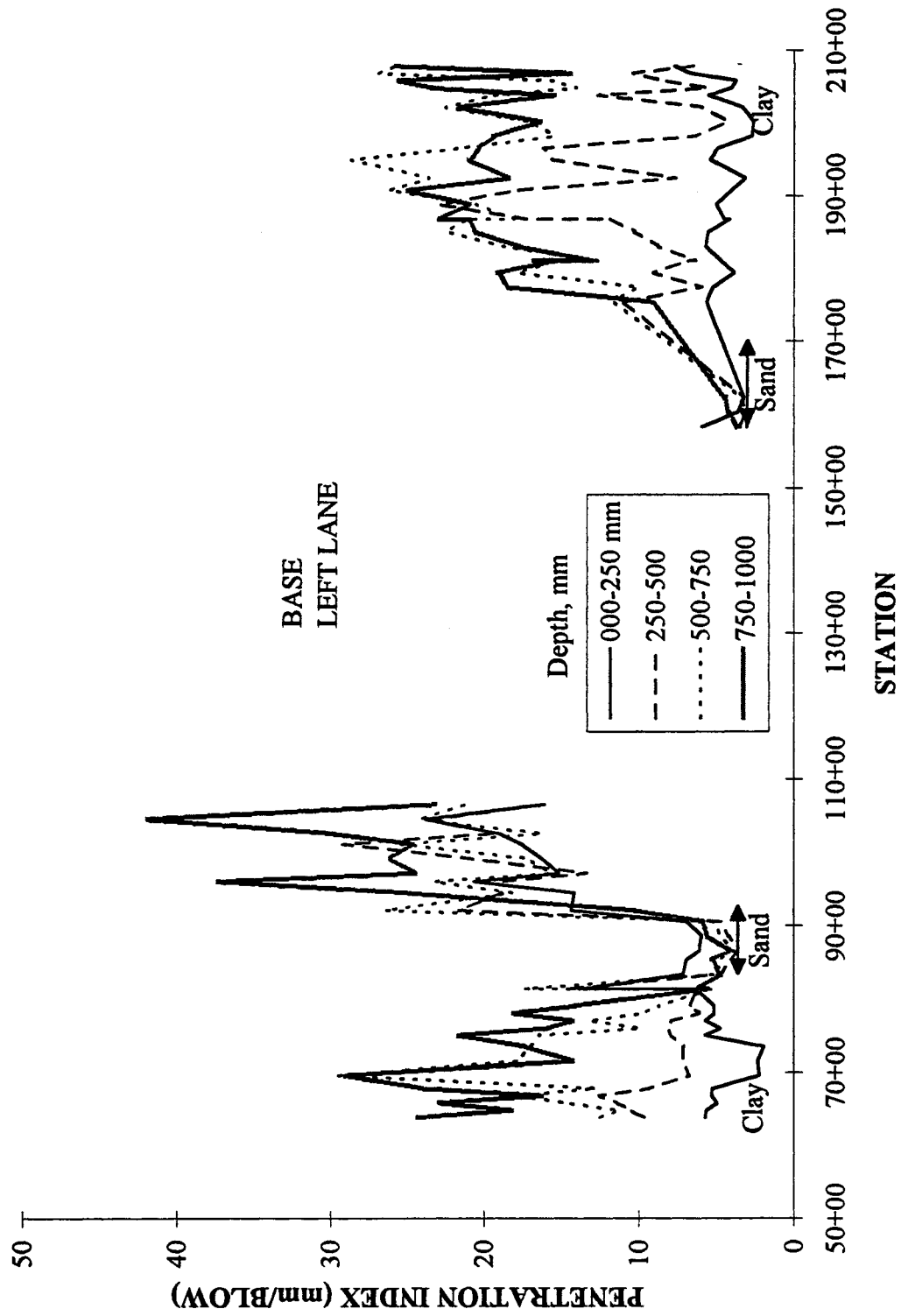


Fig. 56. Variation of sub-layer penetration index values for the low-volume test sections, base testing (left lane).

**VARIATION OF PENETRATION INDEX AND BACKCALCULATED MODULUS
FOR MAINLINE TEST SECTIONS**

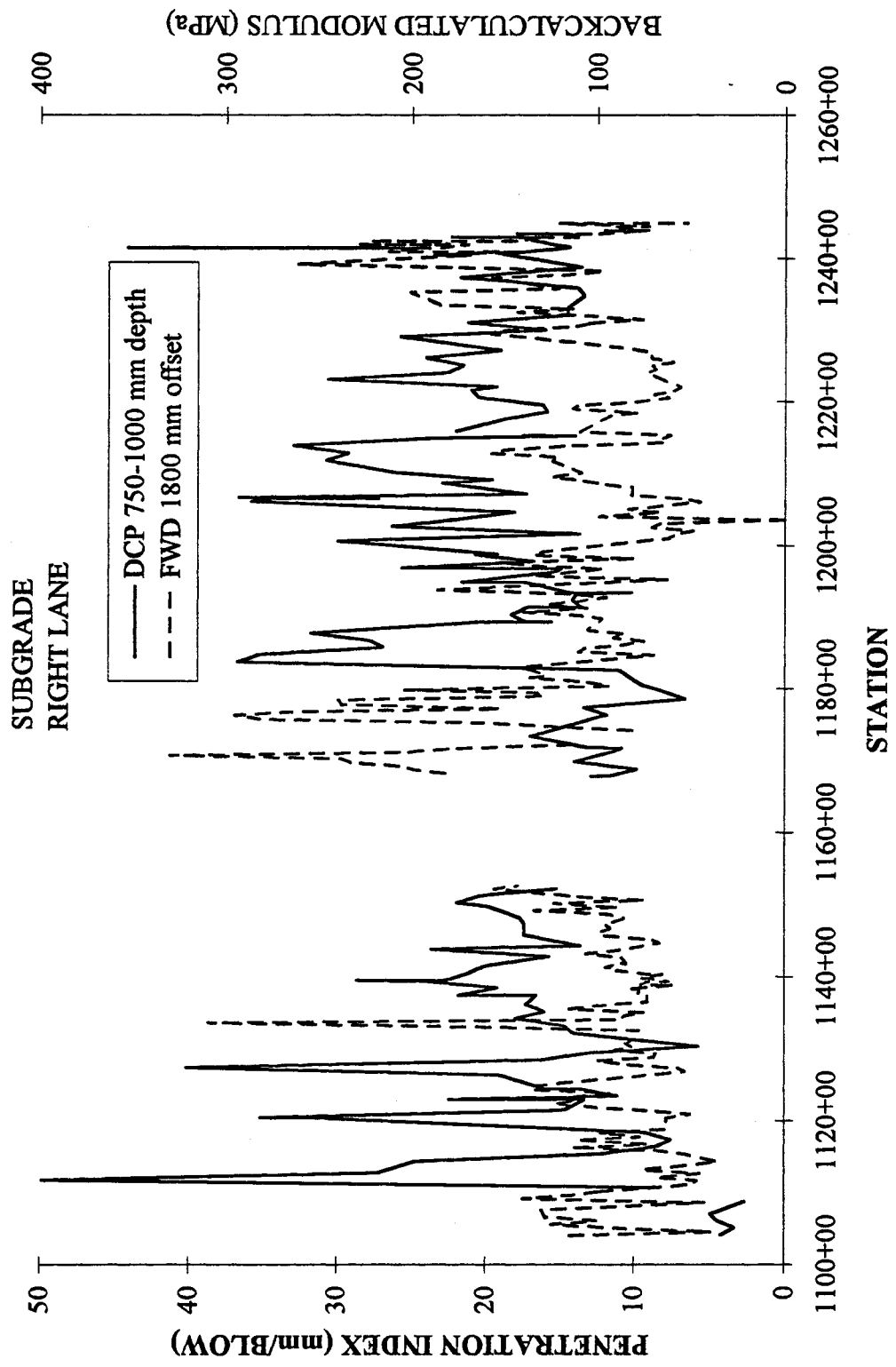


Fig. 57. Variation of penetration index values and moduli for the mainline test sections, subgrade testing (right lane).

**VARIATION OF PENETRATION INDEX AND BACKCALCULATED MODULUS
FOR MAINLINE TEST SECTIONS**

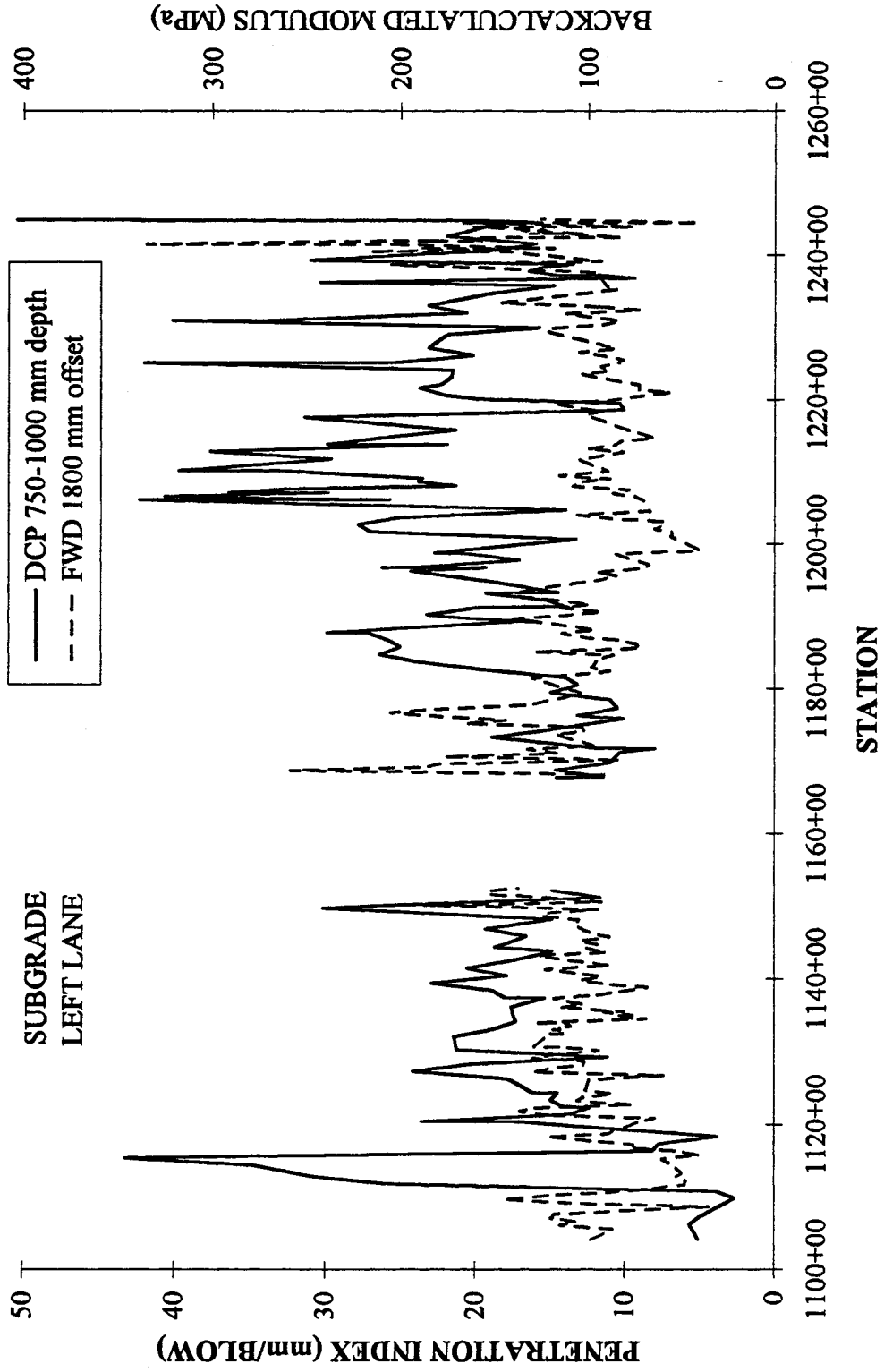


Fig. 58. Variation of penetration index values and moduli for the mainline test sections, subgrade testing (left lane).

**VARIATION OF PENETRATION INDEX AND BACKCALCULATED MODULUS
FOR LOW-VOLUME TEST SECTIONS**

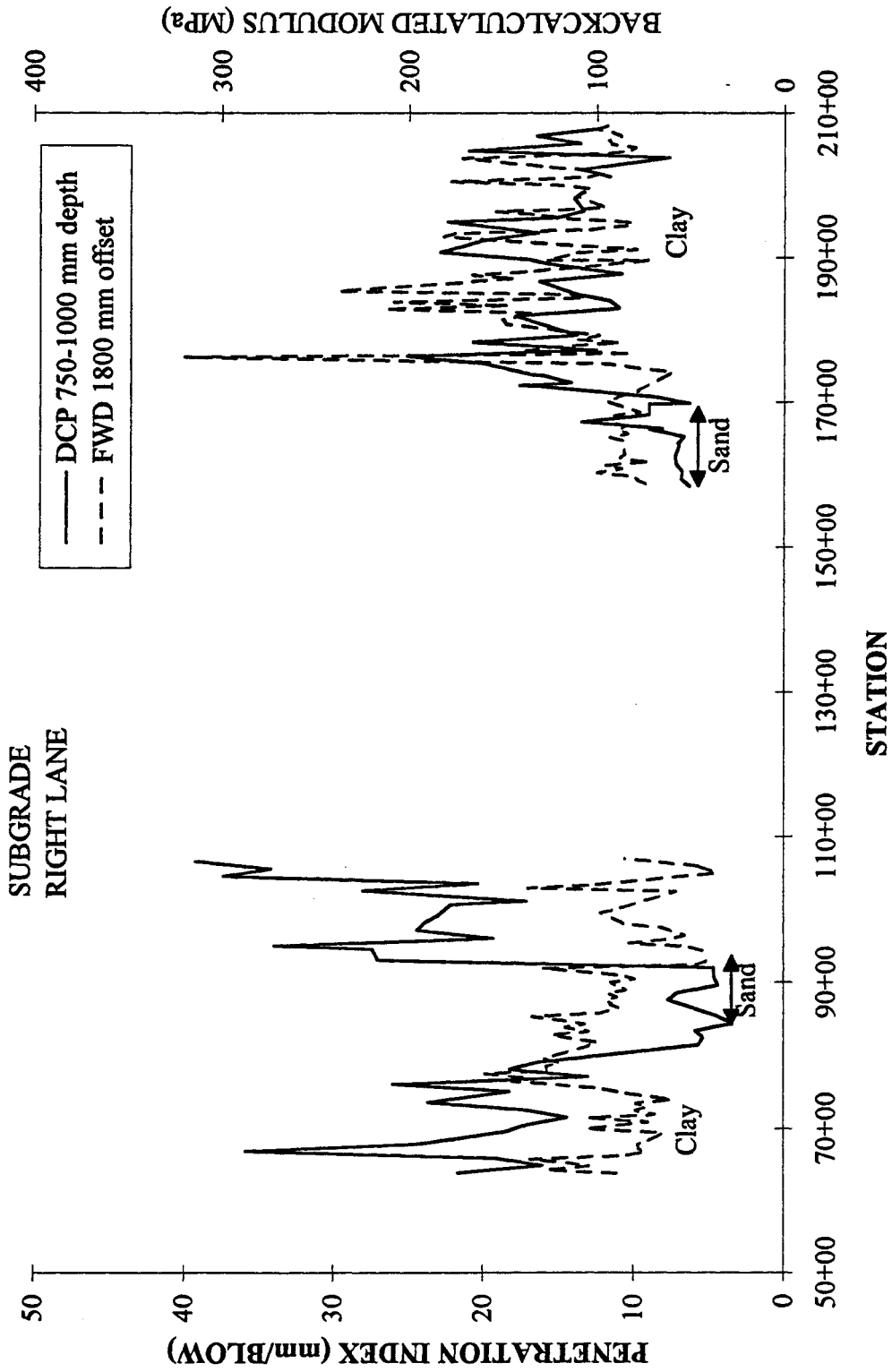


Fig. 59. Variation of penetration index values and moduli for the low-volume test sections, subgrade testing (right lane).

**VARIATION OF PENETRATION INDEX AND BACKCALCULATED MODULUS
FOR LOW-VOLUME TEST SECTIONS**

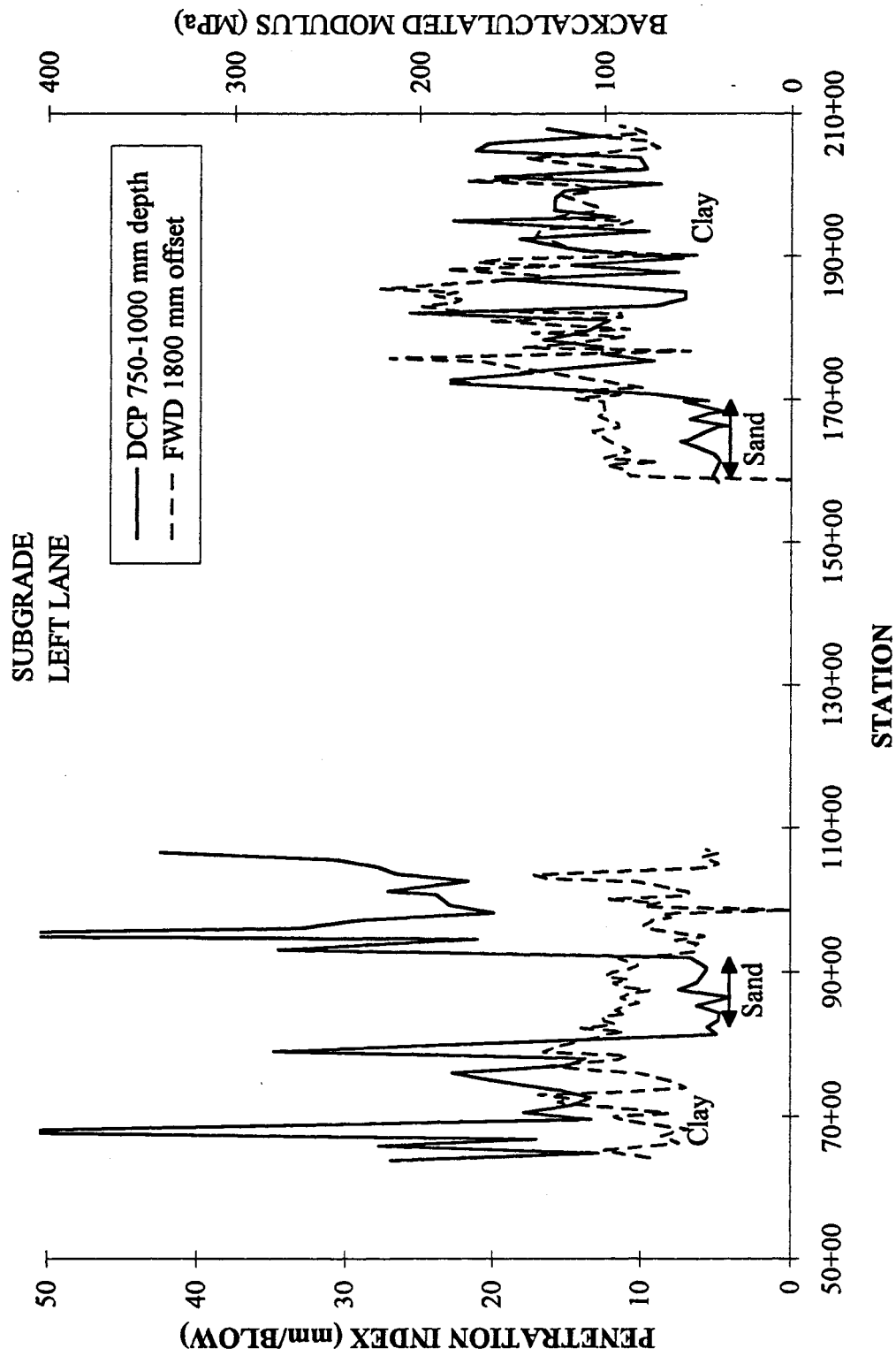


Fig. 60. Variation of penetration index values and moduli for the low-volume test sections, subgrade testing (left lane).

**VARIATION OF PENETRATION INDEX AND BACKCALCULATED MODULUS
FOR MAINLINE TEST SECTIONS**

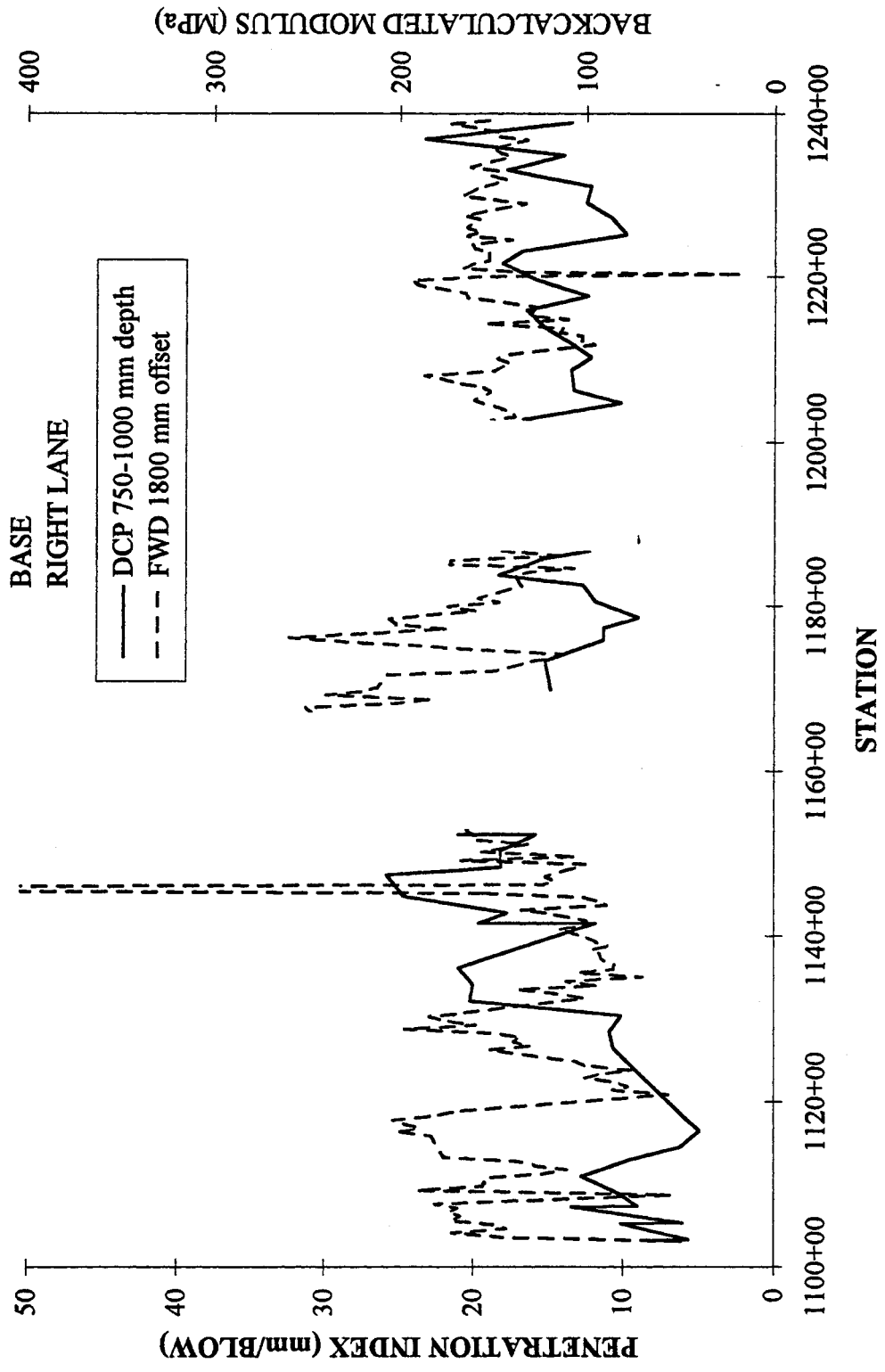


Fig. 61. Variation of penetration index values and moduli for the mainline test sections, base testing (right lane).

**VARIATION OF PENETRATION INDEX AND BACKCALCULATED MODULUS
FOR MAINLINE TEST SECTIONS**

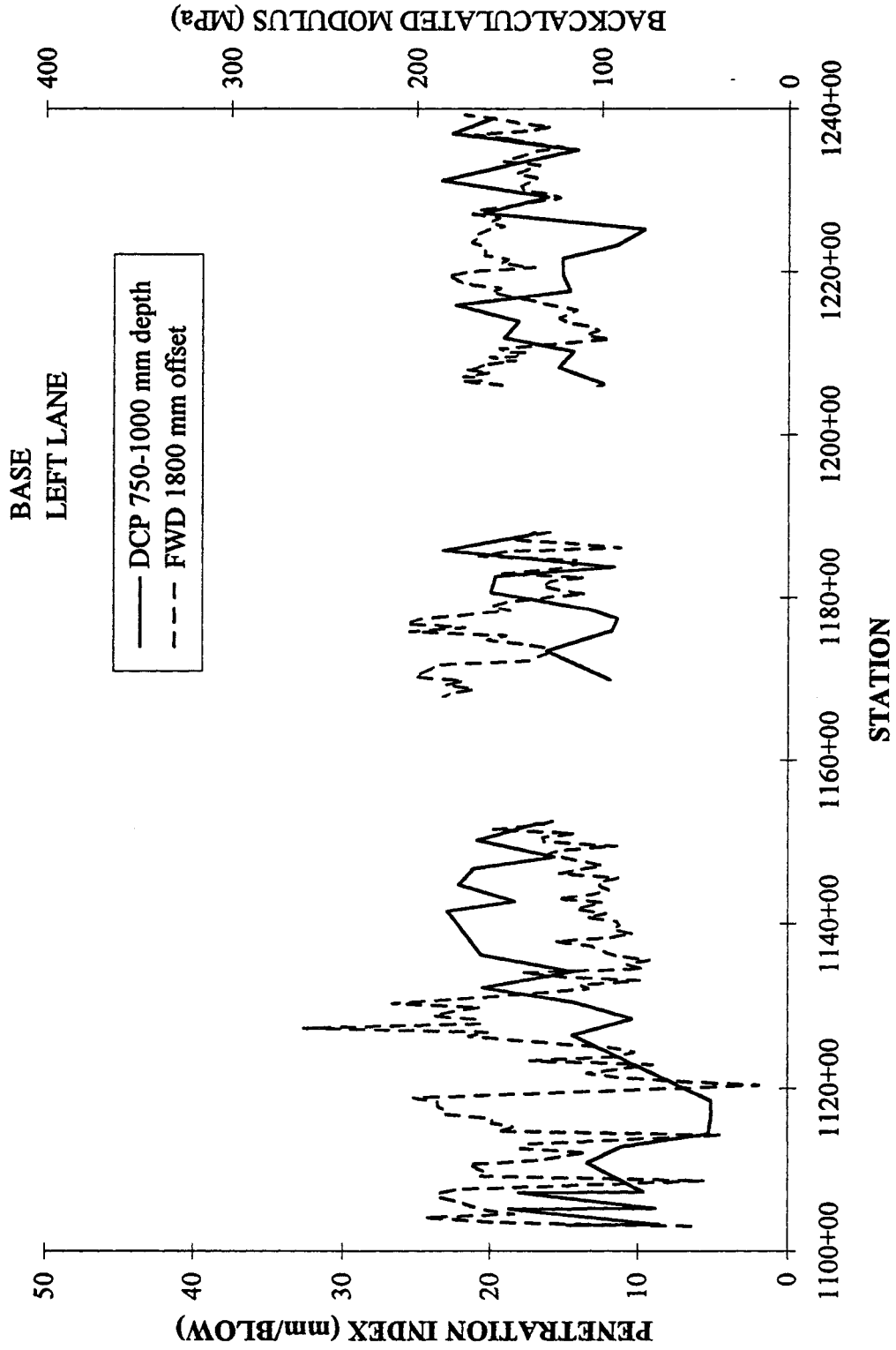


Fig. 62. Variation of penetration index values and moduli for the mainline test sections, base testing (left lane).

**VARIATION OF PENETRATION INDEX AND BACKCALCULATED MODULUS
FOR LOW-VOLUME TEST SECTIONS**

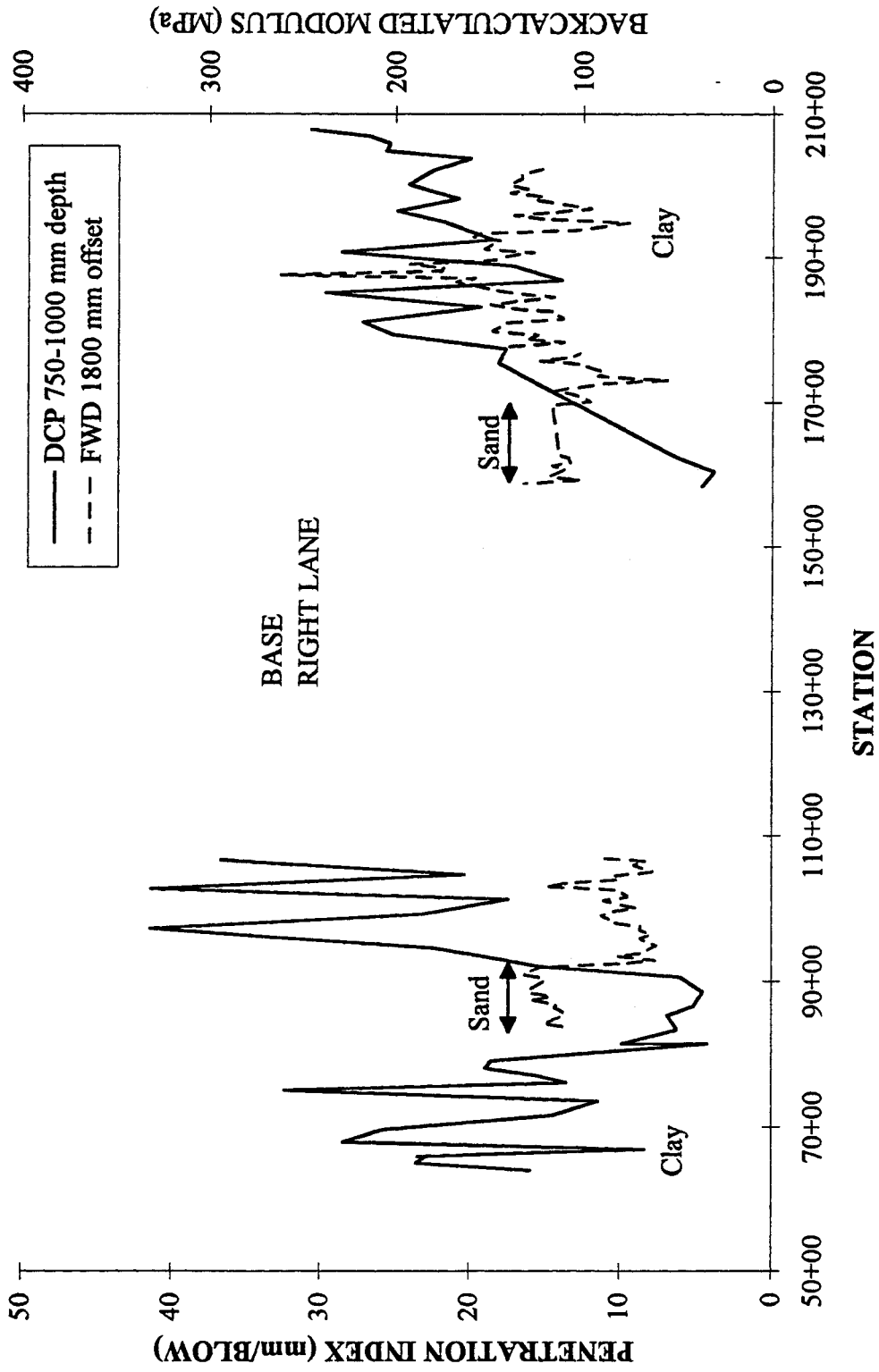


Fig. 63. Variation of penetration index values and moduli for the low-volume test sections, base testing (right lane).

**VARIATION OF PENETRATION INDEX AND BACKCALCULATED MODULUS
FOR LOW-VOLUME TEST SECTIONS**

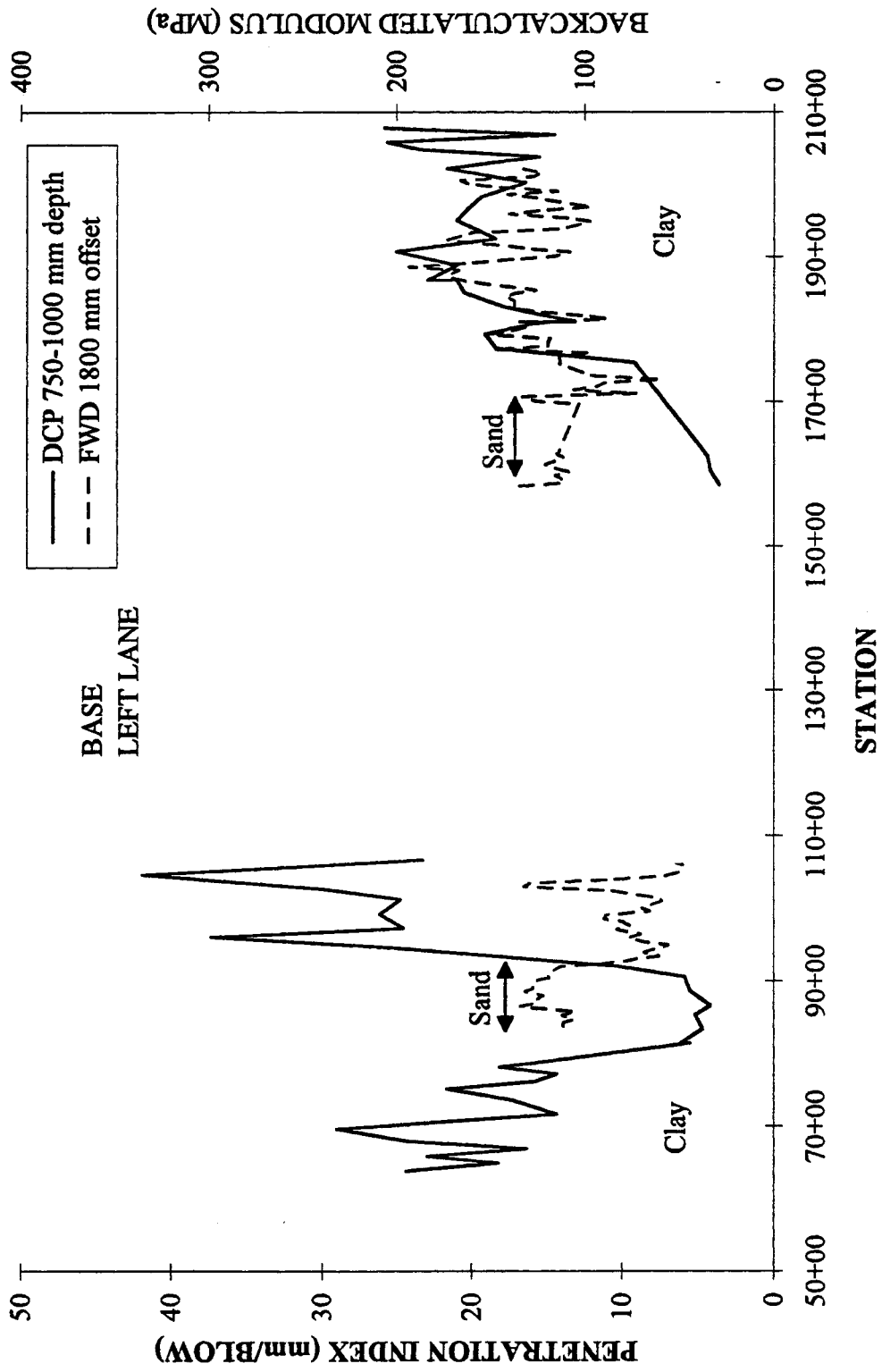


Fig. 64. Variation of penetration index values and moduli for the low-volume test sections, base testing (left lane).

PENETRATION INDEX vs. BACKCALCULATED SUBGRADE MODULUS

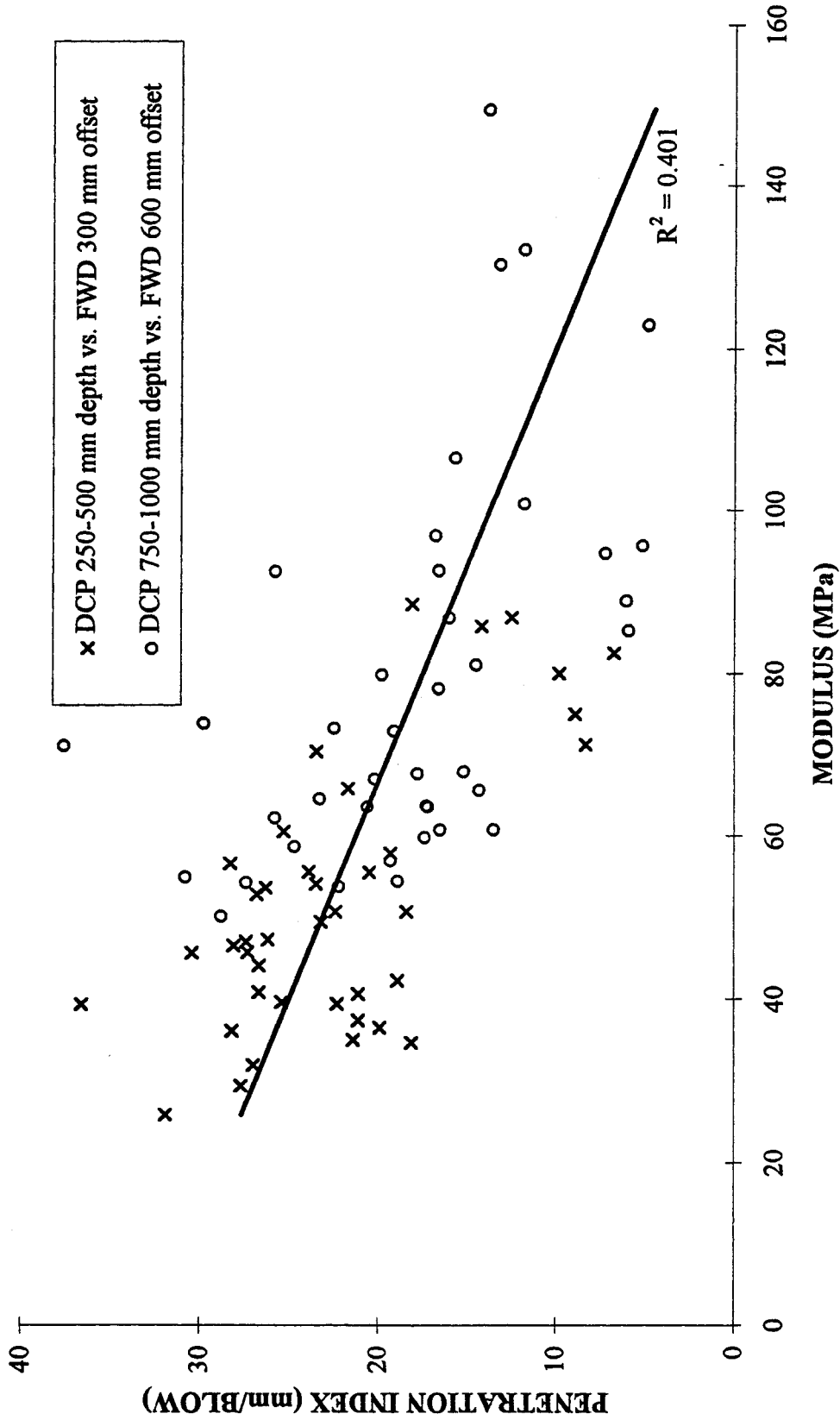


Fig. 65. Comparison of DCP penetration index and backcalculated modulus from subgrade testing.

PENETRATION INDEX vs. BACKCALCULATED SUBGRADE MODULUS

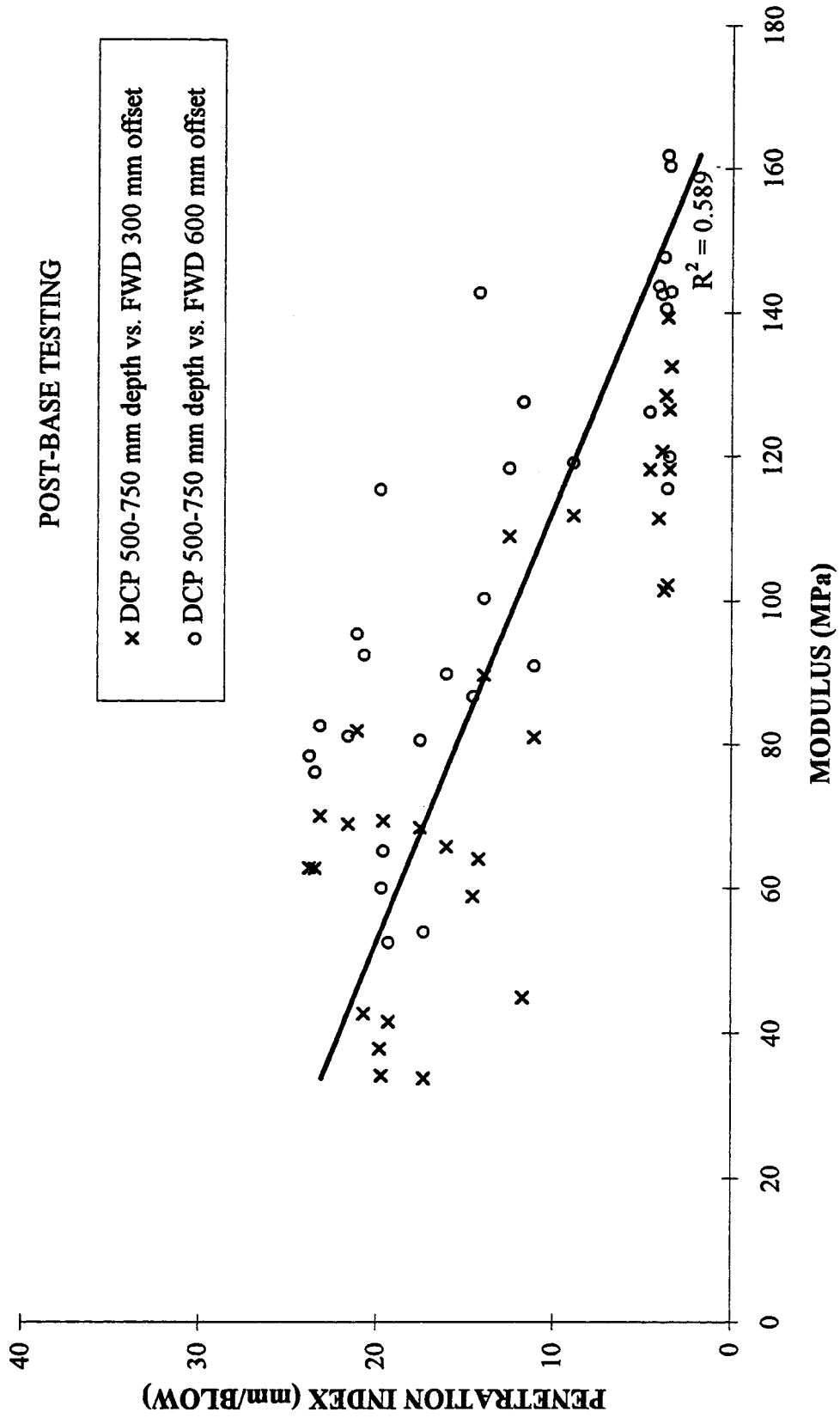


Fig. 66. Comparison of DCP penetration index and backcalculated modulus from base testing.

VARIogram OF BACKCALCULATED SUBGRADE MODULUS

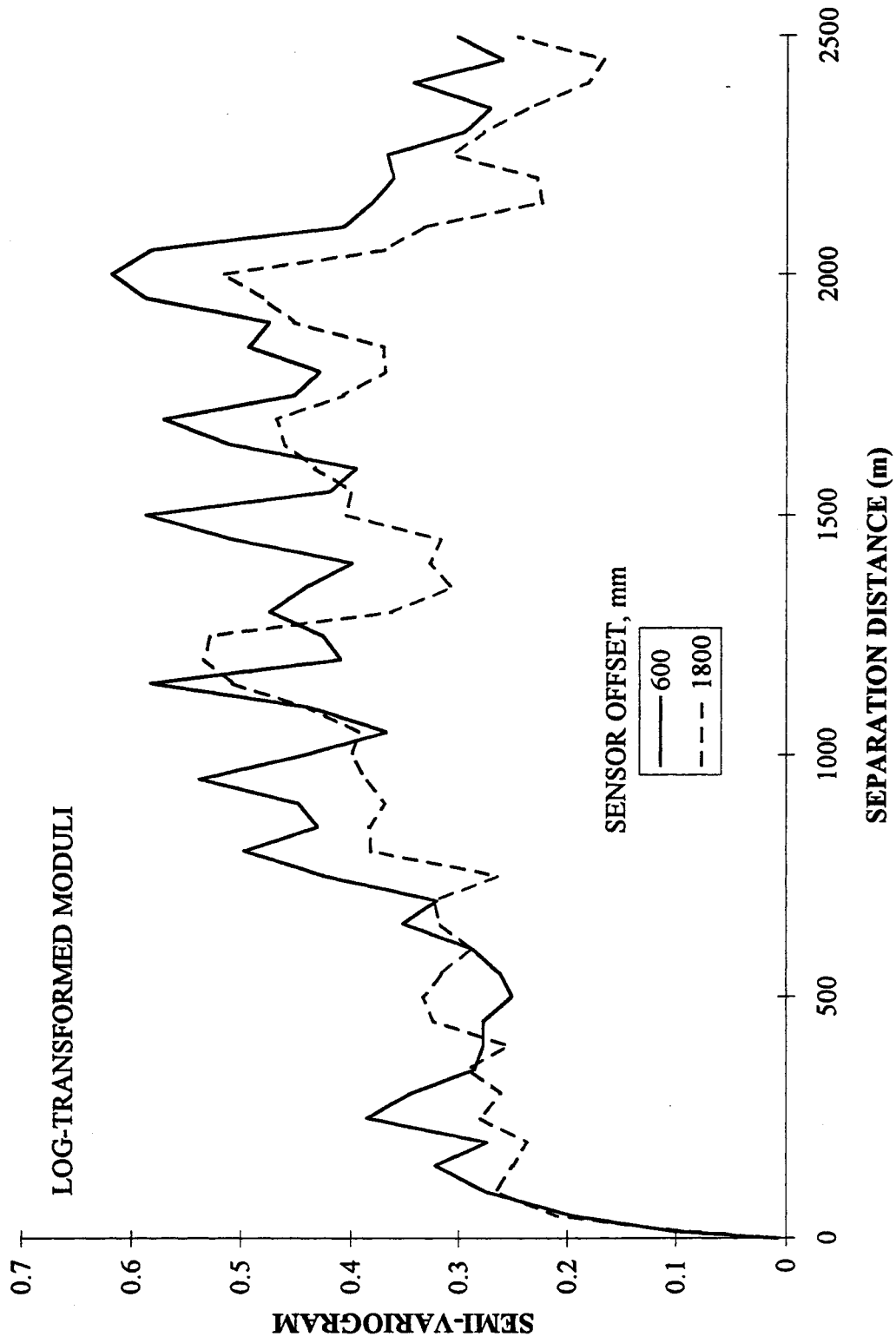


Fig. 67. Variograms for subgrade moduli based on log-transformed data.

VARIATION OF BACKCALCULATED AND KRIGED MODULI

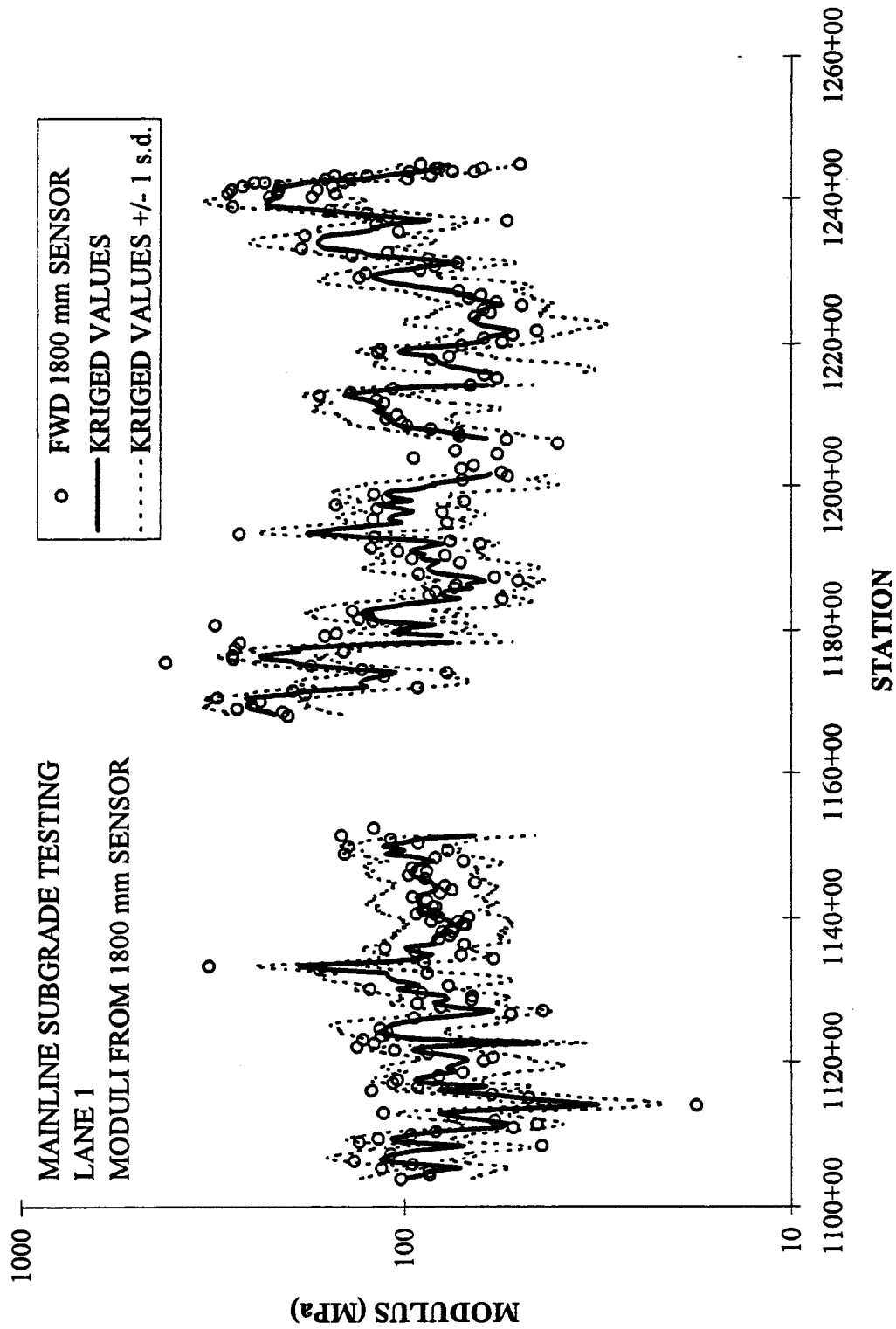


Fig. 68. Variation of backcalculated and estimated (kriged) moduli with station.

**COMPARISON OF LABORATORY
AND INTERPOLATED MODULI**

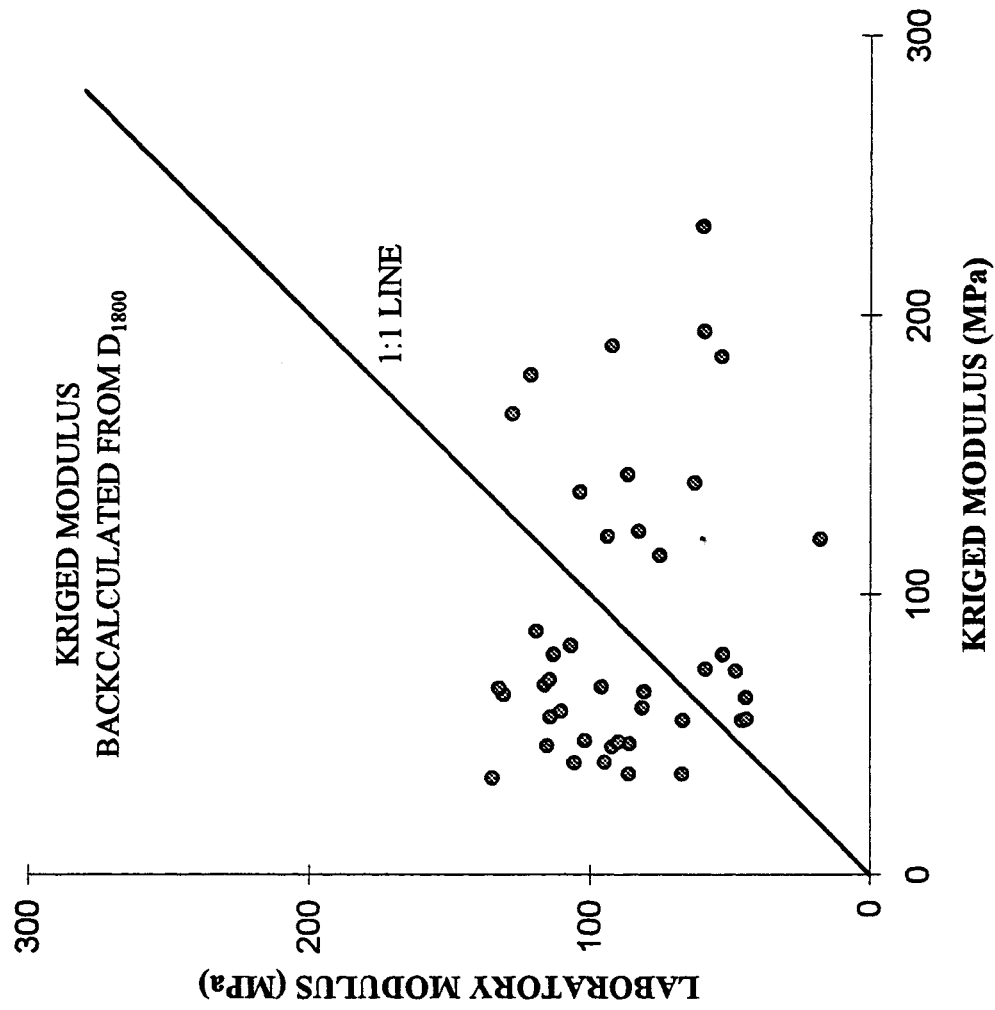


Fig. 69. Comparison of moduli from laboratory data and values estimated at thin-walled locations using kriging.

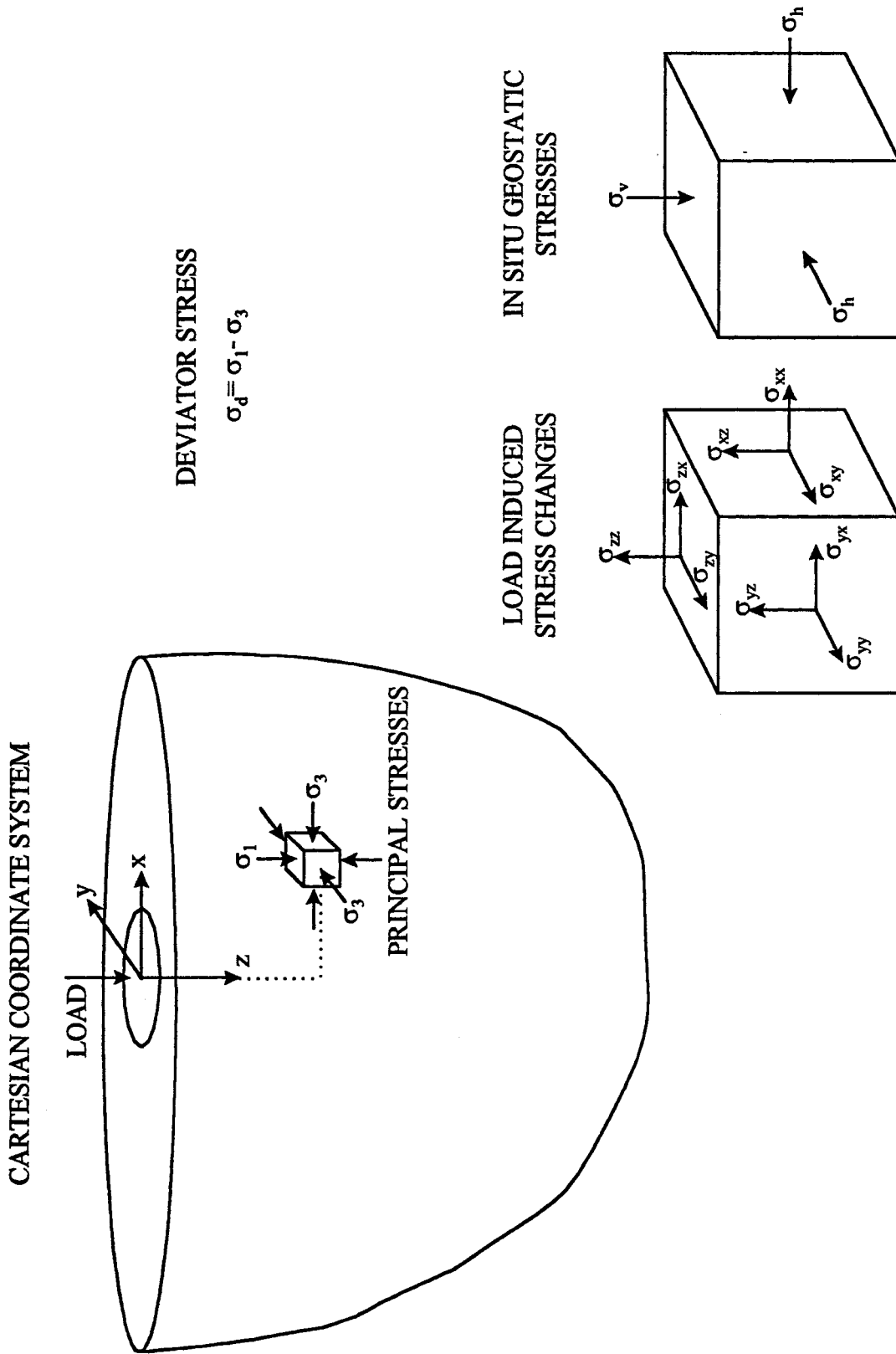
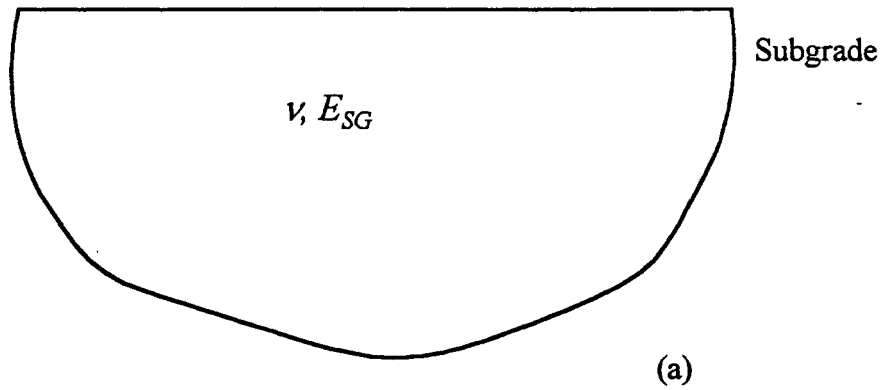
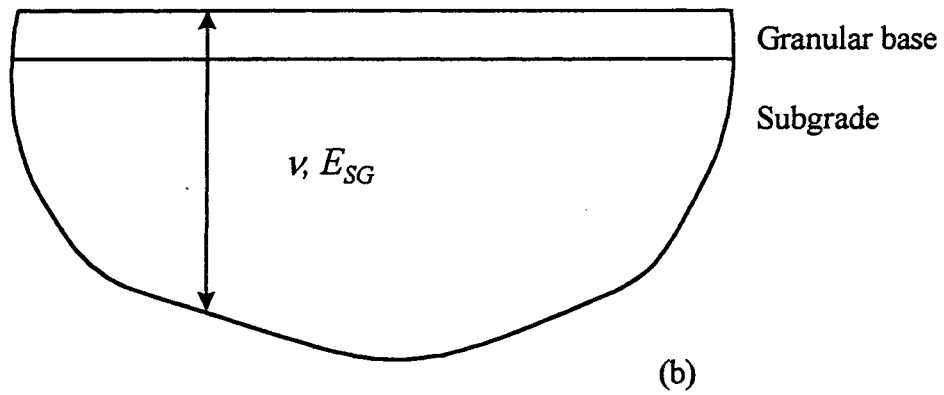


Fig. 70. Contributions of geostatic and load-induced stresses to principal stresses in half-space.

Subgrade testing: homogeneous model



Base testing (thin granular < 125 mm): homogeneous model



Base testing (medium granular 125 to 300 mm): multi-layer system, EVERCALC

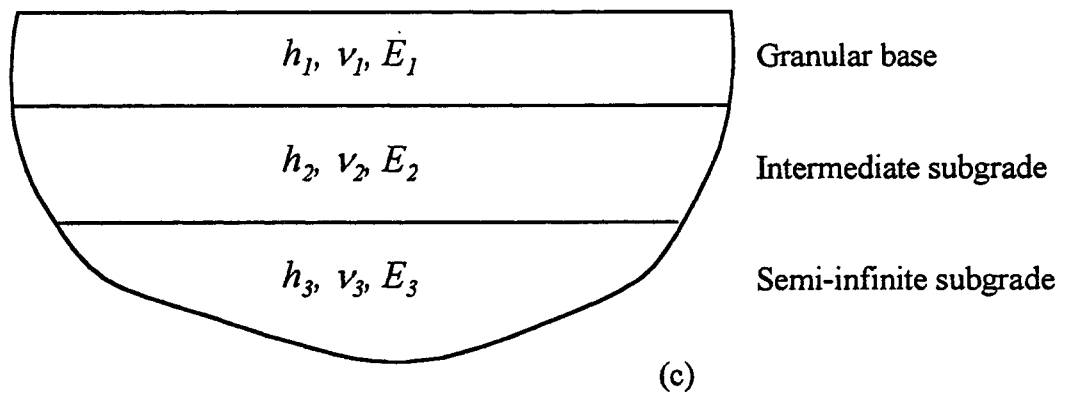
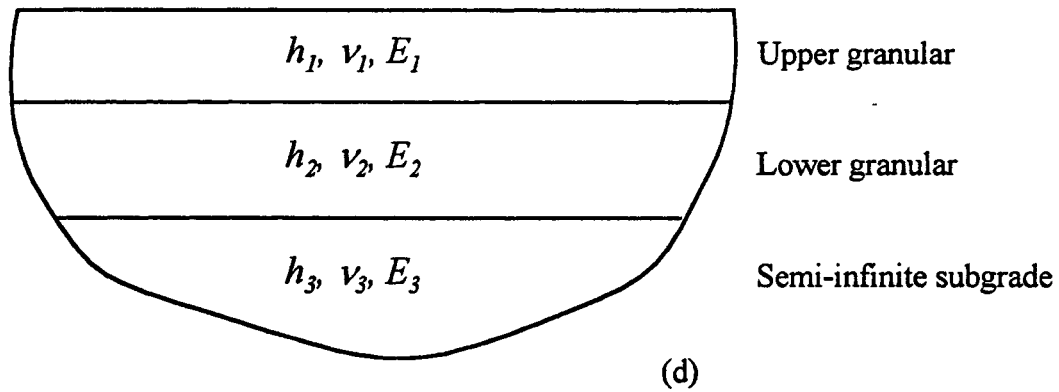
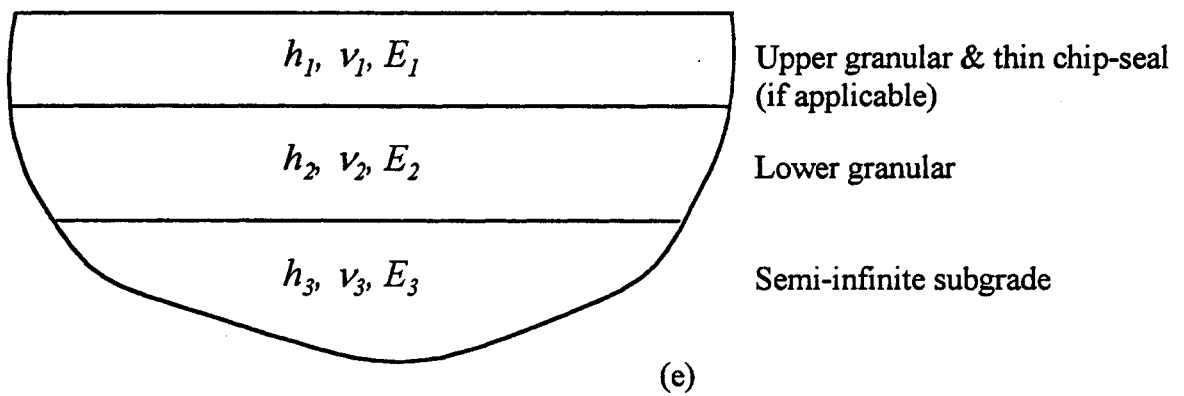


Fig. 71. Backcalculation model configurations.

Base testing (thick granular > 300 mm): multi-layer system, EVERCALC



Aggregate and chip-seal testing: multi-layer system, EVERCALC



PCC section testing: composite layer on subgrade, AASHTO effective pavement and subgrade modulus analysis.

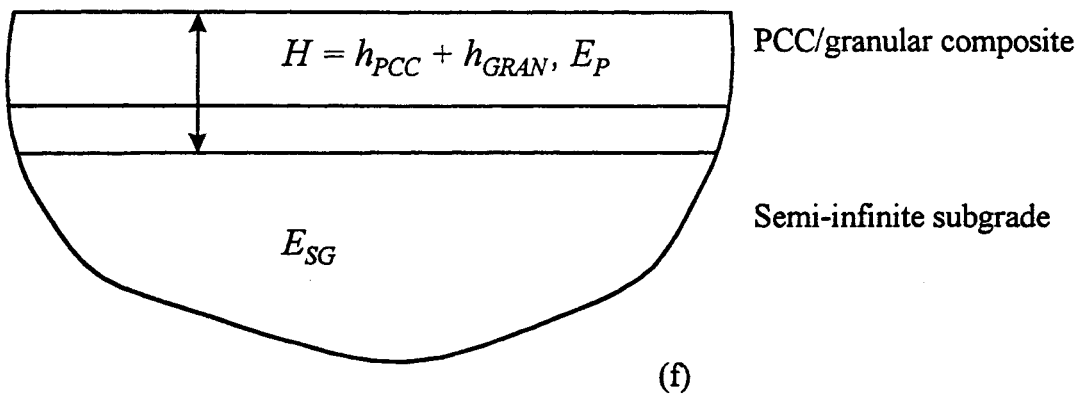
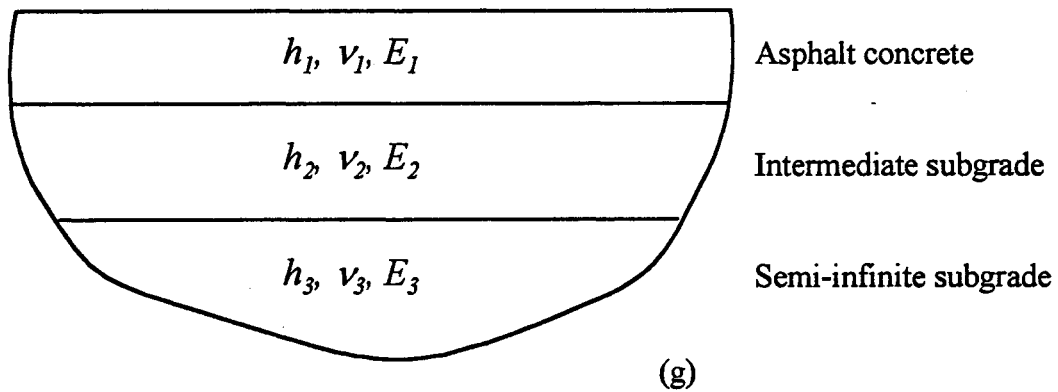
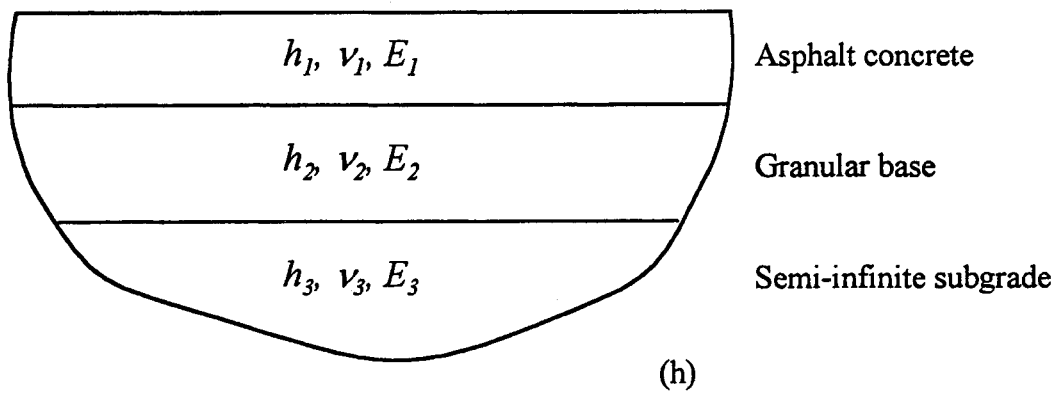


Fig. 71, cont. Backcalculation model configurations.

Full-depth flexible system testing: multi-layer system, EVERCALC



Conventional flexible section testing: multi-layer system, EVERCALC



Permeable asphalt-stabilized base (PASB) testing: multi-layer system, EVERCALC.

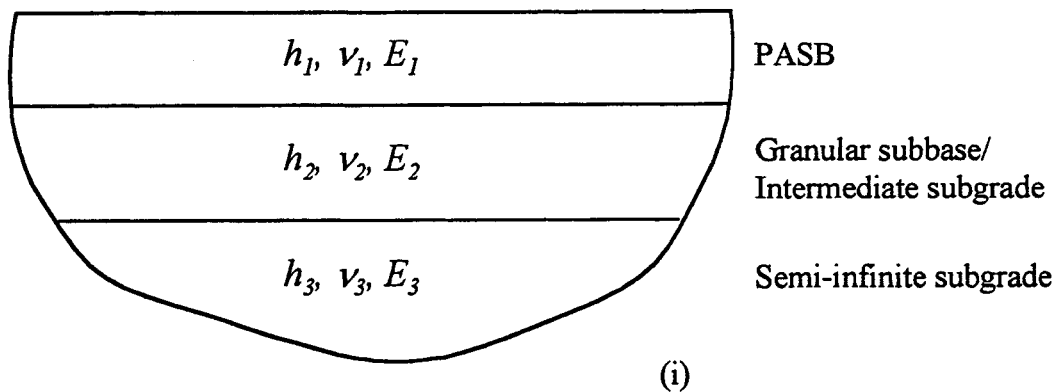
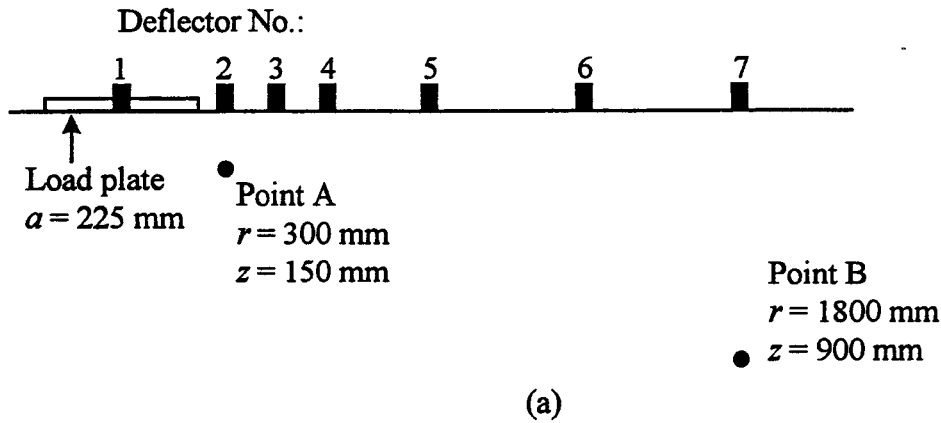


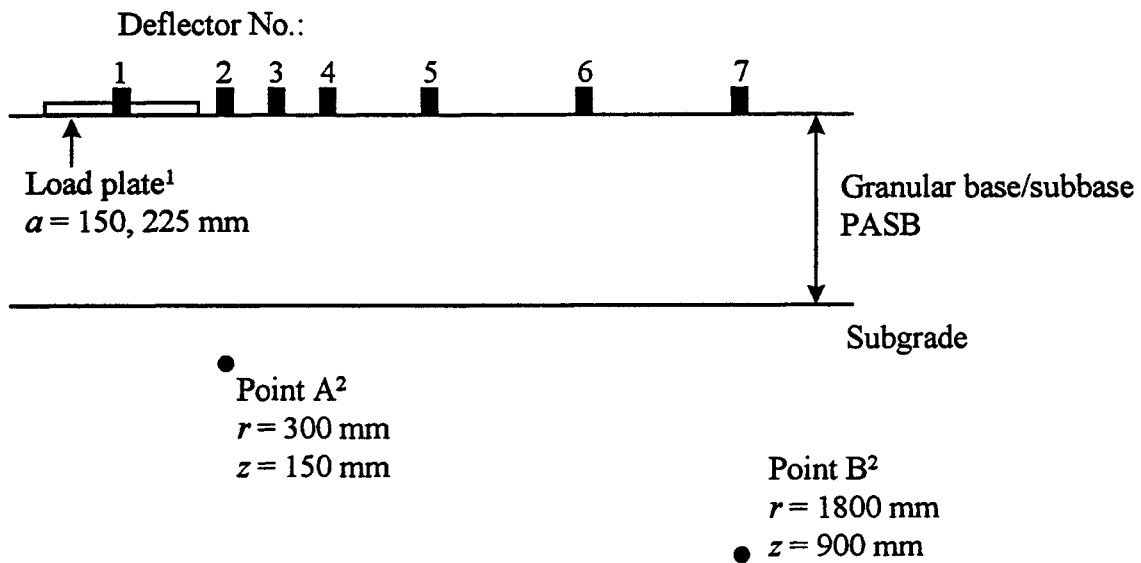
Fig. 71, cont. Backcalculation model configurations.

Locations of points for subgrade stress calculations:

SUBGRADE TESTS



GRANULAR BASE AND PASB TESTS



NOTES:

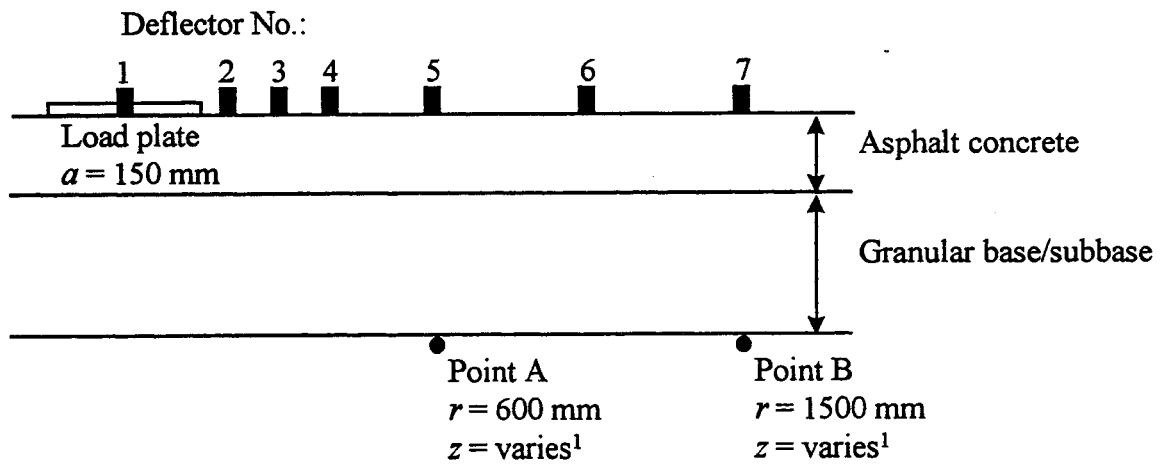
[1] Load plate radius was 225 mm for all granular base tests; a 150 mm radius plate was used for all PASB tests except for TS 9, offsets 1 and 4, and TS 10, offsets 1, 4, and 7.

[2] Points A and B depth relative to granular/subgrade interface.

Fig. 72. Locations of points for subgrade stress calculations.

Locations of points for subgrade stress calculations:

POST-CONSTRUCTION FLEXIBLE PAVEMENT TESTS (CONVENTIONAL)

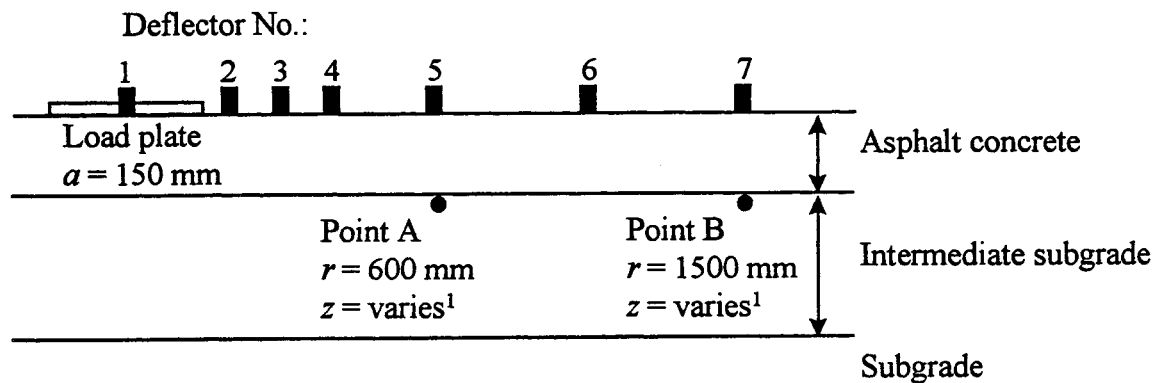


NOTE:

[1] Stresses at Points A and B calculated at point just below top of subgrade at offsets indicated.

(c)

POST-CONSTRUCTION FLEXIBLE PAVEMENT TESTS (FULL-DEPTH)



NOTE:

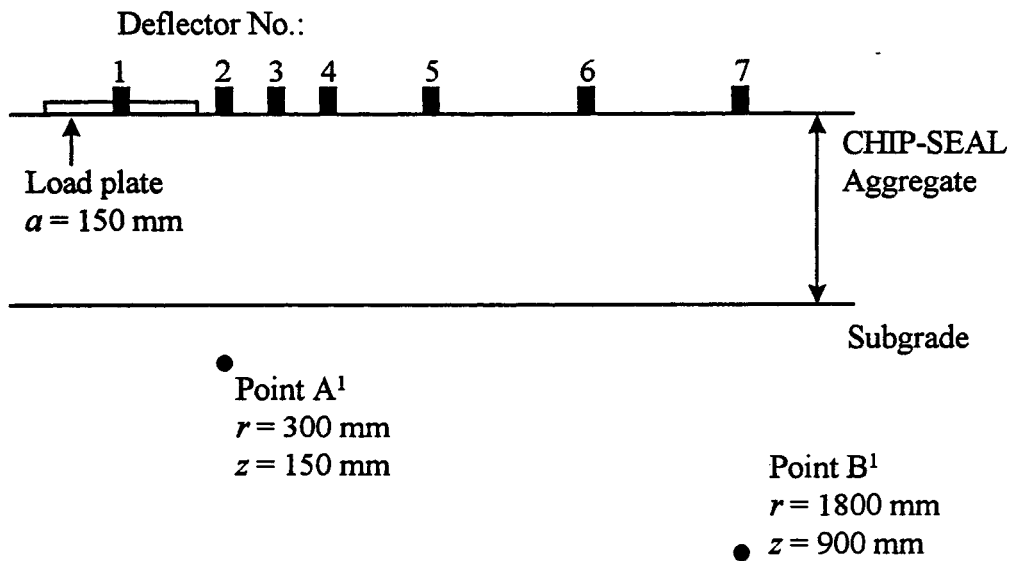
[1] Stresses at Points A and B calculated at point just below top of intermediate subgrade at offsets indicated.

(d)

Fig. 72, cont. Locations of points for subgrade stress calculations.

Locations of points for subgrade stress calculations:

POST-CONSTRUCTION AGGREGATE AND CHIP-SEAL TESTS



NOTE:

[1] Points A and B depth relative to aggregate/subgrade interface.

(e)

Fig. 72, cont. Locations of points for subgrade stress calculations.

**INCREASE IN SUBGRADE MODULUS AFTER CONSTRUCTION
VS. INITIAL SUBGRADE MODULUS AND PAVEMENT THICKNESS**

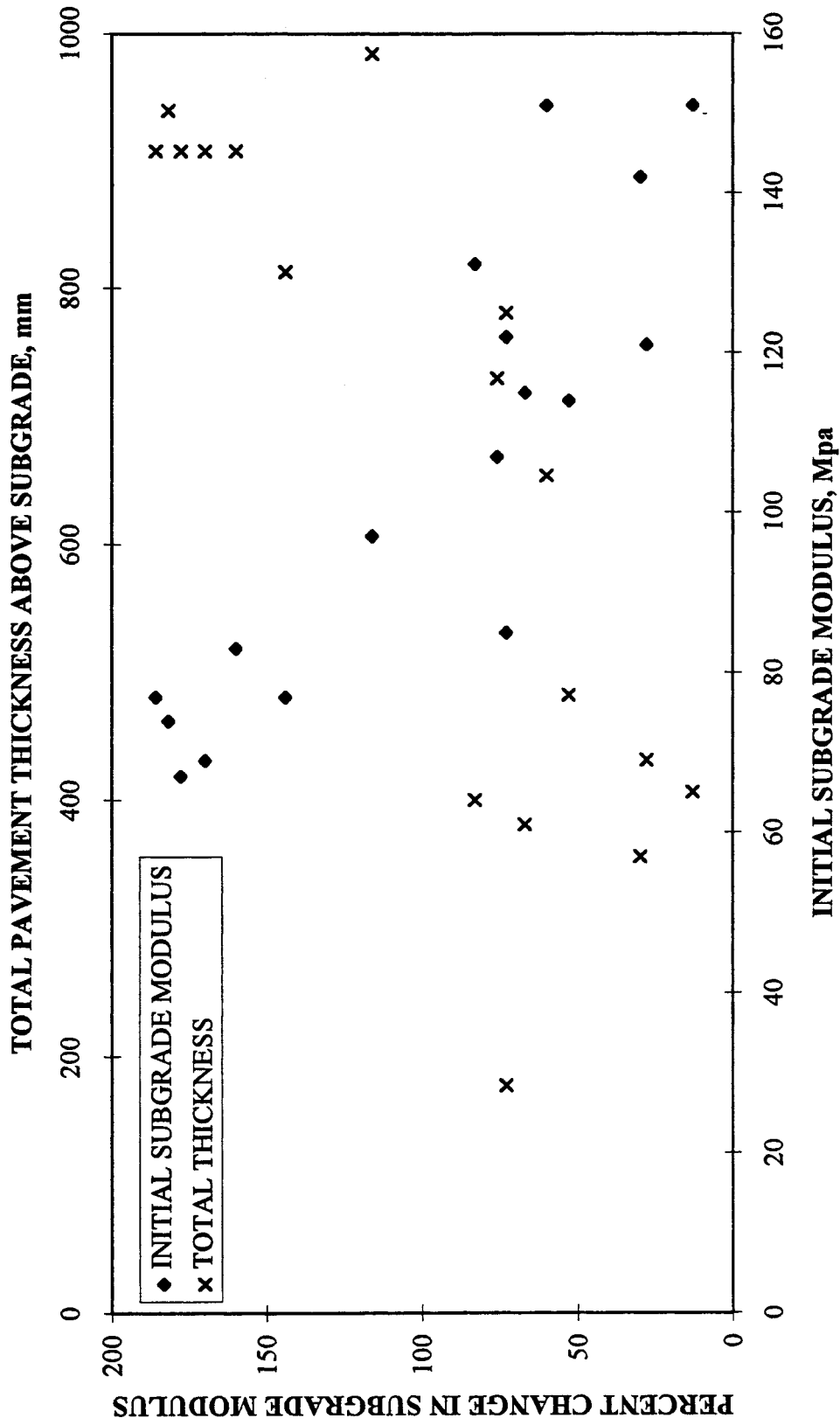


Fig. 73. Increase in subgrade modulus after construction vs. initial subgrade modulus and pavement thickness.

